TUMOR BLOOD VESSEL-ASSOCIATED ANTIGENS AS TARGETS FOR CANCER IMMUNOTHERAPY

by

Kellsye Paula L. Fabian

B.S. in Molecular Biology and Biotechnology, University of the Philippines, 2007

M.S. in Molecular Biology and Biotechnology, University of the Philippines, 2011

Submitted to the Graduate Faculty of the

School of Medicine in partial fulfillment

of the requirements for the degree of

Ph.D. in Immunology

University of Pittsburgh

2017

UNIVERSITY OF PITTSBURGH

SCHOOL OF MEDICINE

This dissertation was presented

by

Kellsye Paula L. Fabian

It was defended on

March 29, 2017

and approved by

Lisa Butterfield, Ph.D., Professor, Department of Medicine

Pawel Kalinski, Ph.D., Professor, Department of Surgery

Adriana Larregina, M.D., Ph.D., Associate Professor, Department of Dermatology

Paul Monga, M.D., Professor, Department of Pathology

Dissertation Advisor: Walter J. Storkus, Ph.D., Professor, Department of Dermatology

TUMOR BLOOD VESSEL-ASSOCIATED ANTIGENS AS TARGETS FOR CANCER IMMUNOTHERAPY

Kellsye Paula L. Fabian, Ph.D.

University of Pittsburgh, 2017

The formation of neovessels is critical in the progression of solid tumors; hence, tumor angiogenesis is an attractive target for cancer therapy. A number of currently available anti-vascular and anti-angiogenic pharmacologic drugs have been shown to induce objective clinical responses, however, the therapeutic effects of these drugs are only transient, with patients developing drug-refractory disease in most cases. Therefore, the development of alternative therapies that durably regulate the tumor vasculature remains an unmet clinical need. Due to the dysregulated angiogenesis within growing tumors, tumor blood vessels are morphologically and functionally aberrant. The cells that make up the tumor vasculature, including pericytes and vascular endothelial cells, exhibit genomic and proteomic profiles that are markedly different than their counterparts in normal tissues. These differences affect the functions of the tumor-associated vascular cells, but they may also represent unique immunological targets for the development of interventional immunotherapies. In this thesis, I demonstrate that DLK1 and DLK2, which represent EGF-like protein antagonists of the Notch signaling pathway, are variably expressed in RENCA renal cell carcinoma-associated vascular pericytes. Vaccines that coordinately target both of these antigens result in the activation and recruitment of DLK1- and DLK2-specific, as well as, tumor-specific $CD8^+$ tumor-infiltrating lymphocytes (TIL). The pro-inflammatory activity of vaccine-induced $CD8^+$ TIL was associated with therapeutic reconditioning of the tumor stroma, and notably, the "normalization" of the tumor vasculature. Moreover, combination of immune checkpoint inhibitors (ICI) with the DLK1- and DLK2-

targeted vaccine yielded a more effective therapy than either component modality, suggesting possible next-generation treatment options for patients with solid forms of cancer.

TABLE OF CONTENTS

LIST OF TABLES

LIST OF FIGURES

ACKNOWLEDGEMENTS

First and foremost, I would like to offer my utmost thanks and sincere gratitude to Dr. Walter Storkus, my mentor, who welcomed me to his lab with open arms and shared his passion for science and research. He is an inspiring role model whose expertise, wisdom, and advice I have always received with the highest degree of respect. His guidance and his confidence in me were instrumental in the completion of my degree. I would also extend my gratitude to the members of my thesis committee, Dr. Lisa Butterfield, Dr. Pawel Kalinski, Dr. Adriana Larregina, and Dr. Paul Monga for their encouragement and valuable feedback. I am grateful to have been surrounded and advised by such great scientists.

I would like to thank the old friends I left behind in the Philippines and the new friends I made in Pittsburgh for supporting me and keeping me sane throughout the whole process. I specifically would like to thank the members of the Storkus lab – Nina, Lu, Aparna, Jen, Devin, Laima, Subha, Aliyah, Ron, and Manoj, who have been excellent co-workers and friends. Grad school wouldn't have been as fruitful and as fun without them.

Last but not least, I'd like to thank my family for their love and support. My parents, for instilling in me the importance of education and always believing that I can achieve whatever I set my mind on to. My siblings, Andri, Kaiser, and Jezka, for inspiring me to be the best eldest

sister they could look up to. My in-laws, for encouraging me and cheering me on. Most importantly, I'd like to thank my husband, Dante, for being with me every step of the way, for being my rock, and for being my biggest fan.

Without a doubt, graduate school is one of the most challenging endeavors that I have undertaken. It would've been impossible to accomplish it alone. To all the people who have encouraged, supported, and guided me along the way, I can't thank you enough.

ABBREVIATIONS

ACT	Adoptive cell transfer
ADAM	A disintegrin and metalloproteinase
Ang	Angiotensin
Arg-1	Arginase I
BM	Basement membrane
CAF	Cancer-associated fibroblast
CAR	Chimeric antigen receptor
CSC	Cancer stem cells
CXCL	CXC-motif chemokine ligand
CXCR	CXC-motif chemokine receptor
DC	Dendritic cell
DLK	Delta-like homolog
Dll	Delta-like protein
DSL	Delta-Serrate, LAG-2 domain
ECM	Extracellular matrix
EGF	Epidermal growth factor
EMT	Epithelial-to-mesenchymal transition
FGF	Fibroblast growth factor

GIST	Gastrointestinal stromal tumors
HGF	Hepatocyte growth factor
HIF	Hypoxia inducible factor
HNSCC	Head and neck squamous cell carcinomas
ICAM-1	Intercellular adhesion molecule-1
IL	Interleukin
LFA-1	Lymphocyte function-associated antigen-1
LPS	Lipopolysaccharide
MDSC	Myeloid derived suppressor cells
MMP	Matrix metalloproteinase
NICD	Notch intracellular domain
NK	Natural killer cell
PD-L1	Programmed death ligand-1
PDGF	Platelet-derived growth factor
PDGFR	PDGF receptor
PNET	Pancreatic neuroendocrine tumors
RCC	Renal cell carcinoma
RTK	Receptor tyrosine kinase
S1P	Sphingosine 1-phospate
SCLC	Small cell lung carcinoma
SDF	Stromal-derived factor
T-ALL	T cell acute lymphoblastic leukemia
TACE	Tumor necrosis factor-α converting enzyme

TAM	Tumor-associated macrophage
TGF	Transforming growth factor
TGF	Transforming growth factor
Th1	T helper type 1
TIL	Tumor infiltrating lymphocytes
TKI	Tyrosine kinase inhibitors
TME	Tumor microenvironment
TNF	Tumor necrosis factor
Tregs	Regulatory T cells
VCAM-1	Vascular adhesion molecule-1
VEC	Vascular endothelial cell
VEGF	Vascular endothelial growth factor
VEGFR	VEGF receptor
VLA-4	Very late antigen-4
vSMC	Vascular smooth muscle cell

1.0 INTRODUCTION

This chapter has been adapted from

Fabian, K.P.L. and Storkus, W.J. Vascular remodeling, T cell trafficking and antitumor immunity. In: *Defects in T Cell Trafficking and Resistance to Cancer Immunotherapy*, Donnadieu, E. (Ed.), Springer, New York, NY, pp. 51-76, 2016.

and

Fabian, K.P.L. and Storkus, W.J. (Immuno)therapeutic targeting of tumor-associated blood vessels. In: *The Microenvironment in Cancer Progression and Cancer Therapy*, Kalinski, P. (Ed.), Springer, New York, NY, *in press*, 2017.

The immune system plays a major role in regulating the growth of cancer. In fact, the presence of tumor infiltrating lymphocytes (TILs), specifically $CD8^+$ T cells and $CD4^+$ T helper type 1 (Th1) cells, has been associated with improved patient survival in a number of clinical studies involving various types of cancers, including melanoma, ovarian cancer, head and neck cancer, breast cancer, esophageal cancer, and colorectal cancer, to name just a few [1-5]. Type 1 TILs can limit tumor progression by directly killing tumor cells or by secreting chemokines and cytokines that mediate anti-tumor activities [6-8]. Therefore, the goal of cancer immunotherapy is to enhance the proliferation, migration, and activity of tumor-specific T cells.

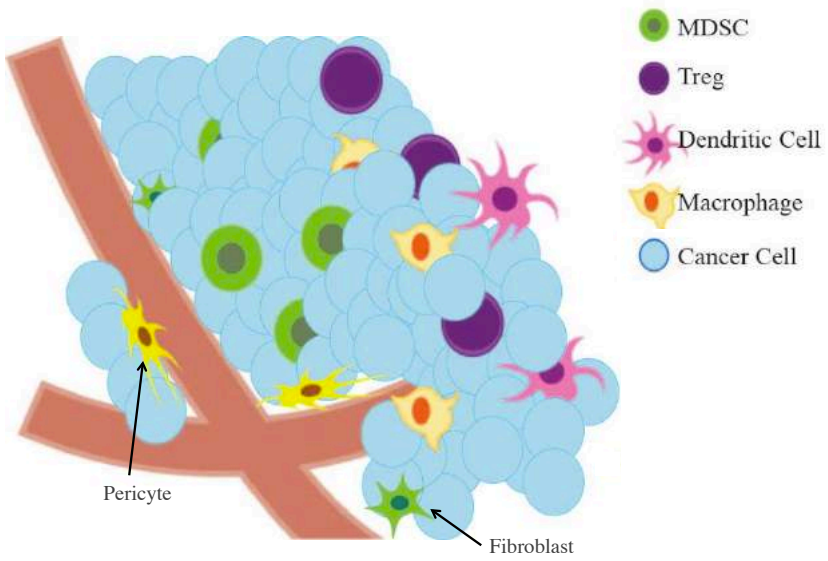

Figure 1. Immunosuppressive populations in the TME.

MDSCs: produce nitric oxide synthase, reactive oxygen species and arginase 1 that suppress T cell activity and proliferation and sequesters cysteine which is essential for T cell functions. Tregs: secrete immunosuppressive cytokines (IL10 and TGFβ) and function as sinks for other important homeostatic and antitumor cytokines, such as IL-7, IL-12, and IL-15. Tolerogenic dendritic cells (DCs): induce Tregs and fail to activate effector T cells. Macrophages (M2): secrete immunosuppressive factors (IL10, TGFβ, and vascular endothelial growth factor (VEGF)) and have impaired tumoricidal activity. (Adapted from Ref. [15])

However, circulating anti-tumor T cells face a hostile, immunosuppressive environment upon interaction with the tumor bed. Tumor and stromal cells could impede T cell recognition and functional activity by down-regulating MHC molecules [9], upregulating inhibitory receptors like programmed cell death protein ligand 1 (PD-L1) [10, 11] and secreting inhibitory factors such as transforming growth factor (TGF)β, interleukin (IL)-10 and prostaglandin E2 [12]. The tumor stroma also contains large populations of immunosuppressive hematologic progeny, such as regulatory T cells (Tregs), myeloid derived suppressor cells (MDSCs) and M2-like tumor-associated macrophages (TAMs) (**Figure 1**; [13, 14]). Despite such therapeutic

concerns, one would be placing the proverbial “cart before the horse”, since in most cases, circulating T effector cells fail to gain entry into the tumor microenvironment (TME) because they are functionally and physically blocked by unique characteristics in the tumor-associated vasculature. Thus, the “tumor endothelial barrier” must be first broken, before worrying about regulatory mechanisms in place within the TME that serve to limit optimal anti-tumor T cell efficacy *in vivo*.

1.1 ANGIOGENESIS AND CANCER

1.1.1 The aberrant tumor vasculature

Pathological angiogenesis is a hallmark of cancer [16]. Solid tumors, like normal tissues, require nutrients and oxygen as well as a mechanism to expel cellular waste and carbon dioxide. These requirements necessitate the formation of neovascular networks for tumor growth and maintenance. In adult normal tissues, angiogenesis is quiescent, occurring only under specific physiological conditions such as wound healing. Notably, in such cases, new vessels mature and stabilize rapidly because of the tightly- regulated balance of pro- and anti-angiogenic factors. During the onset of angiogenesis, the associations between vascular cells are relaxed and the extracellular matrix (ECM) dissolution is promoted by factors like vascular endothelial growth factor (VEGF) and angiotensin (Ang)-2 [17, 18]. The migration of vascular endothelial cells (VECs) is induced by VEGF-A, wherein subsets VECs with high levels of VEGF receptor (VEGFR), called the tip cells, direct the vascular outgrowth by sensing the gradient of the proangiogenic factor, ultimately infiltrating the avascular, hypoxic region of the tissue [19]. In

addition, VEGF also stimulates the tip cells of express the Notch ligand Delta-like protein (Dll)4. Dll4 then activates Notch receptors expressed on adjacent VECs, which causes the adjacent cells to downregulate their expression of VEGFR, becoming less responsive to the VEGF-mediated signals [20]. These neighboring VECs become stalk cells that proliferate and migrate in the direction of the tip cell, thus elongating the sprouting vessel [21]. During the resolution phase of angiogenesis, a new basement membrane is formed and pericytes are recruited to cover the vessel on its abluminal surface. Pericytes signal VECs to stop dividing and to form tight junctions and adherens junctions, in support of overall vascular integrity [21, 22].

On the other hand, in tumors, the production of pro-angiogenic factors is favored over anti-angiogenic factors, turning on the angiogenic switch. Tumorigenic conditions such as hypoxia [23], oncogene activation and tumor-suppressor mutation [24] contribute to the skewing of the balance towards the expression of pro-angiogenic factors. This imbalance leads to the sustained growth of tumor blood vessels that are very distinct from their normal counterparts. Tumor sprouting angiogenesis usually does not reach full resolution. Pericytes atypically remain only loosely-associated with the blood vessels [25] and the basement membrane is abnormally thick or thin [26]. Tumors also employ other mechanisms to instigate neo-vessel growth including: (1) vasculogenesis, in which endothelial progenitor cells are recruited from bone marrow or peripheral blood into the TME to form new blood vessels, (2) intussusception, in which VECs re-organize causing blood vessels to split and give rise to daughter vessels, (3) vessel co-option, in which tumor cells grow along existing blood vessels and (4) vasculogenic mimicry, in which tumor cells may de-differentiate into endothelial-like cells and form vascular tubes [27].

When compared to blood vessels in normal somatic tissues, the tumor vasculature is architecturally and functionally abnormal (**Figure 2**). The tumor vascular network is highly tortuous, disorganized and lacks the normal hierarchical arrangement of arterioles, capillaries and venules [28, 29]. The tumor vessels are also morphologically dilated and leaky with chaotic and variable blood flow, resulting in regions of tumor that are hypoxic and acidic [29]. In conjunction, the cellular components of the tumor blood vessels are also abnormal in their phenotype/function. VECs and pericytes exhibit altered gene expression profiles and elicit a defective basement membrane [26, 30, 31]. These alterations in expression of angiogenesis-associated vascular components in progressor tumors are considered as strong targets for therapeutic intervention in patients with cancer.

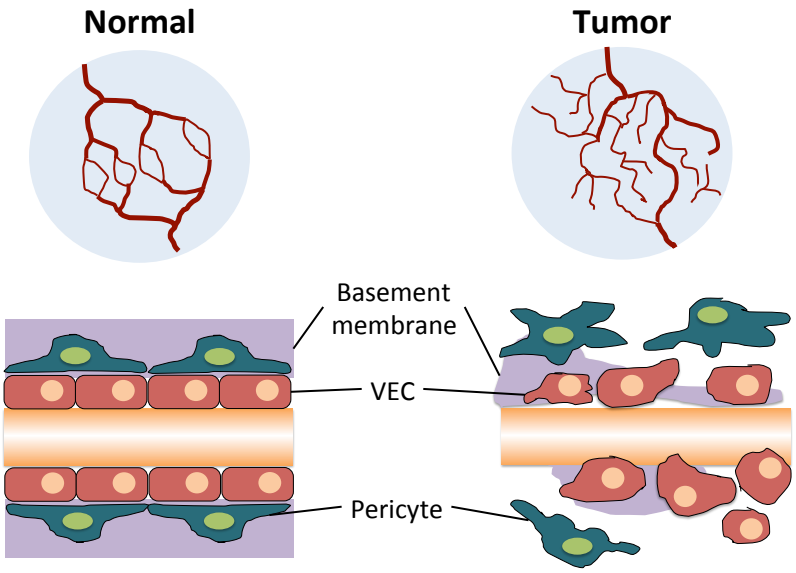

Figure 2. The tumor vasculature is architecturally and functionally abnormal.

In healthy tissues (left panel), the vasculature is organized and has hierarchical architecture. The vascular endothelial cells (VEC) form a monolayer sheath that is covered with pericytes embedded in uniform basement membrane. In tumors (right panel), the vasculature is tortuous and disorganized. The endothelial sheath is porous, fenestrated, lacks pericyte coverage, and has uneven basement membrane.

1.1.2 Constituents of the tumor vasculature

1.1.2.1 Vascular endothelial cells (VECs)

VECs arise from hemangioblast precursors that are derived from the ventral floor of the dorsal aorta in the aorta-gonad-mesonephros region [32, 33]. During *de novo* organization of VECs into vessels (also known as vasculogenesis), newly formed VECs express growth factor receptors like VEGFR1 and VEGFR2 that allow VECs to proliferate, migrate and form tubular structures in response VEGF and fibroblast growth factor (FGF). Once the formed vessels mature, VECs down-regulate their expression of these growth factor receptors. In developing tumor blood vessels, however, VEGFR-1, VEGFR-2 and even VEGFR-3 (which is usually restricted to lymphatic vessels in adults) are re-activated and elevated in the VECs, allowing for the unrestricted proliferation and formation of blood vessels in the VEGF-rich TME [34-36]. Aside from growth factor receptors, tumor VECs also upregulate other genes that are typically not expressed on normal VECs [37, 38]. Most of these genes play a role in the angiogenic process, but some are induced by hypoxia or under conditions of abnormal blood flow [37, 39].

VECs are held together by cell-to-cell junctions to form a continuous monolayer of cells that lines the blood vessel. The normal endothelium acts as a selective barrier that tightly controls the exchange of substances between the blood and the surrounding tissue [33, 40]. Different membrane bound receptors present in the endothelium allow for the active transport of large molecules such as proteins, metabolites and hormones from blood into tissues [41]. The endothelial cells have junctional segments that are very similar to adherens and tight junctions in epithelial cells. These tight junctions are localized in the apical regions to seal the clefts between cells in the luminal surface, therefore, functionally restricting para-cellular permeability. On the other hand, adherens junctions occupy basal positions and function to limit para-cellular

permeability, as well as, to control vessel morphogenesis and stability [42-44]. The adherens and tight junctions also transfer intracellular signals that mediate contact inhibition of cell growth, cell polarity and VEC-pericyte interaction and, hence, allow VECs to adapt quickly to evolving changes in their microenvironment, such as release of growth factors, angiogenic cues and inflammatory conditions [44, 45]. Gap junctions are also present between neighboring cohorts of endothelial cells [42].

The endothelium in tumors is structurally defective, composed of irregularly-shaped endothelial cells that have long, fragile cytoplasmic projections that sometimes extend across the vessel lumen [46] and is characterized by intercellular gaps between endothelial cells, transendothelial holes and endothelial fenestrae (pores) [47-49]. Increased production of VEGF in the TME leads to a dissolution of the VE-cadherins and alternate adherens junction complexes, disrupting VEC cell-to-cell interactions [50]. These abnormalities render tumor vessels unusually leaky and highly-permeable to plasma proteins, and even erythrocytes. The leakiness and uncontrolled extravasation of blood and plasma results in increased interstitial (fluid) pressure within the tumor lesion [51]. Structural abnormalities and high interstitial pressure contribute to irregular blood flow resulting in the uneven and impeded distribution of nutrients, oxygen, and (systemically-administered) chemotherapeutic drugs within tumors. This also leads to areas in the tumor that are highly-acidic and hypoxic. The leaky tumor vessel can also promote the traffic of tumor cells into the blood stream and the eventual formation of distal tumor metastases [47].

1.1.2.2 Pericytes

Pericytes and vascular smooth muscle cells (vSMCs), collectively called mural cells, cover and support the endothelial tubules to maintain vascular integrity. Pericytes are usually found as single cells or as a discontinuous single-cell layer around arterioles, capillaries, and post-capillary venules [52]. On the other hand, vSMCs are generally identified around arteries and veins as multiple concentric layers of cells to mediate vascular tone and contraction [52, 53]. However, the distinction between pericytes and vSMCs is not always clear-cut and it has been suggested that there is a continuum of phenotypes ranging from the canonical vSMCs to classical pericytes rather than two distinct lineages of mural cells [53].

Pericytes have a number of different developmental origins such that within a single region of a given blood vessel, one may identify pericytes that derived from multiple precursor populations [54]. Furthermore, no single consensus pericyte marker has been identified to date. As such, pericytes are typically identified using a combination of different characteristics including location (i.e. cells embedded in a basement membrane that is shared with the endothelium; [55]), in addition to morphology and gene/protein expression profile.

During physiological angiogenesis, pericytes are recruited to the developing vessel via soluble factors such as platelet-derived growth factor (PDGF)β, sphingosine 1-phosphate (S1P), Ang-1 and TGF-β1. The recruited pericytes form tight connections with the underlying endothelial cells with one pericyte usually in coordinate contact with multiple endothelial cells. Such pericyte interactions are very important in maintaining the integrity of the endothelium, playing a central role in regulating endothelial proliferation, differentiation, contractility, tone, stability, and permeability [53, 56-60]. However, the pericyte-endothelial cell interaction is disturbed in the TME, with poor pericyte coverage usually observed in a large proportion of

tumor-associated blood vessels. Tumor pericytes have cytoplasmic processes that extend into the tumor tissue [25] and are loosely associated with the endothelium [22, 25]. This abnormal pericyte-endothelial cell association contributes to increased vascular permeability [47], which results in poor perfusion and hypoxia, and modified basement membrane [61]. Tumor-associated blood vessels are prone to hemorrhaging, and typically exhibit a disrupted basement membrane [61]. The pericyte coverage of the endothelium is also very variable, depending on the type of tumor. For example, islet carcinomas have dense pericyte coverage while glioblastomas have drastically reduced numbers of pericytes per unit of venule area [22]. Variable coverage can also occur within the same tumor [61]. Pericyte coverage is thought to help maintain and stabilize the tumor vessels [62], with naked endothelium seemingly more dependent on VEGF for VEC survival [63]. Moreover, the tumor-associated pericytes exhibit an altered marker/protein expression profile, making them attractive targets for therapeutic intervention. Indeed, in tumors that overexpress PDGF receptor (PDGFR)β (leading to densities of pericytes), blockade of PDGFRβ signaling results in the physical detachment of pericytes from VEC, in association with restricted tumor growth [64-66].

1.1.2.3 Fibroblasts

Cancer-associated fibroblasts (CAFs) are spindle-shaped cells embedded within the ECM that originate from resident fibroblasts and bone marrow-derived mesenchymal precursors [67, 68]. They are phenotypically and functionally distinct from normal fibroblasts and comprise a significant proportion of the population of tumor-associated stromal cells [69].

Although technically not a component of blood vessels, CAFs still play a major role in angiogenesis by promoting tumor blood vessel formation, principally via their production of pro-angiogenic factors. Although cancer cells themselves can secrete VEGF, the principal source of

VEGF in most TMEs are CAFs [70]. In cancers such as pancreatic cancer and breast cancer, CAFs produce stromal-derived factor (SDF)-1 or CXC-motif chemokine ligand (CXCL)12, which contributes to tumor vascularization by recruiting endothelial precursor cells from the bone marrow [71-73]. CAFs may also indirectly promote tumor angiogenesis by secreting chemokines like CXCL1 and CXCL2 that recruit pro-angiogenic macrophages and neutrophils into the TME [74]. Furthermore, CAFs release matrix metalloproteinases that degrade the ECM, thus spatially accommodating the growing blood vessel and, at the same time, releasing VEGF previously sequestered in the ECM [75].

1.1.2.4 Basement membrane

The basement membrane (BM) is a complex of proteins, glycoproteins and proteoglycans. The BM is similar to the ECM but has a different density and is always in contact with cells [26, 76]. The general role of the BM is to serve as boundary between tissue compartments, provide structural support, and regulating local cell behavior [77].

The vascular basement membrane envelops the VECs and pericytes and is primarily composed of Type IV collagen, laminin, fibronectin and heparin sulfate proteoglycan [76]. The BM is integral in the initiation and resolution of angiogenesis, as it possesses both pro- and anti-angiogenic activities. Quiescent endothelial cells are bound to BM, indicating that the primary signals from BM inhibit VEC proliferation [78]. During active angiogenesis, the BM is degraded leading to the detachment of VECs and pericytes and the release of sequestered growth factors. Pro-angiogenic factors induce VEC to produce and embed in a provisional matrix composed of vitronectin, fibronectin, type I collagen and thrombin. Cryptic domains of Type IV collagen in partially degraded BM and the provisional matrix provide proliferative cues to the VECs [76, 79].

Deposition of basement membrane is dependent on VEC-pericyte interaction and disrupting this interaction by blocking pericyte recruitment, for example, results in perturbed or reduced basement membrane deposition [80-82]. Therefore, the abnormalities in tumor basement membrane can be partially explained by the disrupted VEC-pericyte interaction in the tumor. It was previously believed that BM was absent in tumor vasculature. However, more recent studies show that BM is present and can even fully cover tumor vessels albeit in an abnormal manner. Tumor vascular BM has variable thickness and multiple layers, suggesting that the BM has undergone several rounds of remodeling. In addition, the tumor BM exhibits only loose association with VECs and pericytes, which is characteristic of degenerating or forming blood vessels [26].

1.1.3 Tumor vasculature in cancer progression

Several landmark studies have shown that tumor blood vessels and the process of angiogenesis are necessary for tumor progression. When tumor cells were implanted in avascular tissues, tumor growth was inhibited and limited until sprouting vessels were able to access an existing blood supply [83, 84]. Since the importance of the tumor blood vasculature was demonstrated, numerous studies have shown that it not only supports tumor growth by delivering nutrients, it also promotes tumor cell survival, confers drug resistance, helps to limit immune system surveillance, aids in metastasis and promotes stemness (**Figure 3**).

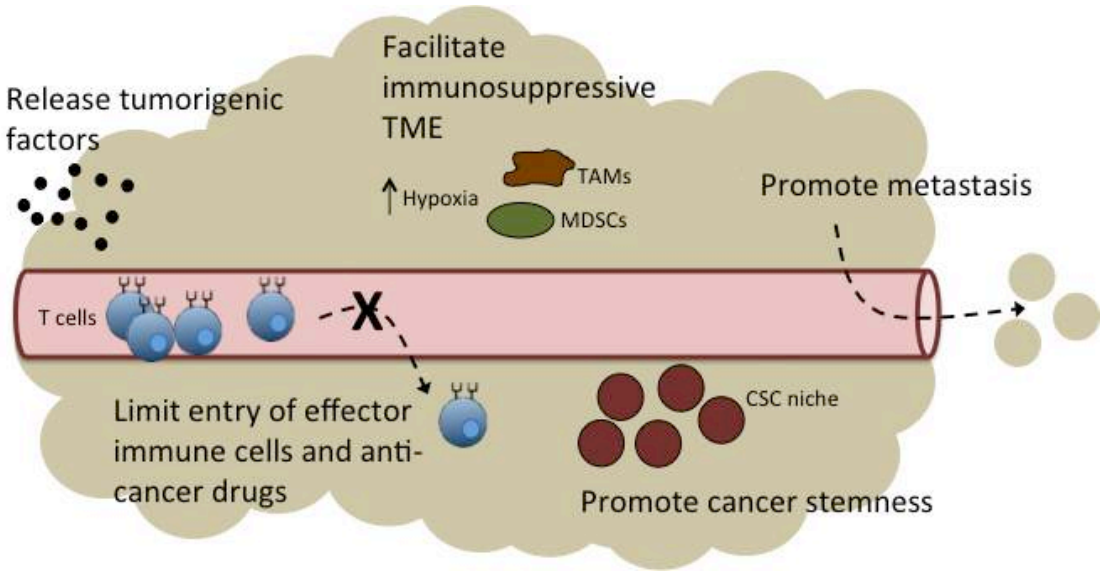

Figure 3. Tumor-promoting mechanisms by the tumor vasculature.

The tumor vasculature support growth and survival of tumor cells by releasing tumorigenic factors (ex.EGF, HGF), impeding drug delivery and entry of effector immune cell infiltration into the tumor bed, supporting immunoregulatory cells, promoting metastasis and providing a niche for cancer stem cells.

1.1.3.1 Tumor vasculature supports tumor growth and survival

The tumor vasculature actively supports tumor growth by secreting factors that promote tumor survival. For example, the CAFs in the TME produce epidermal growth factor (EGF), hepatocyte growth factor (HGF) and heregulin that promote tumor cell proliferation and vitality [85]. VECs in head and neck squamous cell carcinomas (HNSCC) overexpress the anti-apoptotic molecule Bcl-2, which induces the production of VEGF through STAT3 signaling [86]. VEC-derived VEGF binds the VEGFR1 expressed by tumor cells, triggering the production of Bcl-2 in the HNSCC cells and enhancing their survival. IL-6, CXCL8, and EGF derived from VECs also activate STAT3, Akt, and extracellular signal-regulated kinase (ERK) in the tumor cells, enhancing tumor cell migration and preventing their apoptosis. Interruption of these signaling

cascades by silencing Bcl-2 or the factors secreted by the VECs leads to inhibited tumor growth [87].

1.1.3.2 The aberrant tumor-associated vasculature confers drug resistance

The tumor vasculature intrinsically confers therapy resistance by impeding drug delivery into the tumor lesion. The structural aberrations of the vessels cause excessive leakiness that leads to abnormal plasma accumulation and retention. This results in heterogeneous blood flow and high-interstitial fluid pressure in tumor tissue, preventing uniform distribution of systemically-administered anti-cancer drugs. Indeed, the erratic blood flow in the tumor promotes the concentrated delivery of drugs to the perfused outer (cortical) regions of the tumor while delivery to the poorly-perfused medullary tumor regions requires efficient perfusion/diffusion [88]. Furthermore, extravasation of therapeutic drugs into the TME is dependent on fluid movement across the vessel wall, which is influenced by a pressure gradient between the vessels and the interstitial space. The high interstitial fluid pressure in the tumor disrupts the development of an optimal gradient, thus hindering drug delivery to the tumor core [89]. The tumor-associated vasculature may also actively prevent drug delivery by overexpressing efflux pumps that promote rapid drug removal/detoxification [90, 91].

1.1.3.3 The tumor-associated vasculature contributes to immune escape

The abnormal tumor vasculature not only impedes drug delivery, it also obstructs anti-cancer immune response by limiting entry of effector cells while simultaneously contributing to an immunosuppressive TME. The adaptive T cell response is critical to protective anti-tumor immunity and the endothelium plays an important role in regulating the trafficking of T cells and other leukocytes into peripheral (inflamed) tissues. In normal tissues, resting VECs express little

to no adhesion molecules on their luminal surface interfacing with the blood supply. However, during infection or under conditions of tissue injury, pro-inflammatory signals such as lipopolysaccharide (LPS), tumor necrosis factor (TNF)-α and IL-1β induce the expression of adhesion molecules to allow the extravasation of leukocytes from the blood stream [92, 93]. E-selectin and P-selectin expressed on VECs bind to their ligands Sialyl Lewis^X and P-selectin glycoprotein ligand 1 on the activated T cells and other leukocytes [94, 95]. This binding event is a weak affinity interaction that induces the tethering and rolling of the T cells on the inflamed luminal endothelium. The inflamed endothelium also presents chemokines that induce cell surface integrins, such as lymphocyte function-associated antigen-1 (LFA-1) and very late antigen-4 (VLA-4) on rolling T cells, allowing these cells to spread and cluster. Immune cell-expressed LFA-1 and VLA-4 bind strongly to intercellular adhesion molecule-1 (ICAM-1) and vascular adhesion molecule-1 (VCAM-1) on activated VECs, mediating the arrest of interactive T cells on the inflamed endothelium in advance of the subsequent chemokine-driven extravasation of T cells into adjacent tissue. Expression of ICAM-1 and VCAM-1 are down-regulated by an overabundance of angiogenic factors and other VEC-produced proteins (i.e. Egfl7 aka VE-statin) in the TME [96], resulting in the reduced flux of rolling leukocytes and lower densities of adhering leukocytes in tumor-associated blood vessels [97].

Most studies on leukocyte trafficking into tissues focus on VECs, however, a growing literature suggests that pericytes also play significant roles in the extravasation and activation of effector immune cells. During inflammation, pericytes upregulate adhesion molecules, chemokines and cytokines [98-101] and may also display characteristics that are usually associated with antigen-presenting cells [102, 103]. Innate immune cells, specifically neutrophils, have been observed to crawl on pericytes [104]. It was later demonstrated that the

pericyte-expressed molecule NG2 (aka chondroitin-sulfate glycoprotein-4; CSGP4) interacts with neutrophils and macrophages, instructing them to migrate into inflammatory tissue sites [100]. It is currently unknown whether pericytes provide the same homing signals to transmigrating adaptive immune cells in the TME. Moreover, a recent study indicates that pericytes have a direct role in tumor immune escape by inhibiting CD4 T cell activation and by promoting T cell anergy through Regulator of G-protein Signaling-5 (RGS-5)- and IL-6-dependent pathways [105].

1.1.3.4 The tumor-associated vasculature facilitates an immunosuppressive TME

Poor blood perfusion in the tumor leads to hypoxia, which has been shown to promote an immunosuppressive TME. Hypoxia drives the differentiation of tumor-infiltrating myeloid cells into M2-like TAMs. These M2-like TAMs adapt to the hypoxic environment by expressing hypoxia inducible factor (HIF)-1. HIFs are transcription factors that are stabilized under hypoxic conditions and are responsible for the expression of factors that allow cells to survive in a low oxygen environment. M2-like TAMs express high levels of IL-10, arginase I (Arg1) and TGFβ, which are factors known to suppress protective type-1 T cell-mediated immunity, and VEGF, which exerts pro-angiogenic effects [13, 106]. Furthermore, M2-like TAMs preferentially localize within hypoxic regions and TAMs that are situated near functional blood vessels express lower levels of the aforementioned M2-associated immunosuppressive gene products [106]. Hypoxic conditions also promote tumor cells to produce immunosuppressive molecules that inhibit effector T cell and natural killer (NK) cell survival/function, while coordinately supporting the Tregs and MDSCs [107, 108]. Hypoxia decreases the survival and activity of T cells in the TME, partly through inhibition of IL-2 in a HIF-1-dependent manner [109, 110]. HIF-1 also drives expression of FoxP3 associated with Treg differentiation [111].

Interestingly, these immunosuppressive cells also have pro-angiogenic activities, indicating that there are mutually reinforcing interactions between these regulatory cells and the tumor vasculature (**Figure 4**; [112]).

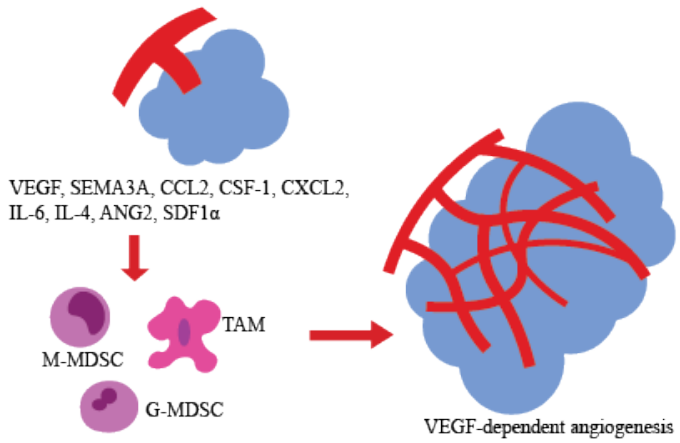

Figure 4. Reciprocal reinforcing interactions between tumor vasculature and regulatory cells.

The tumor vasculature produces factors that recruit and support immunosuppressive cells. The immunosuppressive cells, in turn, promote tumor angiogenesis.

1.1.3.5 The tumor-associated vasculature contributes to metastasis

Metastasis is a multistep process that involves dissociation of tumor cells from the primary tumor mass, invasion of surrounding stroma, intravasation to the vasculature, survival in circulation, extravasation to a distal site and subsequent colonization of new organs [113]. The tumor vasculature is primarily involved in intravasation of tumor cells but can also contribute to other metastatic steps [114, 115].

Hypoxia, due to poor blood perfusion brought about by the structural abnormalities in the tumor-associated vasculature, is a contributing factor to the acquisition of malignant phenotype [116]. During hypoxic stress, HIF-1α together with TGFβ triggers epithelial-to-mesenchymal

transition (EMT) in tumor cells. EMT is the process wherein epithelial markers are down-regulated and mesenchymal markers are up-regulated, leading to the dissociation of epithelial cell-to-cell interactions and the facilitation of cell motility and invasiveness [117].

Invasion of surrounding stroma by tumor cells requires a remodeling of the ECM and the migration of cancer cells through it. CAFs lead the metastatic tumor cells and utilize protease- and force-mediated activities to remodel the ECM [118]. Specifically, fibroblasts implement RhoA and Rho-associated protein kinase 1 to remodel the ECM in an matrix metalloproteinase (MMP)14-dependent manner [119, 120]. Cancer cells then follow these CAF-instructed microtracks in a CDC42-dependent manner [119].

The lack of an intact basement membrane and the disorganized VEC and pericyte interactions make the tumor blood vessels more accessible to motile tumor cells, easing the intravasation process [121]. Studies have shown that a high prevalence of abluminal pericytes limits tumor metastasis [122, 123]. In some tumor models, deficient pericyte coverage of blood vessels, due to a deficiency in pericyte recruitment, can be associated with increased metastatic potential [124]. Conversely, tumor cell intravasation is decreased when pericyte coverage of blood vessels is high within the TME [125].

Cancer cells actively disrupt tumor blood vessel cell interactions in order to facilitate the intravasation process. For example, breast cancer cells express MMP17 which disturbs blood vessel integrity, leading to enhanced tumor cell migration and intravasation [126, 127] Malignant cells also secrete TGFβ1, which causes endothelial junction retraction [128]. Some cancer cells also express Notch receptors that bind to Notch ligands displayed on VECs, assisting their transmigration through the endothelial junctions [129].

In a complementary manner VECs in the TME also express factors that assist cancer cell intravasation. Breast cancer-associated VECs express the enzyme A Disintegrin And Metalloproteinase (ADAM)12 that cleaves vascular endothelial cadherin (VE-cadherin) and TIE2, both of which are also expressed on VECs [130, 131]. VE-cadherin is a component of cell-to-cell adherens junctions that maintains the integrity of the endothelium, hence the ADAM12-induced shedding of this molecule promotes enhanced vascular instability/permeability [131]. TIE2 is the receptor for Ang1 and Ang1/TIE2 ligation is important for pericyte recruitment to nascent blood vessels. ADAM12-mediated disruption of this interaction contributes to vessel destabilization, which is a prerequisite for cancer cell intravasation [130].

1.1.3.6 The tumor-associated vasculature promotes cancer stemness

Although the existence of cancer stem cells (CSC) remains a subject of active debate, some research suggests that within a tumor mass, a minority of cells retain the ability to give rise to all cell types found in the heterogeneous tumor lesion, much like a normal stem cell has the potential to differentiate into many different types of cells. CSCs usually localize in certain specialized areas in the TME. These niches, composed of cells and matrix components, promote the maintenance of CSCs via direct cell contacts and secreted factors [132]. In HNSCC and glioblastoma, such CSC niches are commonly located in close proximity to tumor blood vessels, defining a perivascular niche [133, 134]. In these cancers, tumor-associated VECs appear directly involved in the maintenance of the CSC population through the release of soluble factors that support CSC self-renewal [135-137].

1.2 TUMOR VASCULATURE REMODELING

Methods to inhibit tumor angiogenesis and to normalize tumor blood vessels for improved immune cell recruitment infiltration and anti-tumor function will ultimately be needed to ensure the optimal success of immunotherapeutic intervention. Anti-angiogenic agents were originally developed to prune the excessive neo-vasculature in tumors in order to cut their supply of nutrients and oxygen, leading to disease regression [138]. This was based on the principle that tumors necessitate the formation of new blood vessels to meet their metabolic requirements, as well as, their need to expel metabolic waste. Indeed, vascular pruning using high concentrations of antiangiogenic drugs, caused tumor growth delay and necrosis. However, this effect was only temporary, and eventually, hypoxia was again increased in the TME leading to renewed tumor angiogenesis via drug-refractory pathways. High doses of antiangiogenic drugs have also been shown to increase tumor invasion and metastasis.

One must also consider that the tumor vasculature is required for the delivery of systemically-delivered anti-cancer drugs into the TME. Excessive vascular pruning using antiangiogenic agents actually impedes the effective delivery of chemotherapeutic drugs and renders radiotherapy ineffective [139, 140].

Hence, instead of using anti-angiogenic therapy to ablate the tumor vasculature, it might be more rational to utilize this approach to instead, normalize it. Optimal doses of anti-angiogenic agents, in fact, prune immature vessel branches and remodel the remaining vessels into more normal architectures. The normalized vasculature is less-tortuous, more-organized and less-leaky. This phenotype potentially alleviates hypoxia and interstitial fluid pressure in the TME and, therefore, could improve chemotherapy delivery into the TME. Furthermore, the normalized vasculature improves the oxygenation of the tumor, which is important for the anti-

cancer action(s) of radiotherapy. Importantly, vascular normalization boosts tumor infiltration by immune effector cells and at the same time recondition the TME to become more pro-inflammatory as a consequence of decreased hypoxia [139, 140]. The normalized vasculature also acts as a barrier that prevents cancer cell shedding and intravasation, conditional steps for subsequent metastasis [141].

1.2.1 TNFα therapy targeting tumor blood vessels

TNFα is a vasoactive inflammatory cytokine that has the ability to activate VECs and, hence, if applied to tumors, can potentiate T cell extravasation and infiltration [142]. TNFα therapeutic effects are dose-dependent and associated with VEC activation, increased vascular permeability, VEC apoptosis and hemorrhagic necrosis. To avoid the pathologic effects of high doses of systemic TNFα, low concentrations of the cytokine must be targeted specifically to the tumor vasculature. To achieve this, a Cys-Asn-Gly-Arg-Cys (NGR) sequence serving as a ligand for the CD13 isoform expressed in tumor neovasculature, was fused with TNFα to develop tumor vascular–targeting version of TNFα [143]. Therapy using TNF-NGR resulted in transiently enhanced tumor blood vessel permeability, and the increased efficiency of chemotherapy drugs delivery into murine tumors, without the development of systemic toxicities usually observed for administration of native TNFα. Low doses of NGR-TNF also activated the endothelium as evidenced by VEC upregulated expression of VCAM-1 and ICAM-2, and by VEC release of MCP-1/CCL-2, MCP-3/CCL-7, MIP-2, oncostatin-M and stem cell factor (SCF), factors that serve to attract and activate T cells. This TNF-based therapy also resulted in the loosening of VE-cadherin in the adherens junctions of VECs such that it favors T cell extravasation. Furthermore, this regimen led to reduced hypoxia in the TME, alleviating the

immunosuppressive environment and supporting TIL proliferation and survival. When applied with cancer vaccines and adoptive cell transfer (ACT), TNF-NGR enhances the efficacy of these immunotherapeutic modalities in the absence of significant toxicity [144]. Moreover, in phase II trials in relapsed patients with ovarian cancer, the combination of NGR-TNF and doxorubicin improved progression-free survival and overall survival [145].

1.2.2 Metronomic chemotherapy targeting tumor blood vessels

Most chemotherapeutic agents damage the DNA or inhibit microtubule formation in order to selectively kill rapidly dividing cells, which includes neo-angiogenic endothelial cells. Conventionally, chemotherapeutic drugs are administered at the maximum tolerated dose (MTD) in single doses or short courses followed by prolonged breaks between each therapeutic cycle [146] The two- to three-week break between cycles is necessary to allow the patient to recuperate from adverse drug reactions but it also affords the tumor endothelial cells time to recover and to reestablish pro-angiogenic programming [147].

Metronomic chemotherapy, on the other hand, involves the administration of low doses of chemotherapeutic agents on a frequent or continuous schedule with no drug-free break periods. Metronomic chemotherapy has been shown to have anti-angiogenic effects *in vivo*. It selectively prevents the proliferation and migration of endothelial cells, while blocking their apoptosis. Metronomic chemotherapy also leads to production of thrombospondin-1 (an anti-angiogenic factor) and reduces the content of bone marrow-derived endothelial cell precursors within the treated TME [147].

Metronomic chemotherapy has also been reported to exert immunomodulatory effects that favor anti-tumor response. Several pre-clinical and clinical studies have shown that

metronomic chemotherapy reduces Treg populations and suppresses Treg function. Such interventions have been shown to coordinately improve lymphocyte proliferation and memory T cell expansion [147, 148].

In clinical trials, metronomic chemotherapy when applied as a single modality or in combination with other anti-cancer therapies has demonstrated clinical benefits in patients with advanced breast cancer, recurrent ovarian cancer, hormone-resistant prostate cancer, advanced multiple myeloma, recurrent non-Hodgkins lymphoma, recurrent malignant glioma and glioblastoma, metastatic or locally advanced neuroendocrine carcinoma, among others. Response to metronomic chemotherapy was observed to last for several months and was associated with increased patient overall survival and with progression free-survival [148]. Furthermore, the vascular normalizing and immunomodulatory effects of metronomic chemotherapy make it a potential adjuvant for immunotherapy-based approaches. Indeed, metronomic cyclophosphamide therapy in combination with prophylactic gene-based vaccine targeting mel3 has been reported to inhibit B16.mel3 tumor growth in mice when compared to monotherapy with cyclophosphamide or vaccination [149]. However, several clinical studies have suggested that metronomic chemotherapy does not significantly improve anti-tumor efficacy of immunotherapy, although a trend has been reported for improved overall survival and even increased antigen-specific $CD8^+$ T cell responses in some cases [150].

Metronomic chemotherapy is generally well-tolerated and, thus, has the potential to improve quality of life with minimal toxicity. However, prolonged metronomic chemotherapy can lead to the accumulation of anti-cancer drugs and to the subsequent development of secondary diseases [151]. Furthermore, resistance to metronomic chemotherapy could develop

through reduced vascular dependence, in which resistant tumor cells grow in hypoxic and malnourished environments without the formation of a neovasculature [147].

1.2.3 Anti-VEGF therapies targeting tumor blood vessels

VEGF is an important driver of angiogenesis and is overexpressed in the TME of many forms of cancer. Hence, targeting VEGF has been the focus of numerous studies designed to inhibit tumor angiogenesis (**Figure 5**). To date, two anti-VEGF agents have been approved by the US Food and Drug Administration (FDA) for use as anti-angiogenic therapies for cancer: bevacizumab (Avastin, Genetech), which is a humanized anti-VEGF-A monoclonal antibody [152] and aflibercept (Zaltrap, VEGF-Trap, Regeneron and Sanofi Aventis), which is a recombinant fusion protein consisting of the extracellular domains of VEGFR1 and VEGFR2 and the Fc portion of human IgG [153]. Both bevacizumab and aflibercept bind VEGF and prevent its binding to VEGFR. Treatment with these anti-VEGF agents inhibits VEC proliferation, reduces vessel permeability, lowers tumor blood vessel density, and inhibits tumor growth [154-157].

In pre-clinical studies, anti-VEGF treatment pruned immature tumor vessel branches, with the surviving vessels exhibiting a normalized phenotype and the TME displaying enhanced blood flow/perfusion and reduced hypoxia. However, vascular normalization and, therefore, clinical benefit with anti-VEGF treatments is only transient, with treatment-refractory disease rapidly developing in most cases. Hence, anti-VEGF therapy is typically administered in combination with chemotherapy to effect greater rates of (somewhat more durable) clinical response [158, 159].

Bevacizumab, in combination with chemotherapy, has been approved as a first- or second-line treatment for metastatic colorectal cancer, non-small cell lung cancer (NSCLC), and

metastatic renal cell carcinoma and, as a single-agent, second-line treatment option for patients with recurrent glioblastoma [160]. Aflibercept, also used in combination with chemotherapy, has been approved as a second-line treatment for metastatic colorectal carcinoma [153].

1.2.4 Tyrosine Kinase Inhibitors

VEGF, FGF, PDGF, and other angiogenic factors signal through specific receptor tyrosine kinases (RTKs). In general, RTKs consist of an extracellular ligand-binding region, a transmembrane helix, and a cytoplasmic tyrosine kinase domain. Activation of pro-angiogenic pathway begins with the binding of an angiogenic factor to its cognate RTK and the dimerization/oligomerization of the receptor. Assembly of the RTK complex induces a receptor molecule to phosphorylate one or more tyrosines in the adjacent receptor. The phosphorylated receptor then serves as a docking and activation site for other signaling proteins [161]. Tyrosine kinase inhibitors (TKIs) are small molecules that inhibit downstream signaling of RTKs by competing with ATP binding to the catalytic domain of tyrosine kinase [162].

Several TKIs targeting angiogenesis-related RTKs have been developed as anti-cancer treatment (**Figure 5**). Sunitinib (SU11248, Sutent, Pfizer), sorafenib (BAY43-9006, Nexavar, Bayer, Inc.), pazopanib (GW786034, Votrient, GlaxoSmithKline), and axitinib (Inlyta, AG-013736, Pfizer) target VEGFRs and some of these TKIs also bind PDGFRs, stem cell factor receptor (c-Kit), Flt3 and other RTKs [163-166]. *In vitro* assays using human umbilical vein endothelial cells (HUVECs) demonstrated that sunitinib, sorafenib, pazopanib and axitinib inhibit downstream VEGFR signaling, leading to decreased proliferation, survival, migration and capillary tube formation of HUVECs [167-170]. *In vivo*, these TKIs normalize the tumor-associated vasculature by suppressing angiogenesis and decreasing microvessel density. The

anti-angiogenic effects of these TKIs have been associated with tumor growth inhibition in a range of murine xenograft models [164, 168, 171-173].

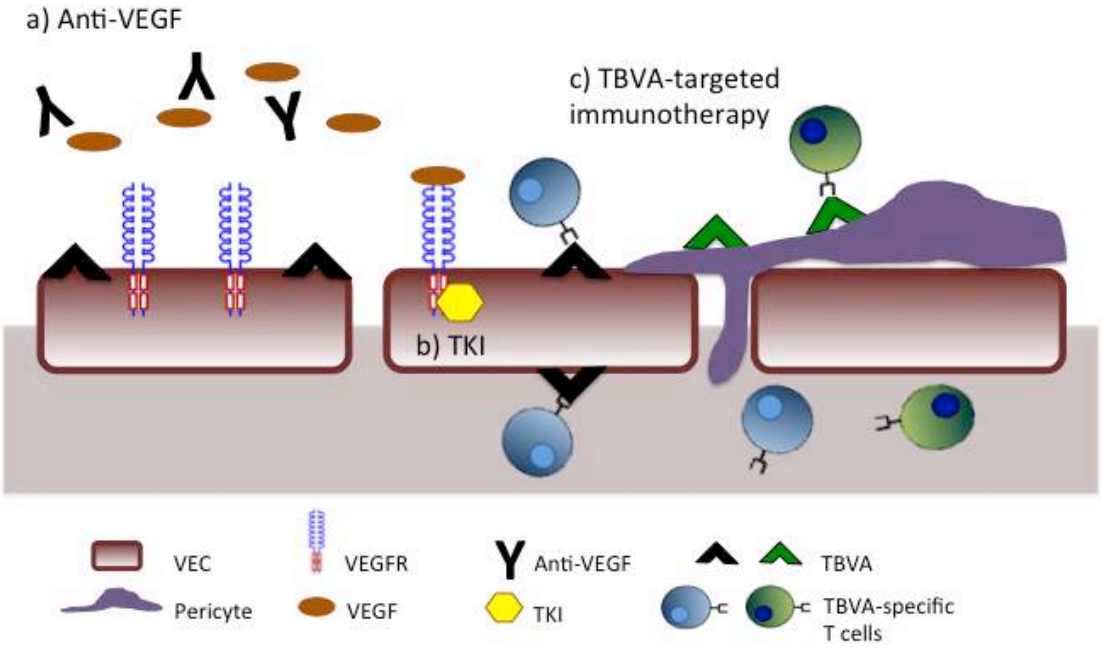

Figure 5. Therapies targeting the tumor vasculature.

a) Anti-VEGF therapies such as monoclonal antibodies and recombinant fusion proteins sequester the angiogenic factor VEGF. b) TKIs block downstream receptor signaling of an array of angiogenic pathways. c) TBVA-targeted immunotherapies promote TBVA-specific T cells that eliminate abnormal blood vessel cells and promote vascular normalization. When applied in combination with other anti-cancer modalities, tumor blood vessel-targeting therapies have been shown to improve delivery and efficacy of chemotherapy and cancer vaccines.

Although developed as an anti-angiogenic drug, several pre-clinical studies have shown that sunitinib also has the capacity to reverse immune dysfunction in the TME. In MCA-26 colon and LLC1-Lewis lung carcinomas, treatment with sunitinib led to a reduction in immunosuppressive MDSCs and Tregs, while coordinately promoting $CD8^+$ and $CD4^+$ effector T cell infiltration into the TME. Type-2 immune responses were also blocked as suggested by the decrease in expression of IL-10 and TGFβ. Furthermore, sunitinib treatment decreased PD-L1

expression on MDSCs and DCs, and CTLA-4 and PD-1 expression in $CD8^+$ and $CD4^+$ T cells [174]. Similarly, sunitinib treatment also restored normal T cell function and suppressed MDSCs in the spleens of mice bearing B16, RENCA, CT26 and 4T1 tumors [175, 176]. Clinical results for sunitinib have provided concordant results. After one cycle of sunitinib treatment, the number of IFN−γ−producing (type-1) T cells increased, while IL-4-producing type-2 T cells were reduced in patients with renal cell carcinoma (RCC; [177]). Although no significant reduction in Treg cell frequency was observed in patient peripheral blood, there was an inverse correlation noted between increased type-1 T cell responses and decreased Treg levels in PBMC after sunitinib treatment. On the other hand, others have reported that sunitinib might have a negative impact on immune cells numbers/function. Sunitinib has been shown to inhibit T cell proliferation and to down-regulate expression of the activation markers CD25 and CD69 on *in vitro* (mitogen)-activated T cells isolated from healthy volunteers and cancer patients [178]. High doses of sunitinib have also been reported to block IL-12 production from DCs matured *in vitro* with IFN-α, TNF-α and poly I:C [179]. These data suggest that the dose and schedule of TKIs, such as sunitinib, must be carefully regulated based on possible (high-dose, chronic) immune-toxicities.

Anti-angiogenic TKIs have been FDA-approved as first-line or second-line treatment for different malignancies. Sunitinib is currently being administered as first-line therapy for patients with RCC and unresectable pancreatic neuroendocrine tumors (PNET). It is also approved as second-line therapy for patients with gastrointestinal stromal tumors (GIST) [180, 181]. Sunitinib is effective in inducing objective clinical responses patients with small cell lung carcinoma (SCLC), breast cancer, thyroid cancer and chondrosarcoma [180]. Sorafenib has been

approved as a therapeutic agent for advanced RCC, unresectable HCC, and recurrent or metastatic differentiated thyroid carcinoma [182, 183]. Pazopanib, on the other hand, has been approved for the treatment of patients with RCC or soft tissue sarcoma after standard-of-care chemotherapy [184, 185]. Axitinib has been approved as a second-line treatment option for patients with RCC [163].

1.2.5 Tumor Blood Vessel-Associated Antigens (TBVA)-Targeted Vaccines

The FDA approval of the first therapeutic cancer vaccine, sipuleucel-T (Provenge, Dendreon), has confirmed that antigen-specific vaccines can elicit the immune system to attack tumor cells in the clinical setting [186]. Sipuleucel-T is a treatment option for castration-resistant prostate cancer, targeting prostate acid phosphatase expressed on cancer cells. Tumor blood vessel cells are also attractive targets for active, specific immunotherapy, and hypothetically, have several advantages over cancer cells as targets. Cellular stressors in the TME cause unique epigenetic programing, resulting in unique phenotypes that allow for differential recognition of tumor stromal cells, including VECs and pericytes, from their normal counterparts by the adaptive immune response [30, 187, 188]. These tumor blood vessel-associated (TBVA) antigens may be targeted immunologically via active, specific vaccination to promote the activation of T effector cells that can selectively target abnormal tumor blood vessel cells, leading to the potential normalization of the tumor-associated vasculature (**Figure 5**). VECs and pericytes are also strategically more visible to immune surveillance being highly-accessible to circulating immune effector cells in the blood. Lastly, VECs and pericytes are more genetically stable than tumor cells and, hence, less prone to adaptive mechanisms associated with immune escape.

Early TBVA-based vaccines targeted VEGFRs, which are highly expressed on the surface of tumor VECs in the neovasculature. In murine tumor models, peptide-based and gene-based VEGFR1- and VEGFR2-targeted vaccines elicited antigen-specific $CD8^+$ T cell responses in association with inhibited tumor angiogenesis and slowed disease progression [189-191]. The success of VEGFR-targeted vaccines in pre-clinical models drove the development of elpamotide, a vaccine against human VEGFR2 containing the HLA-A24-presented peptide epitope RFVPDGNRI [191, 192]. Phase I trials of elpamotide (as a single agent or in combination with other peptide vaccines and/or chemotherapy) demonstrated safety of the treatment and, to some degree, the ability of the approach to induce T cell immune responses associated with reduced angiogenesis in patients with pancreatic cancer, colorectal cancer or NSCLC [193-196]. However, in a Phase II/III clinical trial, elpamotide when used in combination with the chemotherapeutic agent gemcitabine, did not improve the overall survival of patients with advanced-stage pancreatic cancer [192].

Other TBVA that may not be directly involved in angiogenic pathways may also be targeted for use in tumor immunotherapies. Vaccination of HLA-A2 (HHD) transgenic mice bearing HLA-$A2^{neg}$ B16 melanoma or MC38 colon carcinoma with dendritic-based (DC1)-based vaccines incorporating HLA-A2-restricted peptide epitopes derived from TBVAs such as delta-like homologue 1 (DLK1), EphA2, hemoglobin-β (HBB), NG2, NRP-1, PDGFRβ, RGS5 and TEM1 were shown to be effective in providing protective and therapeutic anti-tumor immunity [197]. The vaccination strategy resulted in tumor infiltration by $CD8^+$ T cells that differentially recognized tumor VECs and/or pericytes, in association with a reduction in blood vessel density in the TME. Gene-based vaccination against TEM1 (aka CD248) has also been used as a prophylactic or therapeutic strategy against CT26 (colon), TC1 (cervical), and LLC (lung)

carcinomas, with the vaccine resulting in $CD3^+$ T cell-dependent tumor growth inhibition. These results suggest that TBVA-targeted vaccination can lead to vascular normalization within the TME as a prelude to the more effective delivery of chemotherapeutic agents and ACT in combination treatment approaches.

1.2.6 Chimeric Antigen Receptor (CAR) T cells

CAR T cells are genetically-engineered to express antigen-specific receptors that combine antibody-like recognition and T cell receptor activating functions [198]. CARs are composed of antigen-binding region, usually single-chain variable fragments from monoclonal antibodies, a transmembrane domain and an endodomain derived from the CD3 zeta co-receptor.

Recent clinical studies on CAR T cells, the majority of which were designed to treat B cell malignancies, suggest great promise in the clinic [199]. Thus far, however, CAR T cells have displayed only limited effectiveness in solid tumors due to their inability to actively migrate and extravasate into the TME. As a consequence, TBVA-targeting CAR T cells are being developed to circumvent the need for penetration into the TME (or to potentially improve co-transferred anti-tumor CAR T cells based on vascular normalization mechanisms). CAR T cells engineered to target echistatin, which binds to the $\alpha_v\beta_3$ integrin expressed on tumor VECs, have been shown to lyse αvβ3 $integrin^+$ HUVECs *in vitro* [200]. Treatment of tumor-bearing mice with echistatin-reactive CAR T cells led to the destruction of tumor blood vessels and inhibition of tumor growth. Adoptive transfer of VEGFR-2 CAR T cells co-transduced with cDNA encoding IL-12p70 has also demonstrated anti-tumor efficacy in tumor-bearing mice and prolonged overall survival [201]. Interestingly, this approach also resulted in a treatment-associated reduction in tumor-associated MDSC (as previously observed for the anti-angiogenic

action of TKI as described above). Despite such promising pre-clinical results, TBVA-targeted CAR T cells have yet to be administered to cancer patients in the clinical setting.

1.2.7 Combination therapy: vascular normalizing agents and immunotherapy

Improved understanding of the complexities of cancer heterogeneity, genetics and oncogenic signaling pathways associated with acquired resistance to single modality therapies has reinforced the need to develop combination/multi-modality immunotherapies in order to reproducibly achieve durable objective clinical responses in the cancer setting. As single modality approaches (cancer vaccines, immune checkpoint inhibitors, ACT, among others) have each demonstrated promising (sustained) therapeutic benefits in a minority of treated patients [202, 203]. Cancer vaccines are effective in eliciting anti-tumor immune response but one of the main limitations is the inefficient delivery of vaccine-induced T cells into the tumor lesion [204]. A number of studies have suggested that anti-angiogenic agents may be largely immune-dependent in their anti-tumor action, with many suggesting their use as adjuvants for integration into cancer vaccine formulations. Anti-angiogenic agents normalize the vasculature, increase blood perfusion and improve delivery of chemotherapeutic drugs and immune effector cells in the tumor bed [205]. In addition, some anti-angiogenic agents also have the capacity to reduce hypoxia and immunosuppressive MDSC and T cell populations and to promote the upregulation of vascular adhesion molecules and chemokines that enhance T cell recruitment into the TME [204, 206]. Indeed, in murine melanoma models, specific vaccination combined with systemic delivery of TKIs axitinib, sunitinib or dasatinib has resulted in superior therapeutic benefit when compared to either vaccination alone or TKI treatment alone. Concurrent administration of a DC/peptide vaccine and TKI improved the overall survival of M05 melanoma-bearing mice and

was associated with the upregulated expression of VCAM-1 and CXC-motif chemokine receptor (CXCR)3 ligand chemokines in the tumor endothelium and robust type-1 T cell infiltration in the TME [175, 206, 207]. In another study, treatment of MC38 colon carcinoma-bearing mice with the combination of sunitinib pre-conditioning followed by a CEA gene-based vaccine was used treat mice, resulting in increased tumor infiltration by CEA-specific $CD8^+$ T cells, decreased Treg and MDSC populations, reduced tumor volumes and prolonged survival [208]. Simultaneous administration of sunitinib and the vaccine, or administration of vaccine prior to sunitinib, however, did not did not result in improved survival [208, 209]. In a phase III clinical trial, the combination of a poxvirus-based vaccine encoding the tumor antigen 5T4 (TroVax) followed by administration of sunitinib was evaluated in renal cancer patients, with no benefit for the combined protocol versus sunitinib monotherapy observed [210]. These translational and clinical data strongly suggest that treatment schedule is likely critical to the success of such combination therapies. The temporal interval wherein the anti-angiogenic agents (TKIs, TBVA-based vaccines, others) normalize the tumor vasculature and decrease immunosuppressive cell populations in the TME in advance of the arrival of vaccine-induced or ACT anti-tumor T cells must be determined in order to optimize the clinical benefits of such combination vaccines. This is further complicated by the effective window during which the adjuvant qualities of anti-angiogenic inhibitors impact the TME, in the absence of off-target toxicities (including some manifest in immune cell populations). Hence, biomarkers to predict the efficacy of anti-angiogenic drugs (i.e. increased systemic levels of CXCR3 ligand chemokines, reduced levels of CXCL12, etc.) or techniques to monitor blood perfusion in patients in a non-invasive manner must be developed to define an optimal combination schedule based on vascular normalization criteria [140, 211, 212].

1.3 NOTCH

1.3.1 Notch signaling and cancer

The Notch signaling pathway is a highly evolutionarily conserved pathway that is involved in a myriad of cellular functions in invertebrates and vertebrates. During embryonic development, Notch signaling is vital in the maintenance of stem cell populations, determination of cell fate decision, and the regulation of proliferation and apoptosis. It is also associated with postnatal hematopoiesis, neural stem cell survival, immune regulation, and vascular development [213]. In mammalian systems, there are four known Notch receptors (Notch1, Notch2, Notch3, and Notch4) that contain 29-36 EGF repeats, of which EGF repeats 11-12 are essential for ligand binding and EGF repeat 8 dictates ligand specificity. Canonical Notch ligands (Jagged1, Jagged2, Dll1, Dll3, and Dll4) contain an amino-terminal Notch ligand motif, which (except for Dll3) is followed by a DSL (Delta-Serrate, LAG-2) protein domain and a DOS (Delta and OSM-11) domain [214]. Archetypally, Notch signaling involves two distinct adjacent cells – the signal-sending cell, which presents the ligand and the signal-receiving cell, which express the Notch receptor. The pathway is activated when the DSL domain of the ligand physically interacts with the EGF repeats of the Notch receptor on a neighboring cell (**Figure 6**). This interaction leads to the sequential cleavage of the Notch receptor: first, at the extracellular juxtamembrane region by (ADAM)10/17 metalloproteases and then within the intramembrane region by γ-secretase. The concerted catalytic action of ADAM10/17 and γ-secretase results in the release of the Notch intracellular domain (NICD), which then translocates into the nucleus where it associates with the DNA-binding transcription factor CSL (CBF-1, Su(H), LAG-1) and the transcriptional coactivator Mastermind. Targets of this transcription complex include the

HEY and HES transcription repressors and MYC transcription factor. The pathway is shut off when the NICD is degraded by the proteasome after its phosphorylation and (poly)ubiquitination [215-217].

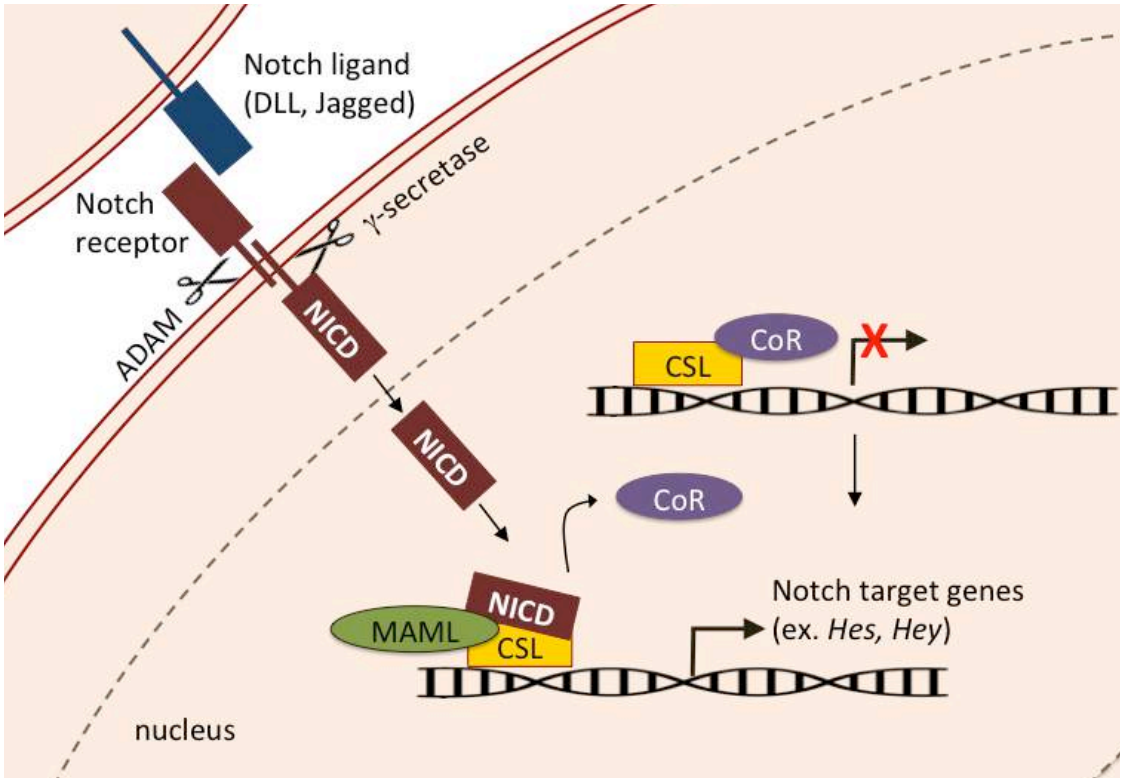

Figure 6. The Notch signaling pathway.

The Notch receptors (Notch 1-4) consist of an extracellular domain composed of multiple EGF-like repeats and an intracellular domain (NICD) that mediates downstream signaling. Upon binding of the extracellular domain to ligands (DLL and Jagged families), the Notch receptor is cleaved by ADAM and g-secretase. This proteolytic event releases the NICD, which subsequently translocates to the nucleus and binds to the transcription factor CSL. The NICD-CSL binding results in the dislocation of co-repressors (CoR) and recruitment of co-activators such as Mastermind (MAML). The heterocomplex then stimulates the transcription of Notch target genes such as members of the HES and HEY families.

The Notch signaling pathway has been implicated in a wide range of human diseases [218, 219]. The involvement of Notch signaling in cancer was first described in T cell acute lymphoblastic leukemia (T-ALL), where it acts as an oncogene that mediates the proliferation, growth, metabolism, and survival of T-ALL cells [220]. Since then, the tumor-promoting effects of Notch have been demonstrated in solid tumors such as breast cancer, colorectal cancer, non-small cell lung carcinoma, medulloblastoma, and melanoma [221, 222], where aside from supporting the proliferation and survival of the tumor cells, Notch signaling also facilitates the invasion and migration of tumor cells [223] and the maintenance, and function of cancer stem cells [224].

Although Notch activation can be oncogenic, a growing body of evidence also shows that components of the Notch signaling pathway have tumor suppressive functions as well. In the skin, Notch activation induces differentiation and cell cycle arrest while the loss of *NOTCH1* results in increased cell proliferation in the basal epidermal layer, spontaneous basal cell carcinomas, and sensitization to chemically-induced skin carcinogenesis [225, 226]. Data also suggests that Notch activation suppresses tumorigenesis by inhibiting the Wnt and Sonic-hedgehog signaling pathways [226]. This suggests that a crosstalk between Notch and other signaling pathways contributes to tumor inhibition in the skin. The Notch pathway has also been reported to act as a tumor suppressor in small cell lung cancer, chronic myelomonocytic leukemia, head and neck squamous cell carcinoma, gastrointestinal stromal cancer, endometrial cancer, and B cell malignancies [221, 222, 227, 228].

As described briefly earlier, Notch1-DLL4 signaling regulates angiogenesis and plays a vital role in the formation of an intact, functionally-mature vasculature under normal physiological conditions [20]. In tumors, DLL4 blockade results in the formation of a highly-

branched vasculature that is dysfunctional [229, 230], however, there is also evidence suggesting that incomplete inhibition of Notch1-DLL4 signaling supports functional angiogenesis [231]. DLL4 inhibition leads to reduced tumor growth in certain models [229, 230] while prolonged DLL4 blockade also results in severe toxicities and the development of vascular tumors [232, 233]. Overall, these data indicate a delicate balance of Notch signaling in the various cell populations within the TME determines pro- versus anti- angiogenic behavior in vivo.

The pleiotropic role of Notch signaling in diverse biological processes transmutes to its dual nature in cancer. In fact, in some cancer types such as pancreatic cancer, prostate cancer, and hepatocellular carcinoma, Notch can act as an oncogene or a tumor suppressor, depending on the cell type expressing the receptor, the strength of the signal or and/or the stage of the disease [234-236]. Hence, further investigation will be required to understand the contrasting roles of Notch activation within the TME in order to enable targeted interventions capable of rendering objective clinical responses in the cancer setting.

1.3.2 DLK1 and DLK2

Delta-like homolog 1 (DLK1, also known as Pref-1, FA-1 and pG2) is a protein that belongs to the EGF-like superfamily of proteins. The membrane-bound form of DLK1 contains six EGF-like repeats, a tumor necrosis factor-a converting enzyme (TACE)-mediated cleavage site, a single transmembrane domain, and a cytoplasmic tail. [237]. The soluble form of DLK1 is released when ADAM17, a TACE, cleaves the protein [238]. Mammalian DLK1 resembles the structure of EGF-like repeats found in invertebrate homeotic proteins (such as Delta, Serrate, Notch and Lin-12) more closely than the mammalian EGF-like structures [237, 239]. However,

DLK1 lacks the DSL domain that is present at the N-terminus of canonical Notch ligands. Despite the absence of the DSL domain, DLK1 interacts with Notch1 and serves as an antagonist to DLL4- and Jagged1-mediated activation of Notch signaling [240, 241].

DLK1 was first identified in the amniotic fluid (hence the alternative name fetal antigen-1 or FA-1) and since then has been shown to be expressed in different embryonic tissues such as the pituitary gland, the adrenal gland, the mesenchymal regions of the developing vertebra, the tongue, the lung, and adipose tissues [237, 239, 242]. Differentiated adult tissues typically do not express DLK1 except in the case of some cells of the pancreas, testes, prostrate, and the ovaries. In some disease models, dysregulated overexpression of DLK1 is associated with the malignant transformation of adipocytes, cancer stemness maintenance in neuroblastomas and hepatocarcinomas, cell proliferation and migration in gliomas, and the faulty myogenic differentiation of mesenchymal cells in nephroblastoma (Wilm's tumor) [243-248]. Conversely, exogenous expression of DLK1 in CAFs reduces tumor growth in a prostate cancer model [249].

Even with the widespread expression of DLK1 during embryogenesis, *Dlk1* knockout mice manifest only mildly abnormal phenotype (growth retardation and abnormalities in the adipose tissue) and are able to reach adulthood and to reproduce [250], suggesting that another gene or set of genes are able to compensate for the absence of *Dlk1*. Another protein, DLK2 (also known as EGFL9) that participates in adipogenesis has recently been reported to be highly homologous to DLK1 [251, 252]. DLK2 contains six EGF-like repeats, a transmembrane domain, and an intracellular region, which includes four putative SH3-binding sites that are absent in DLK1. Like DLK1, DLK2 acts as an inhibitor of Notch signaling and there is some evidence to suggest that these two proteins modulate each other's expression. The role of DLK2

in cancer is largely unknown, with a single report suggesting the pro-oncogenic potential of overexpressed DLK1/2 proteins in SK-MEL2 melanoma cells [253].

1.4 STATEMENT OF THE PROBLEM

In the absence of neovascularization, tumors cannot exceed a certain size or metastasize to distal organs. At the same time, however, without an efficient (normalized) blood vessel network, delivery of anti-cancer agents and therapy-induced or -administered immune effector cells fails to occur. Hence, preventing abnormal angiogenesis while at the same remodeling the tumor vasculature to a more normal state is essential to the clinical success of a broad range of cancer treatments and immunotherapies. However, existing strategies designed to normalize the tumor-associated vasculature, such as those that utilize pharmacologic chemotherapeutic agents, are only transiently effective, with drug-refractory disease inevitably developing. Therefore, alternative therapies targeting the dysfunctional tumor blood vasculature and capable of rendering a sustained state of vascular normalization are being actively pursued.

This thesis describes the generation and assessment of therapeutic vaccines designed to target neoantigens expressed by tumor-associated pericytes, specifically the Notch antagonists DLK1 and DLK2. My findings suggest that vaccination against DLK1/DLK2 results in the activation of antigen-specific $CD8^+$ T effector cells and to tumor vascular normalization, the recruitment of therapeutic immune cells into the TME, and to inhibition of tumor progression.. Furthermore, the anti-tumor efficacy of DLK1/DLK2-targeted vaccines may be improved by combination with current standard of care agents, such as anti-PD-L1. Overall, the results presented in this thesis provide a proof-of-principle that tumor blood vessel-associated antigens can targeted with immunotherapeutic interventions that may ultimately prove clinically-effective against a broad range of solid cancers.

2.0 DLK1: A NOVEL TARGET FOR IMMUNOTHERAPEUTIC REMODELING OF THE TUMOR BLOOD VASCULATURE

Nina Chi Sabins[1], Jennifer L. Taylor[2], Kellsye P. L. Fabian[1], Leonard J. Appleman[3,6], Jodi Maranchie[4,6], Donna Beer Stolz[5], and Walter J. Storkus[1,2,6]

From the Departments of [1]Immunology, [2]Dermatology, [3]Medicine, [4]Urology, and [5]Cell Biology, University of Pittsburgh School of Medicine, Pittsburgh, PA 15213, and the [6]University of Pittsburgh Cancer Institute, Pittsburgh, PA 15213.

These data have been reported in *Molecular Therapy* 2013 21(10): 1958–1968. *Kellsye Fabian* performed the DLK1 immunofluorescence microscopy on human samples and assisted in the DAPT experiment. All authors contributed to the scientific discussion and constructive comments used in developing this manuscript.

2.1 ABSTRACT

Tumor blood vessels are frequently inefficient in their design and function, leading to high interstitial fluid pressure, hypoxia, and acidosis in the TME, rendering tumors refractory to the delivery of chemotherapeutic agents and immune effector cells. Here we identified the Notch antagonist delta-like 1 homolog (DLK1) as a vascular pericyte-associated antigen expressed in RCC, but not in normal kidney tissues in mice and humans. Vaccination of mice bearing established RCC against DLK1 led to immune-mediated elimination of $DLK1^+$ pericytes and to blood vessel normalization (*i.e.,* decreased vascular permeability and intra-tumoral hypoxia) in the TME, in association with tumor growth suppression. After therapeutic vaccination, tumors displayed increased prevalence of activated $VCAM1^+CD31^+$ VECs and CXCL10, a Type-1 T cell recruiting chemokine, in concert with increased levels of Type-1 CD8+ TIL. Vaccination against DLK1 also yielded; i.) dramatic reductions in $Jarid1B^+$, $CD133^+$ and $CD44^+$ (hypoxia-responsive) stromal cell populations, ii.) enhanced tumor cell apoptosis and iii.) increased Notch signaling in the TME. Co-administration of a γ-secretase inhibitor that interferes with canonical Notch signaling resulted in the partial loss of therapeutic benefits associated with DLK1-based vaccination.

2.2 INTRODUCTION

The vasculature of solid tumors is structurally and functionally "abnormal", being composed of an irregular network of blood vessels characterized by aberrant coverage of endothelial tubes and a loosely-attached, largely immature population of mural cells (i.e. smooth muscle cells, pericytes) [25, 122]. In contrast to mature pericyte-VEC interactions found in normal tissues that orchestrates blood vessel integrity/stability [254], in tumors, this relationship is deranged leading to a high-degree of vascular permeability, high interstitial fluid pressure, hypoxia and acidosis [255].

RCC is highly-vascularized and generally considered to represent an immunogenic form of cancer [256-258]. Current treatment options mediate only transient efficacy in a minority of RCC patients, with frequent development of progressive disease that is refractory to conventional chemo-/radio-therapy [259-262]. Vaccines targeting tumor-associated antigens have also thus far demonstrated only modest curative value [202]. The limited perfusion of tumor blood vessels likely contributes to the muted benefits of these treatment approaches by preventing the efficient delivery of chemotherapeutic agents and anti-tumor T cells into the TME [197, 263]. As a consequence, the development of novel therapies that can "normalize" the tumor vasculature (by coordinately improving blood vessel perfusion, reducing tumor hypoxia, and allowing for improved and sustained delivery of anti-cancer agents into the TME) remains a high-priority [139, 197, 264-266].

To achieve the goal of tumor vascular normalization via immunization, we and others have recently advocated the use of vaccine formulations capable of promoting specific Type-1 $CD8^+$ T cell (aka Tc1) recognition of tumor-associated vascular cell antigens [197, 263, 266]. DLK1 is a member of the EGF-like family of proteins which includes Notch receptors and their

ligands [242, 243, 267] and serves as a functional inhibitor of Notch signaling. DLK1 has been reported to inhibit a broad range of Notch-dependent cell differentiation pathways [242]. In the cancer setting, the functional impact of DLK1 modulation cannot be intuitively assumed, since Notch activation has been reported to either promote or suppress tumor development/progression based on the contextual influences of DLK1 on the myriad cell populations located within the evolving TME [242, 243, 267].

In this chapter, we investigated the therapeutic impact of active vaccination against DLK1 in a murine model of RCC (*i.e.,* RENCA tumor cells transplanted s.c. into syngenic BALB/c mice), where the DLK1 antigen is preferentially expressed by blood vessel-associated pericytes in the progressively-growing TME. We show that DLK1 peptide- or gene-based vaccines are both immunogenic and therapeutic against established RCC, with treatment benefits linked to $CD8^+$ T cell-mediated "normalization" of tumor-associated blood vessels (*i.e.,* reduction in blood vessel numbers and extent of arborization, loss of hypoxia and reduced vascular permeability) (98, 182). Responder tumors were highly-infiltrated by $CD8^+$ TIL that localized within the perivascular (pericyte-enriched) space. Residual pericytes lacked expression of DLK1 and were tightly-approximated to $CD31^+$ VEC. Consistent with the vaccine-induced, immune-mediated eradication of tumor-associated DLK1 protein expression, increased Notch signaling was evidenced within the therapeutic TME. These results are consistent with the ability of DLK1-based vaccines to promote therapeutic $CD8^+$ T cell-dependent vascular normalization in the RCC microenvironment, supporting the clinical translation of such approaches in the setting of RCC and other forms of solid cancer.

2.3 MATERIALS AND METHODS

2.3.1 Mice

Female 6-8 week old BALB/c mice (The Jackson Laboratory, Bar Harbor, ME) were maintained in a pathogen-free animal facility, with all animal work performed in accordance with an IACUC-approved protocol.

2.3.2 Tumor cells

The mouse RCC line RENCA derived from a spontaneous renal cortical adenocarcinoma in BALB/cCr mice (CRL-2947; American Type Culture Collection, Manassas, VA) [268] was cultured as previously reported [266].

2.3.3 Stromal cell isolation

Human RCC tumor and adjacent (patient-matched) normal kidney specimens were obtained with written-consent under an IRB-approved protocol. Murine RCC tumors and tumor-uninvolved kidneys were harvested 21 days after s.c. injection of 106 RENCA cells into syngenic BALB/c recipient animals. VEC and pericytes were isolated as previously mentioned in Chapters 2 and 3 with minor modifications [269]. Briefly, tissues were enzymaticaly digested into a single cell suspensions and, for human specimens, labeled with anti- human CD146 FITC (Serotec), anti-human CD34 PE (DAKO), anti-human CD56 PE-Cy7 (Serotec), anti-human CD45 APC (BD-Biosciences) and for murine specimens, labeled with anti-mouse CD34-FITC (eBioscience, San

Diego, CA), anti-mouse CD146-PE (BD-Biosciences, San Diego, CA), and anti-mouse CD45-APC (BD-Biosciences) prior to flow sorting into pericyte ($CD146^{+}CD34^{neg}CD56^{neg}CD45^{neg}$) and VEC ($CD146^{+}CD34^{+}CD56^{neg}CD45^{neg}$) populations.

2.3.4 Real-time PCR

Messenger RNA was isolated from pericytes and VEC using the RNeasy® Plus Micro kit (Qiagen, Valencia, CA) according to manufacturer's instructions. cDNA was then generated using High Capacity RNA-to-cDNA kit (Applied Biosystems, Carlsbad, CA) and real-time PCR performed using Fast SYBR® Green Master Mix (Applied Biosystems) with primer pairs for human or mouse HPRT1 (Qiagen), human DLK1 (Applied Biosystems) or mouse DLK1 (forward primer: TGTGACCCCCAGTATGGATT, reverse primer: CCAGGGGCAGTTACACACTT). Reactions were performed in duplicate in a 96-well reaction plate on a StepOnePlus real-time PCR thermocycler (Applied Biosystems) using cycling conditions of 95°C for 20 min., then 35 cycles of 95°C for 3 min. and 60°C for 30 min.

2.3.5 In vitro generation of bone marrow-derived dendritic cells (DC) and DC.IL12

DC were generated from bone marrow precursors isolated from the tibias/femurs of mice using *in vitro* cultures containing 1,000 U/ml recombinant murine granulocyte/macrophage colony-stimulating factor and 1,000 U/ml rmIL-4 (both from Peprotech, Rocky Hill, NJ), as previously described [266]. The Ad.mIL-12p70 recombinant adenoviral vector was produced and provided by the University of Pittsburgh Cancer Institute's Vector Core Facility (a shared resource), as reported previously [266, 270]. Five million (day 5 cultured) DCs were infected at a multiplicity

of infection = 50 with Ad.mIL-12p70 or the control, empty vector Ad.ψ5. While control DC produced <62.5 pg IL-12p70/ml/48 hour/10^6 cells, DC.IL12 cells produced 1–10 ng IL-12p70/ml/48 hour/106 cells.

2.3.6 Synthetic peptides

The H-2^d class I-presented $DLK1_{158-166}$ (CPPGFSGNF; presented by H-$2L^d$), $DLK1_{161-169}$ (GFSGNFCEI; presented by H-$2K^d$), $DLK1_{259-270}$ (TILGVLTSLVVL; containing overlapping $DLK1_{259-267}$ and $DLK1_{262-270}$ sequences presented by H-$2K^d$) peptide were synthesized as previously described [197].

2.3.7 Recombinant lentiviral vector production

Genes encoding mDLK1 and the reverse sequence of mRGS5 (as a negative control) were cloned into the pLenti6/V5 D-TOPO vector downstream of the CMV promoter using the Lentiviral Directional TOPO® Expression Kit (Invitrogen, Grand Island, NY). To determine insert presence in the plasmid, expression of the V5 tag was detected by immunofluorescence using an anti-V5 FITC antibody (Invitrogen) and by western blot using an anti-V5 HRP antibody (Invitrogen). In the initial production of the lentiviruses, 293FT cells (Invitrogen) were transfected with plasmid DNA pLenti-DLK1 (or pLenti-NEG) using ViraPower™ Packaging Mix (Invitrogen) combined with Lipofectamine 2000 (Invitrogen) according to the manufacturer's instructions. After 48 hours, lentivirus was collected and concentrated using a Fast-Trap Virus Purification and Concentration kit (Millipore). Lentiviral (lvDLK1 and lvNEG) titers, reported in transduction units (TU), were determined by quantitating blasticidin

(Invitrogen)-resistance in HT-1080 cells (kindly provided by Dr. Chuanyue Wu, University of Pittsburgh) according to the manufacturer's instructions. Expanded lentiviral production was performed by the University of Pittsburgh Cancer Institute Lentiviral Vector Core Facility. Lentivirus quality was assessed by infecting HT-1080 cells for 24h and monitoring cells for coordinate V5 protein expression (western blot) and cell-surface expression of DLK1 (flow cytometry using an anti-DLK1-PE conjugated antibody; Adipogen, San Diego, CA).

2.3.8 Animal therapy experiments

BALB/c mice received s.c. injection of 10^6 RENCA tumor cells (right flank) on day 0. Six days later, the animals were randomized into cohorts of 5 mice with comparable mean tumor sizes. On days 7 and 14 after tumor implantation, mice were treated with 100 μl s.c. injections (left flank) of PBS, 10^6 DC.IL12 or 10^6 DC.IL12 that had been pre-pulsed for 2h at 37°C with an equimolar (10 μM) mixture of the $DLK1_{158-166}$, $DLK1_{161-169}$ and $DLK1_{259-270}$ peptides. For lentivirus vaccination experiments, randomized BALB/c mice bearing established (day 10; right flank) s.c. RENCA tumors received a single left flank intradermal injection of lvDLK1 or negative control lvNEG at a dose of 4×10^4 or 2×10^5 TU in a total volume of 50 μl PBS. For all animal experiments, tumor size was assessed every 3 to 4 days and recorded in mm^2, as determined by the product of orthogonal measurements taken using vernier calipers. Data are reported as mean tumor area ± SD. To determine the impact of canonical NOTCH signaling on vaccine efficacy, tumor-bearing animals vaccinated with lvDLK1 or lvNEG were injected i.p. with the g-secretase inhibitor DAPT (10 mg/kg/day in 50 ml DMSO (Sigma-Aldrich) on a 3 consecutive days (followed by 4 days without injections) per week schedule, for 2 weeks beginning on day 12 post-tumor inoculation) or vehicle control (DMSO).

2.3.9 Evaluation of specific $CD8^+$ T cell responses in vitro

Spleens were harvested from three mice per group 7 days after the second DC injection. Splenocytes were then stimulated *in vitro* for 5 days with syngenic DC pulsed with an equimolar (10 μmol/l) mix of the three DLK1 peptides applied in the vaccine. Responder $CD8^+$ T cells were then isolated using magnetic bead cell sorting (Miltenyi Biotec, Auburn, CA) and co-cultured with syngenic DC pulsed with individual DLK1 peptides for 72 hours, 37 °C and 5% CO_2, at which time cell-free supernatants were analyzed for mIFN-γ content using a cytokine-specific ELISA (BD-Biosciences).

2.3.10 Fluorescent imaging of tumors

Tumor tissue samples were prepared and sectioned as previously reported [266]. Six micron tissue sections were analyzed for expression of CD31 (BD-Biosciences), VCAM1 (R&D Systems, Minneapolis, MN), CXCL10 (R&D Systems), NG2 (Millipore), DLK1 (Santa Cruz Biotechnology, Santa Cruz, CA), RGS5, Jarid1b (all from Abcam, Cambridge, MA), CD133 (BD-Biosciences), CD44 (Abcam), and Hes1 (Millipore) by immunofluorescence microscopy, with wide field images collected with fixed illumination conditions using a cooled CCD camera (Olympus Magnafire; Olympus, Center Valley, PA). Using Metamorph software (Molecular Devices, Downingtown, PA), images were thresholded to delineate signal above background and individual structures measured as the integration of pixel number (total number of positive pixels in the structure above background) multiplied by the brightness of each pixel in gray scales. This product provides the integrated pixel intensity of positive structures and is reported as the mean integrated fluorescence intensity ± SD. For the analysis of activated VEC in the TME, cellular

identity was first defined using co-localization of specific markers (cells staining for both CD31 and VCAM-1) using image overlay and manual counting. We found this method was essential to ensure accuracy in cell identification in tissue with complex morphologies. To perform the quantification images were overlaid with Metamorph software and co-localized structures that could be defined as cells were counted. For analysis of cellular apoptosis, tissue sections were labeled using TUNEL kit (Roche, Indianapolis, IN) as per the manufacturer's instructions, followed by incubation with secondary anti-streptavidin Cy3 antibody (Jackson Immunoresearch, West Grove, PA). Some sections were analyzed by confocal microscopy to generate 30 μm 3D reconstructions of images. For the vascular permeability imaging, animals received retro-orbital intravenous injections of FITC-labeled tomato lectin (Sigma-Aldrich) and red 20 nm FluoSpheres (Invitrogen), followed by cardiac perfusion of PBS and 4% paraformaldehyde. Tumors were then immediately resected and imaged by confocal microscopy to generate 17 μm 3D reconstructions. In all depicted tissue images, white ruler insets indicate 50 μm (low magnification images) or 10 μm (high magnification images).

2.3.11 Hemoglobin quantitation

The amount of hemoglobin contained in tissues was quantitated using the Drabkin method [271] and reported as μg hemoglobin per mg wet weight of tissue.

2.3.12 Measurement of tumor hypoxia using pimonidazole

BALB/c mice bearing established (treated or untreated) day 21 s.c. RENCA tumors were injected i.p. with 60 mg/kg pimonidazole hydrochloride (Hypoxyprobe; HPI, Burlington, MA)

30 minutes before euthanasia and tumor harvest and 6 μm tissue sections prepared and analyzed by immunohistochemistry as previously reported [266].

2.3.13 RNA purification and reverse transcription-PCR array

Total RNA was isolated from bulk single-cell suspensions of day 21 tumors harvested from lvNEG- or lvDLK1-treated mice using Trizol reagents (Invitrogen). Total RNA was further purified using the RNeasy Plus Mini Kit (Qiagen) including the gDNA Eliminator spin column. The purity and quantity of the total RNA was assessed using Nanodrop ND-1000 (CelBio SpA, Milan, Italy). Total RNA (1 μg) was reversed transcribed into cDNA using the RT2 First Strand Kit (Qiagen) and the cDNA added to RT2 SYBR Green ROX qPCR Mastermix (Qiagen) and used for quantitative PCR using the RT2 Profiler PCR Array (96-well) for Mouse Notch Signaling Pathway (Qiagen) all according to the manufacturer's instructions. Reactions were performed on a StepOnePlusTM Real-Time PCR thermocycler (Applied Biosystems) using the recommended cycling conditions. All mRNA expression levels were normalized to the expression of GAPDH.

2.3.14 Statistical analysis

Comparisons between groups were performed using a two-tailed Student's *t*-test or one-way analysis of variance with Tukey's *post-hoc* analysis, as indicated. All data were analyzed using SigmaStat software, version 3.5 (Systat Software, Chicago, IL). Differences between groups with a P value <0.05 were considered significant.

2.4 RESULTS

2.4.1 RCC-associated pericytes differentially express the DLK1 antigen

In a previous report [197], we identified several melanoma-associated vascular antigens, including DLK1, which may represent promising therapeutic vaccine targets. Before assessing the therapeutic potential of DLK1 peptide- and gene-based vaccines in the setting of RCC, we first investigated the pattern of DLK1 expression in the TME and tumor uninvolved kidneys of BALB/c mice harboring established syngenic RENCA (an RCC line established from a spontaneously arising renal adenocarcinoma of BALB/c origin) [268] tumors. After enzymatic digestion of tissues, tumor- and kidney-derived pericytes and VEC were isolated *via* flow sorting from single-cell suspensions (**Figure 7a**) and their extracted mRNA (along with mRNA from the cultured RENCA cell line) was analyzed by real-time PCR for DLK1 (and housekeeping control HPRT1) transcript content (**Figure 7b**). We observed that pericytes sorted from RCC tumors were uniquely enriched for DLK1 transcripts (**Figure 7b**) when compared with normal kidney vascular cells or RENCA tumor cells, suggesting that DLK1 may represent a general tumor pericyte-associated antigen. Immunofluorescence microscopy performed on day 21 RENCA tumor sections confirmed that DLK1 protein was coexpressed by $NG2^+$ (a general marker of pericytes in both normal and tumor tissue; [272]) pericytes that were closely approximated to $CD31^+$ VEC *in situ* (**Figure 7c**).

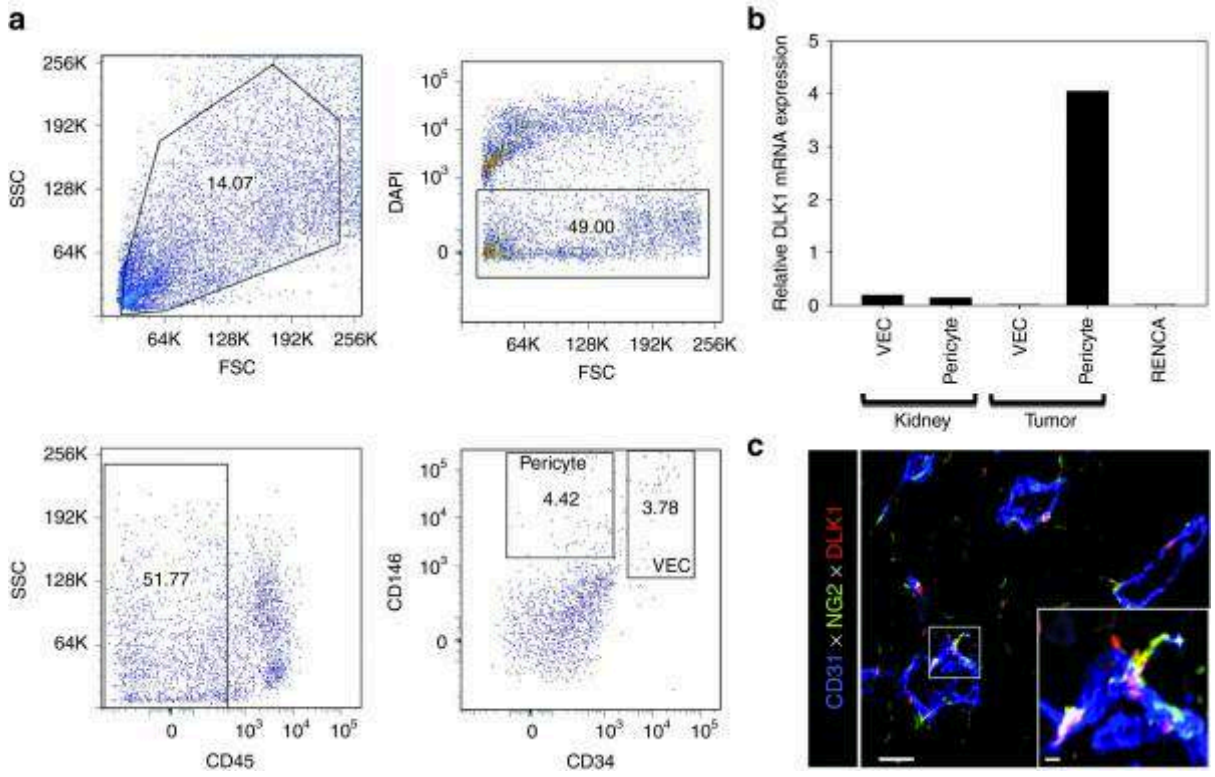

Figure 7. DLK1 is differentially expressed by RENCA tumor-associated pericytes.

The spontaneously arising renal cortical adenocarcinoma RENCA (10^6 tumor cells) was injected s.c. into female BALB/c mice and allowed to progress for 21 days after which animals were euthanized and tumors and normal kidneys harvested. (a) Tissues were processed into single-cell suspensions and sorted by flow cytometry based on forward versus side scatter profiles, DAPI exclusion (to reject dead cells), a $CD45^{neg}$ phenotype (***i.e.,*** non-leukocytic), and then selectively into $CD146^{+}CD34^{neg}$ pericytes and $CD146^{+}CD34^{+}$ VEC populations based on published assignments of these cell lineage-restricted phenotypes [273, 274]. (b) mRNA was then isolated from flow-sorted pericytes and VEC, and analyzed for DLK1 transcript expression by real-time PCR. Relative mRNA expression was normalized to housekeeping HPRT1 mRNA expression. (c) Day 21 RENCA tumor tissue sections were analyzed for expression of CD31 (blue), NG2 (green), and DLK1 (red) by immunofluorescence microscopy. Metamorph quantitation (Materials and Methods) was performed on 10 high power field (HPF) of the fluorescent images, with $28.1 \pm 4.4\%$ of tumor-associated $NG2^{+}$ pericytes coexpressing the DLK1 marker. The analysis also revealed that the majority (***i.e.,*** $58.9 \pm 7.6\%$) of $DLK1^{+}$ cells coexpressed the NG2 marker within the TME. All data are representative of three independent experiments performed. DAPI, 4′,6-diamidino-2-phenylindole; FSC, forward scatter; SSC, side scatter; TME, tumor microenvironment; VEC, vascular endothelial cell.

2.4.2 Treatment of RENCA tumor-bearing mice with a DLK1 peptide-based vaccine is therapeutic and associated with specific type-1 $CD8^+$ T cell (Tc1) activation and recruitment into the TME.

We have previously demonstrated that vaccine formulations composed of interleukin-12 (IL-12) gene-modified dendritic cells (DCs) (*i.e.,* DC.IL12) pulsed with major histocompatibility complex class I-presented peptides promote robust $CD4^+$ T helper cell-independent priming of antigen-specific $CD8^+$ T cells *in vivo* [197, 275]. Using this approach, we analyzed the impact of treating BALB/c mice bearing established s.c. RENCA tumors with a DLK1 peptide (a pooled equimolar mixture of the $DLK1_{158–166}$, $DLK1_{161–169}$, and $DLK1_{259–270}$ peptides)-based vaccine. As depicted in **Figure 8a**, mice treated with the DLK1 peptide-based vaccine, but not a control vaccine (*i.e.,* DC.IL12, no peptide) or phosphate-buffered saline (PBS), exhibited a significant reduction in the growth of RENCA tumors (**Figure 8a**; $P < 0.05$ (analysis of variance) on days >13). On day 21 (*i.e.,* 7 days after the booster immunization), $CD8^+$ splenocytes were isolated and analyzed for secretion of interferon-γ (IFN-γ) in response to stimulation with specific DLK1 peptides presented by syngeneic DC *in vitro*. We noted elevated levels of IFN-γ secretion from $CD8^+$ T cells isolated from mice treated with the DC.IL12 + DLK1 peptide vaccine (versus mice treated with DC.IL12 only or PBS) after stimulation with individual DLK1 peptides, indicating that the vaccine induced poly-specific, anti-DLK1 $CD8^+$ T cell responses *in vivo* (**Figure 8b**).

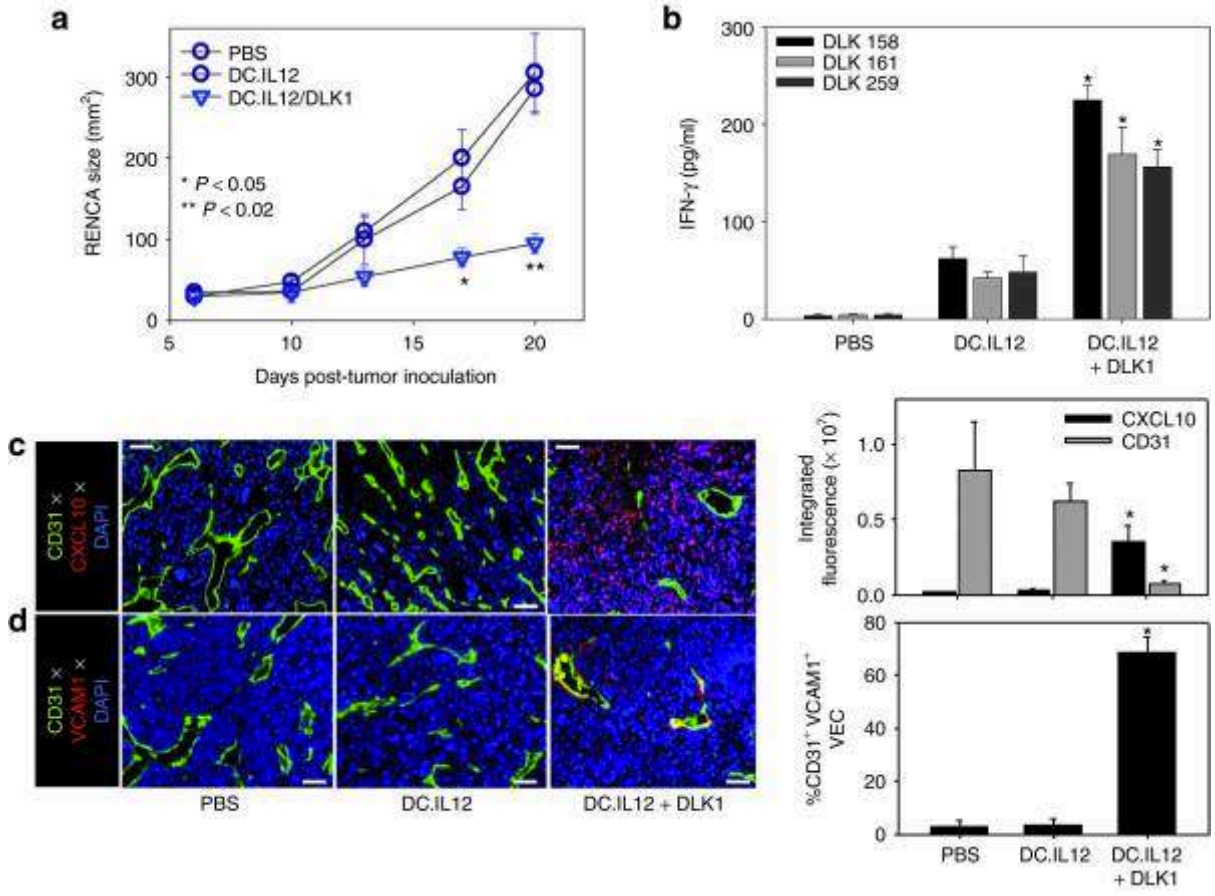

Figure 8. DC/DLK1 peptide-based vaccines are both immunogenic and therapeutic in the murine RENCA model of RCC.

BALB/c mice were inoculated with RENCA tumor cells s.c. on the right flank on day 0. (**a**) After randomizing for similar mean tumor size per treatment cohort (n = 5), mice were injected s.c. on their left flank on days 7 and 14 (post-tumor inoculation) with PBS, 10^6 DC.IL12 or 10^6 DC.IL12 pre-pulsed with equimolar mix (10 μmol/l each) of the three synthetic DLK1 peptides. Tumor growth (mean ± SD) was then monitored over time. (**b**) On day 21 post-tumor inoculation, splenic $CD8^+$ T cells were isolated from each cohort and co-cultured with syngenic DC pre-pulsed with individual DLK1 peptides for 24 hours, at which time, IFN-γ ELISA were performed on the harvested cell-free supernatants. (**c**,**d**) Day 21 tumors were fixed, sectioned and analyzed by immunofluorescence microscopy; CD31 (green in **c**,**d**), CXCL10 (red in **c**), VCAM1 (red in **d**). The percentage of VCAM1 co-localization with CD31 is depicted as a yellow signal in **d** and was quantitated using Metamorph software as described in Materials and Methods. Histograms to the right of images reflect mean fluorescence intensity quantitation of the indicated markers (±SD) from three independent fields per slide as described in Materials and Methods. Data are representative of

three independent experiments performed. *$P < 0.05$ versus control treatments (analysis of variance). DC, dendritic cell; IFN, interferon; PBS, phosphate-buffered saline; RCC, renal cell carcinoma.

Since therapeutic type-1 $CD8^+$ T cells preferentially express a VLA-4^+ $CXCR3^+$ phenotype [175, 276], we next determined whether specific vaccination resulted in the altered expression of VLA-4 and CXCR3 ligands, VCAM-1 and CXCL10, respectively in the TME. A coordinate immunofluorescence microscopy analysis of the TME after DLK1 peptide-based vaccination versus control treatment revealed fewer $CD31^+$ tumor blood vessels (**Figure 8c**), and these vessels contained VEC enriched in the activated $VCAM1^+$ phenotype (**Figure 8d**). We also observed that these same tumors contained elevated levels of CXCL10/IP-10 chemokine protein expression versus control tumors (**Figure 8c**), suggesting that the DLK1-based vaccination induces a proinflammatory TME that is competent to recruit type-1 T effector cells.

2.4.3 Vaccination with a recombinant lentivirus encoding murine DLK1 cDNA is therapeutic in the RENCA model of RCC

Clinical trials implementing synthetic tumor peptide-based vaccines have needed to restrict patient accrual to those individuals expressing relevant human leukocyte antigen class I (peptide-presenting) allotypes. To develop a more universal immunization platform, we next engineered a genetic vaccine that would theoretically allow for virally transduced host antigen-presenting cells to cross-prime a more comprehensive anti-DLK1 T effector cell repertoire. Given the reported superiority of lentiviral-based vaccines to promote prolonged antigen-specific $CD8^+$ T cell responses after a single administration *in vivo* [277], we first constructed a recombinant

lentivirus encoding full-length murine DLK1 (lvDLK1) and a negative control virus (lvNEG; **Figure 9**).

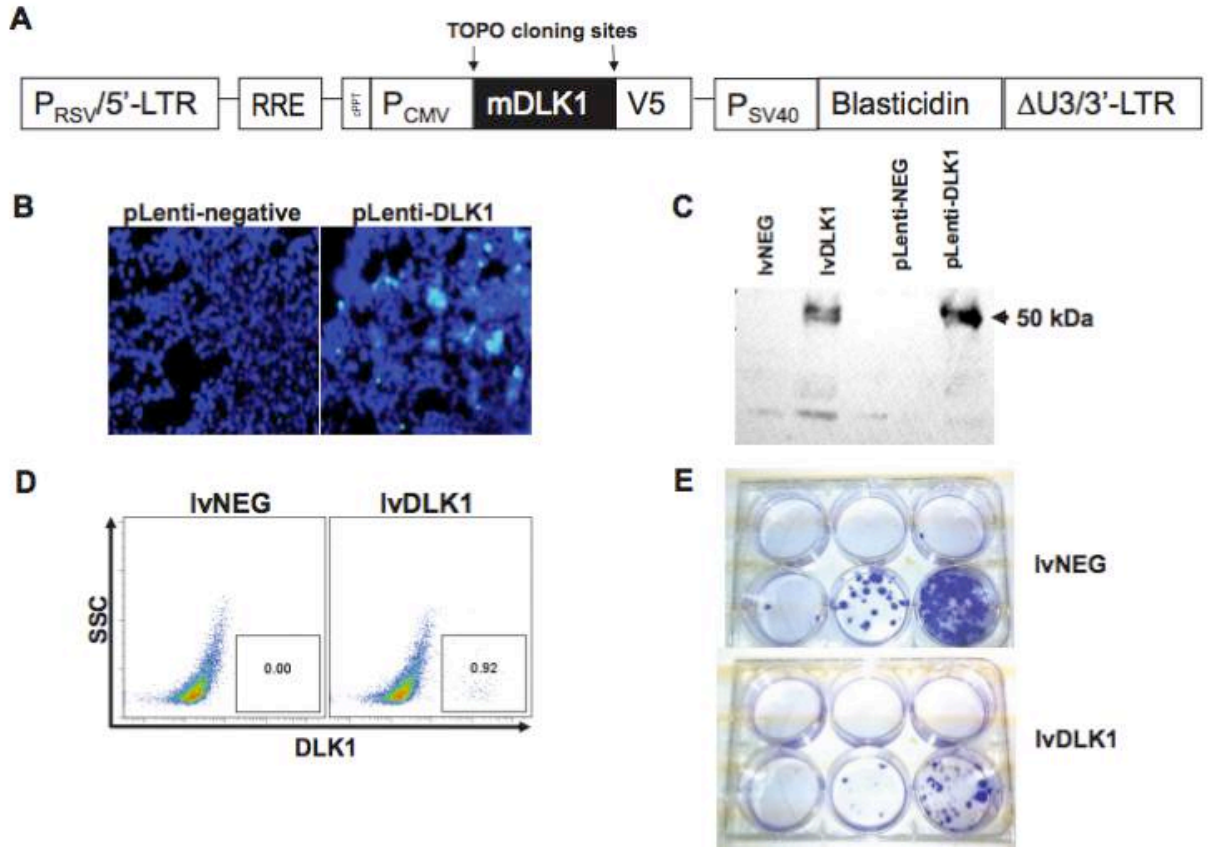

Figure 9. Production of recombinant lvDLK1 and control lvNEG lentiviruses.

In (**a**), a schematic diagram is provided for lvDLK1. pRSV/5′LTR, RSV LTR and HIV LTR chimeric promoter; RRE, Rev response element sequences; CMVp, CMV promoter used to drive transgene expression; whole mouse DLK1 gene with V5 reporter tag; SV40p-Blasticidin, SV40 virus promoter used to drive selection marker blasticidin gene expression; ΔU3/HIV 3′LTR, promoter deleted in U3 region so that the lvv become selfinactivated; TOPO cloning sites also indicated. 293T cells were transfected with plasmid DNA pLenti-DLK1 (or pLenti-NEG) and analyzed for V5 protein expression by (**b**) immunofluorescence and (**c**) western blot. HT-1080 cells were infected with lentivirus and analyzed for (**c**) V5 protein expression by western blot and (**d**) DLK1 protein expression by flow cytometry. (**e**) Production of a live functional virus (lvNEG) is confirmed by the formation of blasticidin-resistant colonies of lentivirus-infected HT-1080 cells stained with crystal violet.

To assess the therapeutic efficacy of specific genetic vaccination against the full-length DLK1 antigen, BALB/c mice bearing established day 7 RENCA tumors received a single intradermal injection of lvDLK1 or control lvNEG at a site distal to tumor (*i.e.,* contralateral). Animals treated with lvDLK1 exhibited significant reductions in tumor growth compared with animals treated with lvNEG (**Figure 10a**). As was the case for DLK1 peptide-based vaccines, immunofluorescence microscopy analysis of tumor sections supported decreased vascularity and loss of ($DLK1^+$) vascular pericytes (**Figure 10b**), and increased presence of the CXCR3 ligand chemokine, CXCL10, and $VCAM1^+CD31^+$ VEC in the TME of mice treated with lvDLK1 versus lvNEG (**Figure 10c**,**d**). Enhanced expression of CXCL10 and VCAM1 in the TME was associated with greater numbers of $CD8^+$ TIL in mice receiving LvDLK1-based vaccines (**Figure 10e**). These findings suggest that immune targeting of DLK1 *via* a single administration of lvDLK1 can effectively limit tumor growth and induce a proinflammatory TME promoting the improved recruitment of TIL.

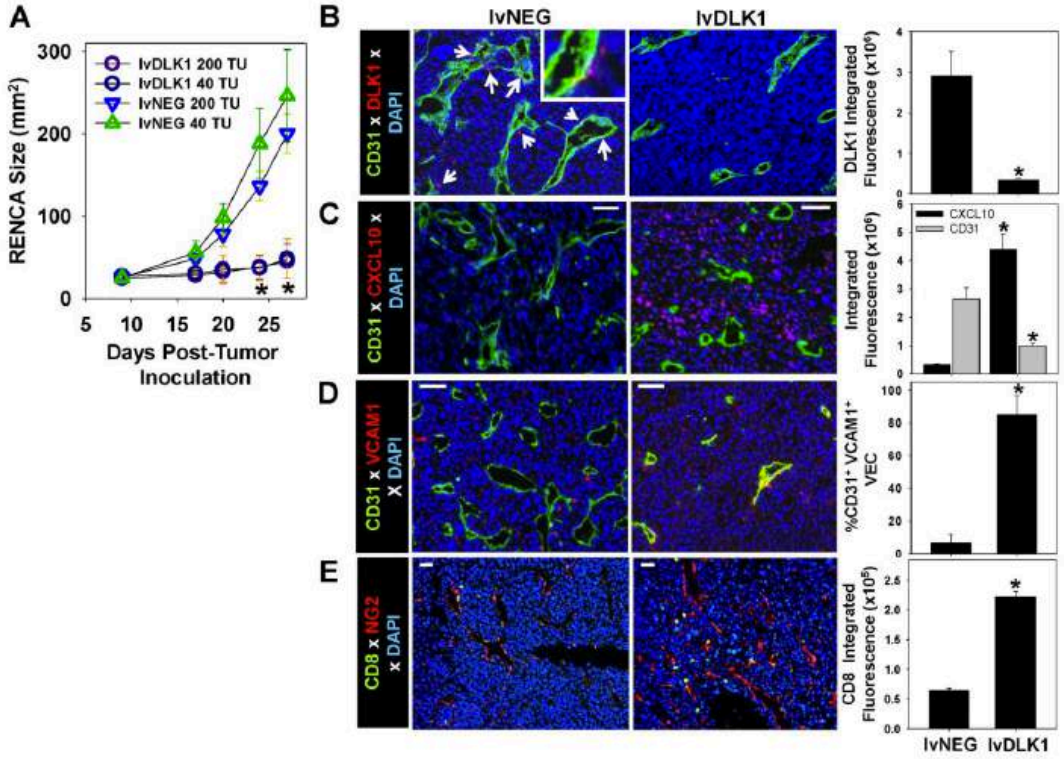

Figure 10. Recombinant lvDLK1-based vaccines are therapeutic and promote a type-1–polarized TME.

(**a**–**d**) BALB/c mice were inoculated s.c. with RENCA tumor cells in the right flank on day 0. (**a**) After cohort (n = 5) randomization for similar mean tumor size on day 10 post-tumor inoculation, mice were treated i.d. in the left flank with 40 or 200 transduction units (TU) of lvDLK1 or control virus, lvNEG. Tumor size was then monitored longitudinally. (**b**–**e**) On day 27 post-tumor inoculation, mice were euthanized, with harvested tumors fixed, sectioned and analyzed by immunofluorescence microscopy for expression of (**b**) CD31 (green) and DLK1 (red) with white arrows indicating $DLK1^+$ cells, (**c**) CXCL10, (**d**) co-localization of VCAM1 with CD31, and (**e**) $CD8^+$ TIL (green) and NG (red). Histograms to the right of images reflect mean fluorescence intensity quantitation of the indicated markers (±SD) from three independent fields per slide as described in Materials and Methods. Data are representative of three independent experiments performed. *$P < 0.05$ versus control treatments (analysis of variance). i.d., intradermal.

2.4.4 Vaccination with lvDLK1 normalizes the RENCA vasculature

It has been suggested that the tumor-associated vasculature of mice deficient in immature pericytes appears "normal" with minimal arborization and reduced vascular permeability [264], supporting therapeutic strategies to selectively reduce or eradicate immature vascular pericytes within tumor sites. Given the ability of our lvDLK1-based genetic vaccine to reduce the content of $DLK1^+$ (immature) pericytes in the tumor stroma, we sought further evidence supporting therapeutic vascular remodeling as a consequence of treatment with this modality. We noted that RENCA tumors harvested from mice treated with lvDLK1 appeared "anemic" when compared to control tumors (**Figure 11a**), a subjective index that was subsequently confirmed based on an analysis of hemoglobin content in tumor lysates (**Figure 11b**). When we analyzed tumors for expression of NG2 using immunofluorescence microscopy, we observed that animals vaccinated with lvDLK1 exhibited tumors with significant reductions in numbers of $NG2^+$ pericytes in their TME versus tumors from animals vaccinated with lvNEG (**Figure 11c**,**d**). Residual tumor pericytes in lvDLK1-treated animals were tightly approximated to $CD31^+$ VEC, unlike the randomly distributed pattern of pericytes detected in the stroma of tumors isolated from control mice. To investigate changes in tumor vascular permeability, vaccinated animals received intravenous injections of two fluorescently labeled probes, tomato lectin-FITC to bind/mark the vascular endothelium and small 20 nm (red) FluoSpheres to determine vessel leakiness into tissue. When compared with controls, the tumor blood vessels in mice vaccinated with lvDLK1 displayed a simple tubular architecture devoid of extensive branching (**Figure 12a**). Furthermore, while the perivascular stroma of tumors in control animals was littered with the red FluoSpheres, these probes were virtually undetected in tumors harvested from lvDLK1-vaccinated mice, consistent with diminished vascular permeability in the TME of these latter

animals (**Figure 12a**). These data suggest that immunization against DLK1 allows for the immunotherapeutic "normalization" (*i.e.,* reduction in blood vessel numbers and arborization, reduced vascular permeability) of tumor blood vessels *in vivo*.

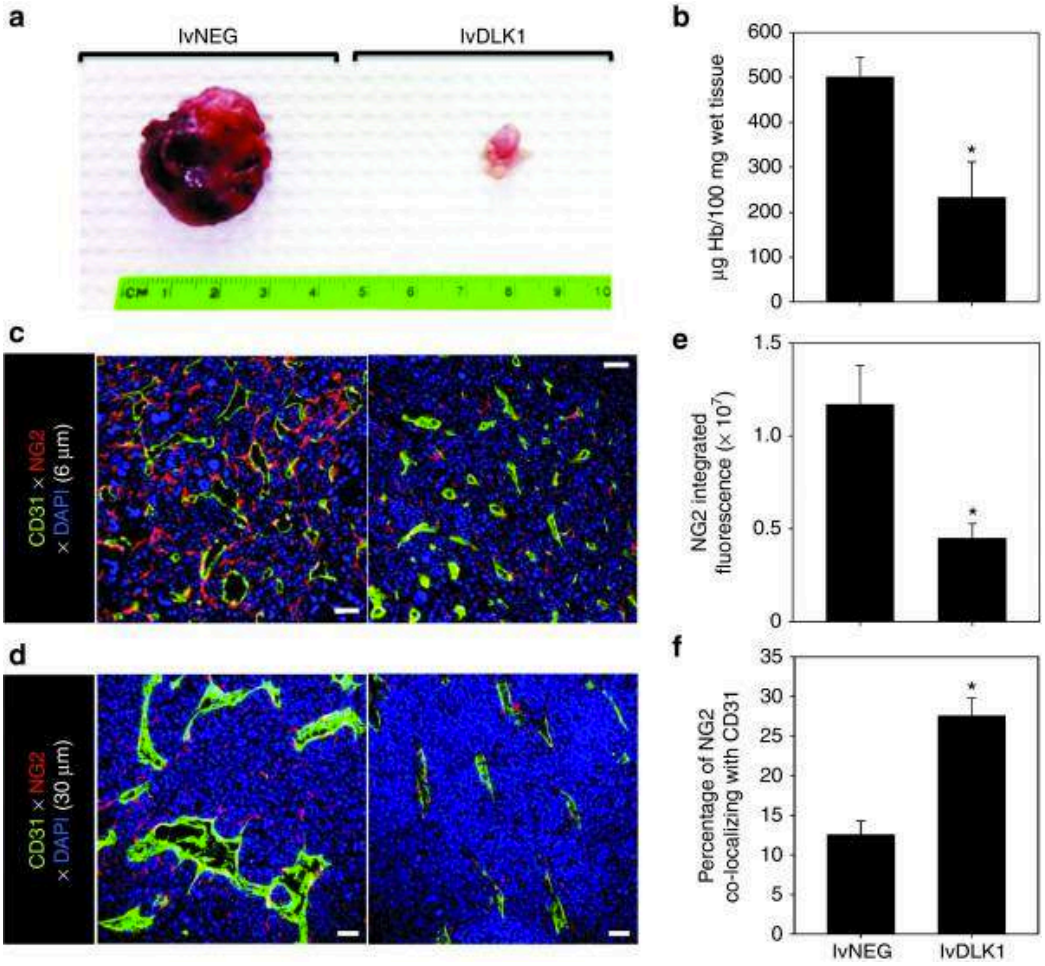

Figure 11. Recombinant lvDLK1-based vaccines promote normalization of the tumor vasculature.

Mice bearing day 10 RENCA tumors were treated with 200 TU of lvDLK1 or lvNEG as outlined in **Figure 10**. On day 27 post-tumor inoculation, mice were euthanized and the (**a**) tumors were resected and evaluated macroscopically and (**b**) for hemoglobin content. In **c** and **d**, tumor sections were analyzed by immunofluorescence microscopy for expression of CD31 (green) and NG2 (red). In **e**, 6 µm sections were imaged by wide field microscopy, while in **d**, 30 µm sections were imaged by confocal microscopy to generate 3D reconstructions. For **e**, mean data ± SD of three independent fields per slide in **c** is reported for each group from one representative experiment of three performed. (**f**) The percentage of NG2 fluorescence signal overlapping CD31 fluorescence

signal was calculated using Metamorph software as described in Materials and Methods, and is reported as mean ± SD of three independent fields per slide. *$P < 0.05$ for lvDLK1 versus lvNEG (*t*-test).

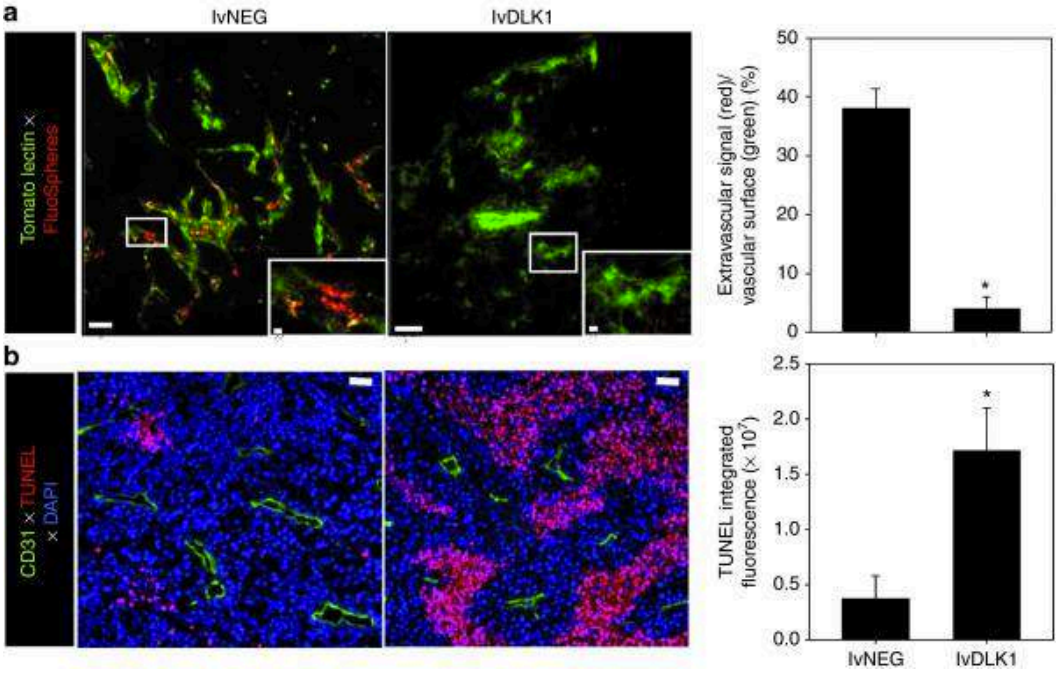

Figure 12. Recombinant lvDLK1-based vaccination reduces tumor vascular permeability resulting in the development of apoptotic "dead zones" in the TME.

In repeated experiments as outlined in **Figure 10**, (**a**) treated mice received intravenous injections of tomato lectin-FITC to label vascular endothelium (green) and 20 nm FluorSpheres to assess vascular permeability (red) on day 24 post-tumor inoculation. Whole tumor tissue was then imaged immediately by confocal microscopy at a depth of 17 μm. *$P < 0.05$ for lvDLK1 versus lvNEG (*t*-test). (**b**) On the same day, unlabeled mice were euthanized, with tumors resected, fixed, sectioned, and analyzed for expression of CD31 (green) and apoptotic nuclear staining with TUNEL reagent (red). Histograms to the right of images reflect mean fluorescence intensity quantitation of the indicated markers (±SD) from three independent fields per slide as described in Materials and Methods. Data are representative of three independent experiments performed. *$P < 0.05$ for lvDLK1 versus lvNEG (*t*-test).

2.4.5 Therapeutic vaccination with lvDLK1 results in increased cellular apoptosis in the treated TME

Given the apparent trimming of vascular branches in the RENCA TME, and reduction in vascular permeability after vaccination with lvDLK1 (but not lvNEG), we hypothesized that plasma nutrients required for sustaining tumor cell viability would be limited to regions adjacent to the remaining normalized blood vessel network. TUNEL analyses revealed that indeed, the level of cellular apoptosis in the TME of lvDLK1-treated mice was substantially increased when compared with tumors isolated from control treated animals (**Figure 12b**). Furthermore, virtually all apoptotic events (*i.e.,* "dead zones") in RENCA tumors isolated from lvDLK1-vaccinated mice were located in tissue regions >~60 μm away from residual $CD31^+$ blood vessels in planar tissue imaging analyses (**Figure 12b**).

2.4.6 Therapeutic vaccination with lvDLK1 results in reduced hypoxia and a lower incidence of cell populations expressing hypoxia-responsive markers in the TME

Hypoxia frequently occurs in solid cancers as a consequence of inefficient perfusion of oxygen into tumors by "aberrant" blood vessels [278, 279], resulting in reduced recruitment and function of TIL, increased prevalence of immunosuppressive cells/modulators, dysregulated angiogenesis, and the accumulation of "stem-like" cell populations (*i.e.,* cancer stem cells/tumor initiating cells, cells undergoing epithelial-to-mesenchymal transition) in the TME [280, 281]. To investigate changes in hypoxia within tumors after vaccination with lvDLK1 versus lvNEG, we injected mice intraperitoneally (i.p.) with pimonidazole (a hypoxia marker that undergoes reductive activation and then conjugates to thiol-containing proteins specifically in hypoxic cells,

allowing for immunohistochemical detection of tissue regions exhibiting low (<1.3%) O_2 tension) [282]. Using this imaging technology, we found that tumors isolated from mice receiving lvDLK1 vaccines had a very low hypoxic index when compared to tumors culled from control animals (**Figure 13a**). Given this large reduction in TME hypoxia postvaccination with lvDLK1, we next investigated treatment impact on expression of hypoxia-responsive gene products associated with immature vascular stromal cells (*i.e.,* RGS5) and/or stem-like cell populations (*i.e.,* Jarid1B aka histone demethylase lysine demethylase 5b; CD133, CD44) [283-285]. Immunofluorescence microscopy analysis of day 27 tumor sections revealed that the expression of these markers was coordinately reduced in RENCA tumors after host vaccination with lvDLK1 (**Figure 13b–f**). When taken together, these data indicate that vaccination with lvDLK1 results in the recovery of normoxia in the TME in association with the conditional alteration in the phenotype (and presumably function) of a range of stromal cell subpopulations *in vivo*.

2.4.7 Loss of DLK1 expression in the TME after therapeutic vaccination with lvDLK1 leads to increased locoregional activation of NOTCH

Since lvDLK1-based vaccination leads to loss of DLK1 expression in the TME (**Figure 10**) and DLK1 represents a functional inhibitor of NOTCH signaling [242], we hypothesized that this therapeutic vaccine would promote enhanced canonical NOTCH signaling in therapeutic RENCA TME. As shown in **Figure 14a**,**b**, RENCA tumors isolated from lvDLK1-treated (but not control) mice contained cells strongly expressing cytoplasmic/nuclear Hes1 protein, a NOTCH transcriptional target required for the tumor suppressor action of activated NOTCH [222, 267]. $Hes1^+$ cells included both $CD31^+$ VEC and non-VEC stromal cell populations in the

TME (**Figure 14a**). Corollary gene array analyses also supported the enhanced transcription of numerous NOTCH target genes (including the canonical NOTCH ligands (DLL1, DDL3, DLL4, and Jag1/2) and the NOTCH1-4 receptors, among others), but not control β_2-microglobulin, in lvDLK1- versus lvNEG-treated tumors (**Figure 14c**).

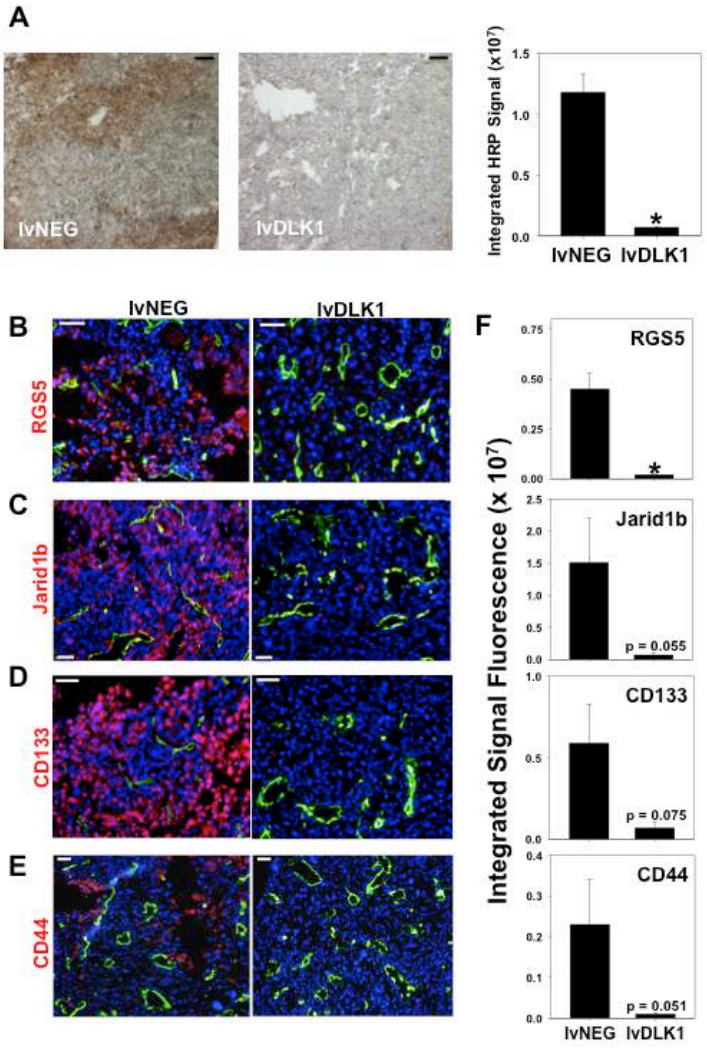

Figure 13. Recombinant lvDLK1-based vaccines promote normoxia in the TME in association with the loss of cells bearing stem cell-like phenotypes.

Mice bearing day 10 RENCA tumors were treated with 200 TU of lvDLK1 or lvNEG as outlined in **Figure 10**. (**a**) On day 21, mice were injected intraperitoneally with the hypoxia probe pimonidazole hydrochloride and euthanized,

with tumors resected, sectioned, and analyzed by HRP immunohistochemistry. (**b–e**) Day 21 tumor-bearing mice that did not receive pimonidazole hydrochloride were euthanized, with tumors harvested, fixed, sectioned and analyzed by immunofluorescence microscopy for expression of (**b**) CD31 and RGS5, (**c**) Jarid1b, (**d**) CD133, and (**e**) CD44. (**f**) Histograms to the right of panel **b**–**e** images reflect mean fluorescence intensity quantitation of the indicated markers (±SD) from three independent fields per slide as described in Materials and Methods. Data are representative of three independent experiments performed. **P* < 0.05 for lvDLK1 versus lvNEG (*t*-test). TME, tumor microenvironment; TU, transduction unit.

2.4.8 Therapeutic benefits associated with lvDLK1-based genetic vaccination are partially dependent on canonical NOTCH signaling

To determine the importance of canonical NOTCH signaling on the antitumor efficacy of genetic vaccination against DLK1, we immunized BALB/c mice bearing established s.c. RENCA tumors with lvNEG or lvDLK1 as described in **Figure 10a**, with cohorts of lvDLK1-vaccinated animals injected i.p. with the γ-secretase inhibitor DAPT (N-[N-(3,5-Difluorophenacetyl-L-alanyl)]-(S)-phenylglycine t-butyl ester; which inhibits the generation of the NOTCH intracellular domain required for downstream NOTCH signaling events, ref. [286]) or vehicle control DMSO. As shown in **Figure 14d**, administration of DAPT partially suppressed the antitumor action of lvDLK1-based therapeutic vaccination.

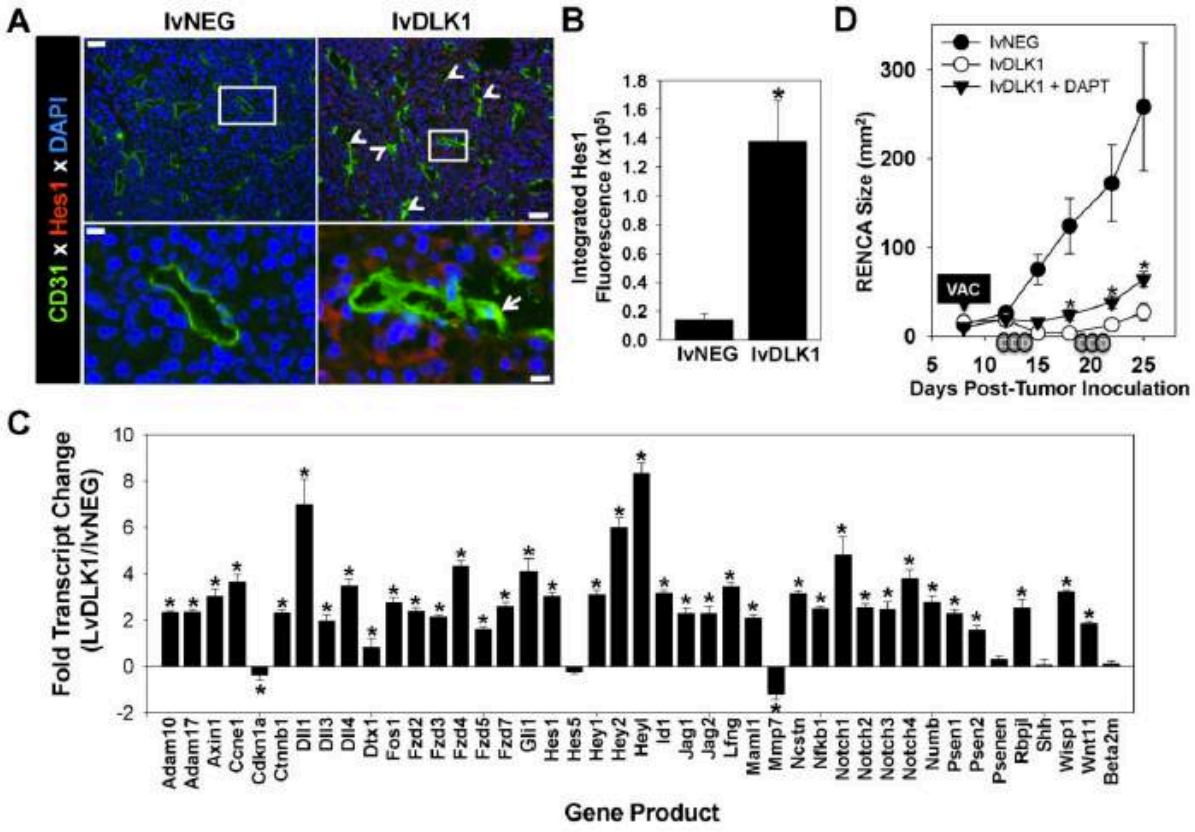

Figure 14. Treatment with lvDLK1 vaccines results in NOTCH activation in the TME, which is partially responsible for the antitumor effectiveness of this treatment strategy.

(**a**) Tumor sections were isolated as described in **Figure 10** and evaluated by fluorescence microscopy using specific antibodies against CD31 (green) and Hes1 (red). DAPI counterstaining was used to image cell nuclei (blue). White arrows in image insets indicate $Hes1^{+}CD31^{+}$ VEC. (**b**) Mean fluorescence intensity quantitation of Hes1 protein expression (±SD) from three independent fields per slide is reported as described in Materials and Methods. Data are representative those obtained in three independent experiments performed. $^{*}P < 0.05$ (*t*-test). (**c**) mRNA transcripts of NOTCH target genes were analyzed using an reverse transcription-PCR gene array. The ratio of transcript levels for a given gene product among total tumor mRNA isolated from lvDLK1- versus lvNEG-treated mice is reported. Negative control transcript = β_2-microglobulin (beta 2-m). (**d**) Established day 8 s.c. RENCA tumors were treated with 200 TU of lvNEG or lvDLK1 (*i.e.,* VAC) as described in the **Figure 10a** legend and Materials and Methods. DAPT (in DMSO; depicted as small gray ovals labeled "D" on the *x*-axis) or vehicle control DMSO was then provided as indicated for three consecutive days/week/cycle for two cycles beginning on day 12 post-tumor inoculation. Tumor size was then monitored longitudinally. $^{*}P < 0.05$ for lvDLK1 + DAPT treatment versus

lvDLK1 treatment; also $P < 0.05$ for the lvDLK1 + DAPT and lvDLK1 treatments versus lvNEG control treatment on days ≥15 post-tumor inoculation (analysis of variance). DAPI, 4′,6-diamidino-2-phenylindole; TME, tumor microenvironment; TU, transduction unit; VAC, vaccination.

2.5 DISCUSSION

The major finding in this report is that DLK1 is a tumor pericyte-associated antigen that can be immunologically targeted *via* specific peptide- or gene-based vaccination *in vivo*, leading to the effective "normalization" of the vasculature in the TME and a drastic reduction in solid tumor (*i.e.,* RENCA) growth *in vivo*. Effective therapeutic vaccination resulted in the activation of type-1 (IFN-γ–producing) DLK1-specific $CD8^+$ T cells in the periphery and the improved recruitment of $CD8^+$ T cells into/around residual blood vessels in the TME. Therapeutically normalized blood vessels in RENCA tumors exhibit a simplified conduit design with tightly approximated (abluminal) $NG2^+DLK1^{neg}RGS5^{neg}$ mature pericyte populations that appear improved in their structural integrity based on a reduction in vascular permeability. RENCA tumors in DLK1-vaccinated mice became normoxic and displayed a dramatic increase in the rate of apoptotic death in regions of the tumor that were further away from residual blood vessels. The relationship between loss of hypoxia and promotion of tumor cell apoptosis in the therapeutic TME may not be intuitively obvious. We hypothesize that consistent with the paradigm of Jain [139], therapeutic vascular normalization results in the coordinate loss of vascular permeability and hypoxia in the TME. In turn, loss of hypoxia (and hypoxia-responsive genes such as HIF-1α) has been associated with enhanced rates of tumor cell apoptosis [287] and reduced expression of a broad range of tumor growth and survival/antiapoptotic gene products [288]. As such, under normoxic conditions post-therapy (as in the case of lvDLK1-based vaccination), tumor cells most removed from blood vessels may be rendered most susceptible to undergo apoptosis based on limited access to pro-survival/growth factor gradients emanating from normalized blood vasculature. Overall, our findings support a model in which specific

immune effector T cells may serve as regulators of the "angiogenic switch" [139, 197, 264, 266, 278] by monitoring and controlling the status of $DLK1^+$ pericytes within the TME.

Vaccination against DLK1 also induced a proinflammatory TME based on the acquisition of activated $VCAM1^+$ VEC and concomitant production of the CXCR3 ligand chemokine CXCL10, responsible for recruiting type 1 TIL. We hypothesize that an initial wave of DLK1-reactive type-1 TIL results in perivascular secretion of IFN-γ and tumor necrosis factor-α in the TME, leading to locoregional upregulation of IFN-γ/tumor necrosis factor-α–responsive gene products such as VCAM-1 and CXCL10 [289]. Such alterations in the TME would then be expected to foster improved uptake of tumor debris (*i.e.,* apoptotic bodies) by recruited/activated antigen-presenting cells and the corollary reiterative cross-priming of an expanded, protective T cell repertoire reactive against both tumor- and tumor vascular-associated antigens [197] that may be directed into the proinflammatory TME.

Interestingly, a recent report by Reis *et al [289],* suggests that the conditional activation of the Wnt/β-catenin/NOTCH signaling pathway can lead to vascular normalization, as indicated by reduced vascular density and improved mural cell attachment, in intracranial murine glioma models. Our data support such a paradigm, with specific vaccination resulting in removal of DLK1 expression (and NOTCH antagonism) [242] in the TME. Such immune pressure improved NOTCH signaling based on a dramatic increase in the intratumoral expression of Hes1 protein and the transcriptional activation of multiple NOTCH target genes. The transcriptional profiling also supports differentially increased expression of Frzd2, Frzd4, Frzd7, and β-catenin (Ctnnb1) in RENCA tumors harvested from lvDLK1-vaccinated mice supporting the coactivation of canonical Wnt/β-catenin signaling [290] in the therapeutic TME, consistent with the model proposed by Reis *et al* [289]. As such, our data suggest that vaccination against DLK1 (as an

integral transmembrane protein or *via* its shed extracellular domain) [291][41] may derepress canonical NOTCH/Wnt/β-catenin signaling in endothelial cells (and other stromal cell populations) within the TME, thereby promoting vascular quiescence/normalization [242, 289, 292]. Vaccination against DLK1 may also improve type-1 functionality of TAMs and DC (*i.e.,* enhanced IL-12p70 and CXCL10 production) and T cells [293]. Indeed, we observed that the functional antagonism of NOTCH signaling *in vivo* (based on administration of the γ-secretase inhibitor DAPT) partially ablated the antitumor benefits associated with lvDLK1-based therapeutic vaccination, suggesting a supporting role for canonical NOTCH signaling in treatment outcome. Future studies will investigate the potential role of Wnt/β-catenin signaling in therapeutic benefit associated with DLK1-based vaccines by applying specific inhibitors of these pathways in our therapeutic model.

The TME of progressively growing, control RENCA tumors was enriched in cells expressing markers known to contain HRE in their promoter regions, such as CD44, CD133, and Jarid1B [283-285], that have been previously linked to cell populations with "stem-like" characteristics [280, 281]. Notably, the "normalized" TME after therapeutic vaccination with lvDLK1 was normoxic and largely devoid of cells expressing these hypoxia-responsive antigens. Although the most simplistic reason for this change reflects the transcriptional silencing of these gene products in the TME of lvDK1-vaccinated animals, it is also conceivable that the therapeutic TME is poor in recruiting cells bearing these phenotypic markers, and/or that the vaccine evoked corollary cross-priming [197, 275] of cytotoxic $CD8^+$ T cell responses capable of eradicating $CD44^+$, $CD133^+$, and $Jarid1B^+$ target cells in effectively treated RENCA tumors. With regard to the latter scenario, we currently plan to longitudinally evaluate the reactivity of the evolving therapeutic $CD8^+$ T cell repertoire against peptide epitopes derived from the CD44,

CD133, and Jarid1B (as well as alternate "stem cell"-associated/hypoxia-responsive markers such as ALDH1, Oct4, and Nanog) [285] antigens in RENCA-bearing mice treated with DLK1 peptide/gene-based vaccines.

The antiangiogenic action mediated by the DLK1 vaccine-induced $CD8^+$ T cell repertoire would be anticipated to differ, and likely complement, that of alternative pharmacological antiangiogenic treatment modalities such as antivascular endothelial growth factor antibodies (*i.e.,* bevacizumab) and small molecule tyrosine kinase inhibitors [261, 294, 295]. In most cases, tumors treated with these agents rapidly become drug-refractory due to their adoption of compensatory growth/progression pathways. As such, DLK1-based vaccines could represent a logical second-line approach in the many cases of developed resistance to bevacizumab, sunitinib or similar antiangiogenic drugs. DLK1-based vaccines may also represent effective co-first line therapeutic agents, since the specific activation, recruitment and function of anti-DLK1 T effector cells in the TME would be anticipated to be improved by the coadministration of antiangiogenic tyrosine kinase inhibitor that reduce suppressor cell populations (most notably in RCC patients) and activate a proinflammatory TME *in vivo [174, 175, 177]*. Based on these expectations, we plan to evaluate the comparative therapeutic efficacy of combined sunitinib + lvDLK1 vaccination treatment in our existing s.c. RENCA model, as well as, in an orthotopic RCC model using RENCA.luc (RENCA cells transduced with luciferase cDNA) to allow for vital bioluminescence monitoring of tumor growth and metastasis. Although we have not observed signs of off-target autoimmune pathology as a consequence of DLK1-targeted vaccination (*i.e.,* inhibition of cutaneous wound healing [197], tissue vasculitis; data not shown) to date, these new models will provide us with additional opportunities to investigate potential combination treatment-associated toxicities in future.

Consistent with our findings in the RENCA model, pericytes from freshly isolated human RCC (but not patient-matched normal adjacent kidney tissue) also differentially (over)express the DLK1 antigen *in situ* (**Appendix Figure 1**). When coupled with the knowledge that anti-DLK1 $CD8^+$ T cell responses can be developed from human cancer patients after *in vitro* sensitization [275], we believe that DLK1-based vaccines (as single agents or in combination approaches) represent attractive candidates for clinical translation in the setting of RCC and alternate well-vascularized forms of solid cancer.

3.0 THERAPEUTIC EFFICACY OF COMBINED VACCINATION AGAINST TUMOR PERICYTE-ASSOCIATED ANTIGENS DLK1 AND DLK2 IN MICE

Kellsye Paula L. Fabian[1], Nina Chi-Sabins[1], Jennifer L. Taylor[2], Ronald Fecek[2], Aliyah Weinstein[1] and Walter J. Storkus[1,2,3]

From the Departments of [1]Immunology and [2]Dermatology, University of Pittsburgh School of Medicine, and the [3]University of Pittsburgh Cancer Institute, Pittsburgh, PA, 15213.

These data have been reported in *OncoImmunology* 2017 (In Press). All data in this chapter were obtained by Kellsye Paula L. Fabian. All authors contributed to the scientific discussion and constructive comments used in developing this manuscript.

3.1 ABSTRACT

When compared to vascular cells in normal tissues, pericytes and (VEC) in tumor blood vessels exhibit altered morphology and epigenetic programming that leads to the expression of unique antigens that allow for differential recognition by $CD8^+$ T cells. We have previously shown that the Notch antagonist delta-like homolog 1 (DLK1) is a tumor pericyte-associated antigen expressed in setting of melanoma and a range of carcinomas. In this report, we show that therapeutic vaccination against DLK1 in murine models results in slowed tumor growth, but also to the compensatory expression of the DLK1 homolog, DLK2, by tumor-associated pericytes. Vaccines targeting both DLK1 and DLK2 resulted in superior anti-tumor benefits in association with improved activation and recruitment of antigen-specific Type 1 $CD8^+$ T cells, reduced presence of MDSC and Treg, and tumor vascular normalization. The anti-tumor efficacy of vaccines coordinately targeting DLK1 and DLK2 was further improved by inclusion of PD-L1 blockade, thus defining a combination immunotherapy theoretically suitable for the treatment of a broad range of solid (vascularized) cancers.

3.2 INTRODUCTION

Progressive neoplasms require an expansive blood vessel network to supply nutrients and oxygen, as well as, to expel metabolic wastes and carbon dioxide, making the tumor vasculature a viable target for interventional anti-cancer therapy [296]. Indeed, therapies integrating neutralizing anti-vascular endothelial growth factor (VEGF) antibodies or tyrosine kinase inhibitors (TKIs) that interfere with proangiogenic signaling pathways have exhibited some degree of therapeutic efficacy in the pre-clinical and clinical settings [297, 298]. However, the protective benefits resulting from anti-angiogenic therapies have typically proven to be transient in nature, with the consequent evolution of treatment-refractory disease [299]. Hence, there remains a great clinical need to develop novel anti-angiogenic therapies that are adaptive and support the sustained normalization of the tumor vasculature in cancer patients.

Blood vessels in solid tumors differ structurally and functionally from those found in normal tissues. In normal tissues, vascular endothelial tubes are found in close physical approximation with abluminal pericytes, where these cell types communicate via intimate cell-to-cell contact, as well as, via mutually secreted factors. This results in the coordinated proliferation and differentiation of VEC, and the formation of an efficient and organized mature blood vessel network. In stark contrast, in the TME, VEC-pericyte associations are estranged, resulting in highly-permeable blood vessels and a local tissue milieu that is characterized by high interstitial fluid pressure, acidosis and hypoxia [22, 25]. Such environmental stressors promote unique epigenetic programming amongst stromal cell populations that leads to abnormal genomic and proteomic profiles of tumor-associated VECs and pericytes [187, 300]. Notably, disease-associated tumor-blood vessel-associated antigens (TBVA) may be targeted immunologically by specific $CD8^+$ T cells that can be elicited via active, specific vaccination.

Indeed, our lab has previously shown that TBVA-targeted vaccines are competent to promote therapeutic $CD8^+$ T cell responses that are capable of extending overall survival in murine tumor models [197].

In a previous study (Chapter 2), we demonstrated that pericytes within human renal cell carcinoma (RCC) biopsies or *in vivo* grown murine renal carcinomas (RENCA) express abnormally high levels of the TBVA delta-like homolog 1 (DLK1), and that therapeutic vaccination against DLK1 in RENCA-bearing mice results in tumor growth inhibition, increased frequencies of $CD8^+$ tumor infiltrating lymphocyte (TIL) and vascular normalization (VN; ref. [197]). Interestingly, DLK1 (over)expression has also been correlated to the malignant transformation of adipocytes and to cancer stemness in the setting of hepatocellular carcinomas and neuroblastomas [243-246]. DLK1 and its homolog, delta-like homolog 2 (DLK2), belong to the Notch EGF-like family of receptors and ligands. DLK1 and DLK2 both contain six EGF-like repeats in the extracellular region, a single transmembrane region, and a short intracellular tail [237, 251]. Despite lacking the characteristic Delta, Serrate, and Lag-2 (DSL) domain of canonical Notch ligands, DLK1 and DLK2 interact with Notch1 and serve as antagonists to DLL4- and Jagged1-mediated activation of Notch signaling [240, 241, 252] that are required for normal vascular maturation [301].

Consistent with previous reports that the *Dlk1* and *Dlk2* genes reciprocally regulate each other's expression [251], we report that targeted therapeutic vaccination against DLK1 in RENCA-bearing mice leads to the loss of DLK1 expression in the TME, but also to a compensatory increase in the expression of DLK2 by tumor-associated vascular pericytes. We also show that combined vaccination against DLK1 and DLK2 leads to superior anti-tumor benefits when compared to vaccination against either single antigen in both the RENCA and B16

melanoma tumor models. The combined vaccine resulted in superior activation and recruitment of antigen-specific $CD8^+$ TIL and to VN in the TME. In the B16 tumor model, tumor-associated antigen (TAA)-specific T cells were also activated as a consequence of combined DLK1 + DLK2-targeted vaccination, via an apparent "epitope spreading" mechanism. Furthermore, we demonstrate that the anti-tumor efficacy of DLK1/DLK2-targeted vaccines may be improved when further combined with programmed death ligand-1 (PD-L1) blockade, thus defining a combination immunotherapy suitable for the treatment of many solid forms of cancer.

3.3 MATERIALS AND METHODS

3.3.1 Animals and cell lines

Female 6-8 week old Balb/c and C57BL/6 mice were purchased from Jackson Laboratory and were maintained in a pathogen-free animal facility. All animals were handled under aseptic conditions per an Institutional Animal Care and Use Committee (IACUC)-approved protocol and in accordance with recommendations for the proper care and use of laboratory animals. The RENCA (CRL-2947) and B16-F10 (CRL-6475) cell lines were purchased from American Type Culture Collection. These cell lines were free of Mycoplasma contamination and were maintained in complete medium [CM: RPMI-1640 media (Gibco, Cat. No. 21870-076) supplemented with 10% heat-inactivated fetal bovine serum (Sigma, Cat. No. F442), Pen/Strep [100 μg/mL streptomycin and 100 U/mL penicillin (Gibco, Cat. No. 15140-22)], and 10 mmol/L L-glutamine (Gibco, Cat. No. 25030-081)] at 5% CO_2 tension in a 37°C humidified incubator.

3.3.2 Generation of bone marrow-derived DCs and DC-based vaccines

Bone marrow precursors isolated from the tibias and femurs of mice were cultured for 5 days in CM supplemented with 1000 U/mL rIL-4 and 1000 U/mL rGM-CSF (both from Peprotech) to generate DCs. The resulting DCs were then purified using CD11c microbeads (Miltenyi, Cat. No. 130-108-338) according to the manufacturer's instructions. To generate DC/adenovirus-based vaccines, purified DCs were infected with rAd.mIL-12p70 at a multiplicity of infection (MOI) of 50, alone or in combination with or rAd.mDLK1 or rAd.mDLK2 (MOI = 100 each) and cultured for 2 days in rIL-4 and rGM-CSF supplemented CM, prior to harvest and use as

vaccines. All recombinant adenoviral vectors were produced and provided by the University of Pittsburgh Cancer Institute's Vector Core Facility (a shared resource). To generate DC/peptide-based vaccines, DCs transduced with Ad.mIL-12p70 (DC.IL12; as described above) were pulsed with a pool of the $DLK1_{158–166}$, $DLK1_{161–169}$, and $DLK1_{259–270}$ peptides (10 μM each; ref.[302]) for 2 hours. DLK1 peptides were synthesized by the University of Pittsburgh Cancer Institute's Peptide Synthesis Facility (a shared resource) and analyzed for purity by the University of Pittsburgh Cancer Institute's Protein Sequencing Facility (a shared resource).

3.3.3 Generation of recombinant lentiviral vector

Lentiviral vectors (lv) encoding mDLK1 (lvDLK1), mDLK2 (lvDLK2) and a reverse RGS5 sequence (used as a negative control vector designated as lvNEG) were generated as previously described [302]. Briefly, full-length murine DLK1, DLK2, and reverse RGS5 (control) were cloned into pLenti6/V5 D-TOPO using the Lentiviral Directional TOPO Expression Kit (Invitrogen, Cat. No. K495000). To produce the lentiviral vectors, 293FT cells (Invitrogen, Cat. No. R700-07) were transfected with the pLenti plasmids with DLK1, DLK2 or control inserts using ViraPower Packaging Mix (Invitrogen, Cat. No.44-2050) combined with Lipofectamine 2000 (Invitrogen, Cat. No. 11668019) according to the manufacturer's instructions. The lentiviral vectors were collected using a Fast-Trap Virus Purification and Concentration kit (Millipore, Cat. No. FTLV00003) 48 hours after the transduction. Lentiviral titers were determined via blasticidin-resistance assay (Invitrogen, Cat. No. R210–01) in HT1080 cells (kindly provided by Dr. Chuanyue Wu, University of Pittsburgh, Pittsburgh, PA) according to the manufacturer's instructions.

3.3.4 Animal experiments

Balb/c mice received subcutaneous (s.c.) injection of 10^6 RENCA cells on the right flank. Six days after tumor inoculation, the animals were randomized into cohorts of five mice, with each cohort exhibiting comparable mean tumor sizes. For the DC/peptide-based vaccine experiments, RENCA-bearing mice were injected s.c. on the left flank (i.e. contralateral to tumor) with 100 μl PBS, 10^6 DC.IL12 or 10^6 DC.IL12 that had been pre-loaded with an equimolar (10 μM) mixture of DLK1 peptides on Days 7 and 14 post-tumor inoculation. For the lentiviral vaccine experiments, RENCA-bearing mice (on day 10 post-tumor inoculation) received intradermal injection of 50 μL PBS, 10^4 transduction units (TU) of lvNEG, 10^4 TU lvDLK1, 10^4 TU lvDLK2 or 10^4 TU lvDLK1 + 10^4 TU lvDLK2. The dose of 10^4 TU was selected for analysis based on previous results using lvDLK1-based therapeutic vaccines in the RENCA model [302]. For the checkpoint inhibitor experiments, 200 μg PD-L1 blocking antibody (BioXCell, Cat. No. BE0101) was administered via i.p. injection into lentivector-vaccinated RENCA-bearing mice on days 7, 10, 13, and 17 after tumor injection. C57BL/6 mice received s.c. injections of 10^5 B16-F10 cells on the right flank. Six days post-tumor inoculation, the animals were randomized into cohorts of five. On days 7 and 14 post-tumor inoculation, tumor-bearing mice received s.c. injection of 100 mL PBS, 10^6 DC.IL12, 10^6 DC.IL12.DLK1, 10^6 DC.IL12.DLK2 or 10^6 DC.IL12.DLK1 + 10^6 DC.IL12.DLK2 on their left flank. Tumor size was assessed every 3-4 days using a vernier caliper. Data are reported as mean tumor area ± SEM.

3.3.5 Stromal cell isolation

Kidneys and tumors were isolated from control or vaccinated mice 21 days after initial tumor inoculation. After the tissues were mechanically minced and enzymatically digested with 0.5 mg/mL collagenase IA (Sigma, Cat. No. C5894), 0.5 mg/mL collagenase II (Sigma, Cat. No. C1764), 0.5 mg/mL collagenase IV (Sigma, Cat. No. C1889), and 20 U/mL DNase I (Sigma, Cat. No. D5025), the resulting single cell suspensions were labeled with anti-mouse CD45-APC (BD Biosciences, Cat. No. 559864), anti-mouse CD34-FITC (eBioscience, Cat. No.11-0341-82), and anti-mouse CD146-PE (BD Biosciences, Cat. No. 562196). The cells were flow sorted into pericytes ($CD45^{neg}CD34^{neg}CD146^{+}$) and VECs ($CD45^{neg}CD34^{+}CD146^{+}$) using a FACSAria II Cell Sorter (BD Biosciences). Sorted cells were > 95% pure for the specified phenotype.

3.3.6 Real time PCR

Messenger RNA from whole murine RCC tumors and murine kidney- and murine RCC-associated pericytes and VECs was isolated using the RNeasy Plus Micro kit (Qiagen, Cat. No. 74034) according to the manufacturer's instructions. cDNA was then generated from the RNA samples using the High Capacity RNA-to-cDNA kit (Applied Biosystems, Cat. No. 2017-08-31) and real-time PCR was performed using the Fast SYBR Green Master Mix (Applied Biosystems, Cat. No. 2017-07-31). PCR reactions were performed in duplicate on a StepOnePlus real-time PCR thermocycler (Applied Biosystems) using the primers listed in **Table 1** and cycling conditions of 95°C for 20 minutes, then 40 cycles of 95°C for 3 seconds and 60°C for 30 seconds followed by post-amplification melting curve analysis at 95°C for 15 seconds and 60°C for 1

minute. Assays were normalized to HPRT1 gene (Qiagen, Cat. No. 249900) and the results were analyzed by the $2^{-\Delta\Delta Ct}$ method.

Table 1. qPCR primers

Primer name	**Sequence**
mDLK1 forward	TGTGACCCCCAGTATGGATT
mDLK1 reverse	CCAGGGGCAGTTACACACTT
mDLK2 forward	GCCTGCCAGAGCGGATGAC
mDLK2 reverse	CACACCTGCAGGAGCCGTC
mPDGFR forward	GACATTGAGTCCCCCAGCTA
mPDGFRb reverse	GAGCACTGGTGAGTCGTTGA
Igf1r forward	CTGATGTCTGGTCCTTCGGG
Igf1r reverse	CACCCTCCATGACGAAACGA
Vegfr1 forward	TACCTCACCGTGCAAGGAAC
Vegfr1 reverse	AAGGAGCCAAAAGAGGGTCG
Vegfr2 forward	GCTCATCATCCTAGAGCGCA
Vegfr2 reverse	ATGGTCTCGCCAATGGTTGT
Vegfr3 forward	GATGCTGAAAGAGGGCGCTA
Vegfr3 reverse	ACGTTGAGATGGTTGCCGAT

3.3.7 Fluorescent imaging of tumors

Tumor tissue samples were fixed in 2% paraformaldehyde for 2 hours and dehydrated in 30% sucrose for 24 hours at 4°C. Six-micron tissue sections were analyzed using specific pAb against mNG2 (gift from Dr. William Stallcup, Sanford Burnham Prebys Medical Discovery Institute), mDLK1 (Santa Cruz Biotechnology, Cat. No. sc-25437), mDLK2 (Aviva Systems Biology, Cat. No. ARP49784_P050), mCD31 (BD Biosciences, Cat. No.550274), mVCAM1 (R&D, Cat. No. AF643), mNICD1 (Abcam, Cat. No. ab8925), mHes1 (Miltenyi, Cat. No. AB5702), and mCD8 (BD Biosciences, Cat. No. 558733) paired with secondary antibodies donkey anti-guinea pig Cy3 (Jackson ImmunoResearch, Cat. No. 706-165-148), donkey anti-goat Cy3 (Jackson ImmunoResearch, Cat. No. 705-165-147), donkey anti-rabbit Alexa Fluor 488 (Molecular Probes, Cat. No. A-21206) or donkey anti-rat Alexa Fluor 488 (Molecular Probes, Cat. No. A-21208) via immunofluorescence microscopy using a cold CCD camera (Olympus Magnafire; Olympus; Olympus, Central Valley, PA) to collect wide-field images. The Metamorph software (Molecular Devices, Downingtown, PA) was used to determine fluorescence signals over background and to measure individual structures as the integration of pixels (total number of positive pixels in structure above background) multiplied by the brightness of each pixel in grey scale. The same software was used to measure co-localization of specific labeled markers.

3.3.8 *In vitro* evaluation of Ag-specific $CD8^+$ T cell responses

To evaluate specific $CD8^+$ T cells responses in vaccinated tumor-bearing mice, spleens were harvested from animals 14 days after lentiviral injection or 7 days after the second DC/adenovirus vaccination. Splenocytes were re-stimulated *in vitro* with syngeneic DCs

transduced with mDLK1 and mDLK2 recombinant adenovirus for 5 days (1:10 DC:splenocyte ratio). Afterwards, $CD8^+$ T cells were isolated from the splenocytes using a $CD8^+$ T cell enrichment kit (Stemcell Technologies, Cat. No. 19753A) and were then assessed for antigen-specific secretion of IFN-γ (Mabtech, Cat. No. 3321-3-1000 and 3321-6-250) or granzyme B (R&D, Cat. No. SEL1865) via ELISPOT, or by intracellular staining for IFN-γ (BD Biosciences, Cat. No. 554714) and flow cytometry according to manufacturer's protocol. To test for anti-DLK1 and anti-DLK2-specific responses, syngeneic DCs transduced with rAd encoding mDLK1 or mDLK2, respectively, were used as target cells. To test for Ag-specific responses in melanoma models, C57BL/6 DCs were pulsed with 1 μM human $gp100_{25\text{-}33}$ (Anaspec, Cat. No. AS-62589) or 1 μM mouse $TRP2_{180\text{-}188}$ (AnaSpec, Cat. No. AS-61058), and used as stimulator cells. As positive controls, purified T cells or splenocytes were stimulated with 2 μg/mL conA (Sigma, Cat. No. C0412) or 0.5 μg anti-mCD3e antibody (eBioscience, Cat. No. 16-0031-82) along with 0.5 μg anti-mCD28 antibody (eBioscience, Cat. No. 16-0281-82).

3.3.9 Flow cytometry

Spleens and tumors were harvested from mice 14 days after lentiviral injection or 7 days after the second DC/adenovirus vaccination, with single-cell suspensions then prepared as previously described (9,10). Fluorescently-labeled antibodies against the following target molecules were used for cell surface staining: CD3e-BUV395 (BD Biosciences, Cat. No. 563565), CD4-PEDazzle (Biolegend, Cat. No. 100566), CD8a-FITC (BD Biosciences, Cat. No. 553031), CD8-PECy7 (BD Biosciences, Cat. No.552877), CD11b-APC (eBioscience, Cat. No.17-0112-82), Gr-1-PE (BD Biosciences, Cat. No. 553128), PD-1-FITC (eBioscience, Cat. No. 11-9985-81), and PD-L1-PE (Biolegend, Cat. No. 124308). Cell staining was performed in FACS buffer (PBS

with 5% FBS and 0.1% NaN_3). To stain for intracellular cytokine, the BD Cytofix/Cytoperm kit (BD Biosciences, Cat. No. 554714) was used with anti-IFNγ-PE (BD Biosciences, Cat. No. 554412). To stain for intracellular transcription factors, FoxP3/Transcription factor staining buffer set (eBioscience, 2017-11) was used with the anti-FoxP3-APC (eBioscience, Cat. No.17-5773-82) and anti-Tbet-APC (Biolegend, Cat. No. 644814) antibodies.

3.3.10 Statistical Analyses

Comparisons between groups were performed using a two-tailed Student's t-test or analysis of variance (ANOVA; one-way or two-way) with Tukey's *post-hoc* analysis. All data were analyzed using GraphPad Prism software, version 6.07 (GraphPad Software, Inc., La Jolla, CA). Differences between groups with a P value <0.05 were considered significant.

3.4 RESULTS

3.4.1 Treatment of RENCA tumor-bearing mice with DLK1 peptide-based vaccine leads to a compensatory increase in DLK2 expression in tumor-associated pericytes

We have previously reported that pericytes within murine RENCA and melanoma TME overexpress DLK1 protein when compared to their normal tissue counterparts, permitting the differential recognition of tumor-associated pericytes by DLK1-specific $CD8^+$ T cells (Chapter 2; [197, 302]). Indeed, treatment of RENCA-bearing Balb/c mice with DC/DLK1 peptide-based vaccines or lentivirus-based DLK1 genetic vaccines effectively promote the activation and recruitment of Type-1 anti-DLK1 $CD8^+$ TIL in concert with removal of $DLK1^+$ target cells in the TME and delayed tumor growth (Chapter 2; [302]). Since DLK1 and its homolog, DLK2, both function as Notch antagonists and may counter-regulate each other's expression [252], we first investigated DLK2 expression in the tumor stroma of untreated versus DLK1-vaccinated mice. We confirmed that RENCA-bearing mice receiving DC/DLK1 peptide-based vaccines on days 10 and 17 post-tumor inoculation exhibited slowed disease progression when compared with cohorts of animals that were left untreated or that had been treated with DC control (no peptide) vaccines (**Figures 15a and 15b**). To determine whether DLK2 was differentially expressed by pericytes and VECs in tumor vs. (tumor-uninvolved) kidneys +/- treatment, tissues were enzymatically-digested, with each cell type was then isolated from single-cell suspensions by fluorescence-activated cell sorting (**Figure 15c**). mRNA was extracted from the sorted cells and real-time PCR was performed to quantify the amount of *DLK2* transcript in each sample. We observed that *DLK2* transcript was minimally expressed by pericytes and VECs sorted from normal kidneys and untreated RENCA tumors. However, *DLK2* mRNA was enriched in tumor-

associated pericytes isolated from animals that had been vaccinated against DLK1 (**Figure 15d**). This observation was confirmed in immunofluorescence microscopy analysis of tumor sections, where DLK2 protein was selectively (co)expressed with $NG2^{+}$, a marker that is specifically expressed by pericytes but not by RENCA cells [302], within the TME of DLK1-vaccinated mice. DLK2 was not expressed within the tumors of mice in any other treatment cohort (**Figure 15e**). These data suggest that DLK2 may represent a "covert" antigen expressed by tumor-associated vascular pericytes that can be therapeutically targeted in the cancer setting, particularly under conditions in which DLK1 expression is silenced (i.e. as a consequence of targeted vaccination).

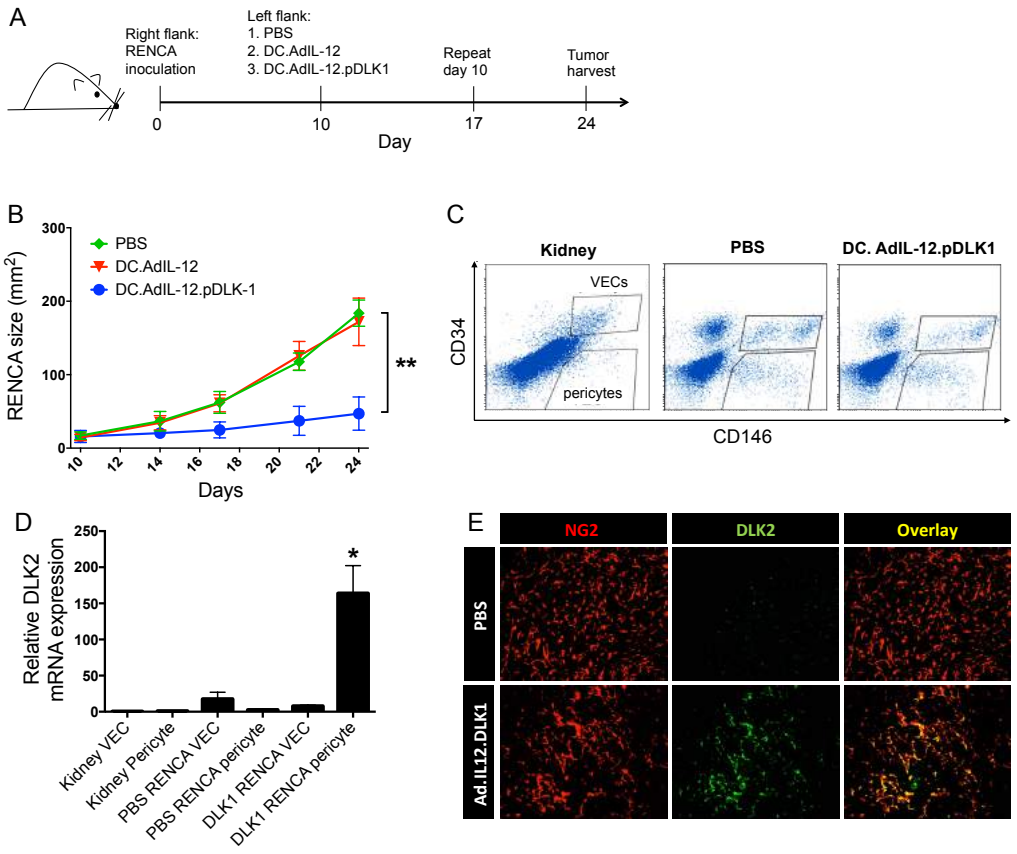

Figure 15. Vaccination of RENCA-bearing mice against DLK1 results in slowed tumor growth, the loss of DLK1+ pericytes in the TME, and a compensatory increase in DLK2 expression by tumor-associated vascular pericytes.

(A) Female Balb/c mice with established day 10 s.c. RENCA tumors on their right flanks were treated with s.c. injection (left flank) of PBS, 10^6 DCs transduced with rAd.IL12 (i.e. DC.IL12) or DC.IL12 pulsed with DLK1-derived peptide epitopes (i.e. DC.IL12.DLK1) per Materials and Methods. An identical s.c. booster vaccination was provided on day 17 post-tumor inoculation. **(B)** Tumor growth was monitored every 3-4 days and is reported as the mean ± SEM for 5 animals per group. *$P < 0.05$, two-way ANOVA. **(C)** On day 21, tumor tissues and (tumor-uninvolved kidneys from matched animals) were harvested and then digested mechanically and enzymatically as described in the Materials and Methods, yielding single-cell suspensions. Live cells (DAPI negative) cells were flow-sorted to select for $CD45^-CD146^+CD34^-$ pericytes and $CD45^-CD146^+CD34^+$ VEC populations. **(D)** Total mRNA was isolated from sorted populations of pericytes and VECs and analyzed for DLK2 expression by quantitative real-time PCR. Relative mRNA expression was normalized to HPRT1 expression. *$P < 0.05$, one-way

ANOVA compared with kidney pericyte DLK2 levels. In **(E)**, RENCA tissue sections were analyzed for expression of DLK2 (green) in $NG2^{+}$ pericytes (red) by immunofluorescence microscopy. Scale bar = 1mm. All data are representative of those obtained in 2 independent experiments.

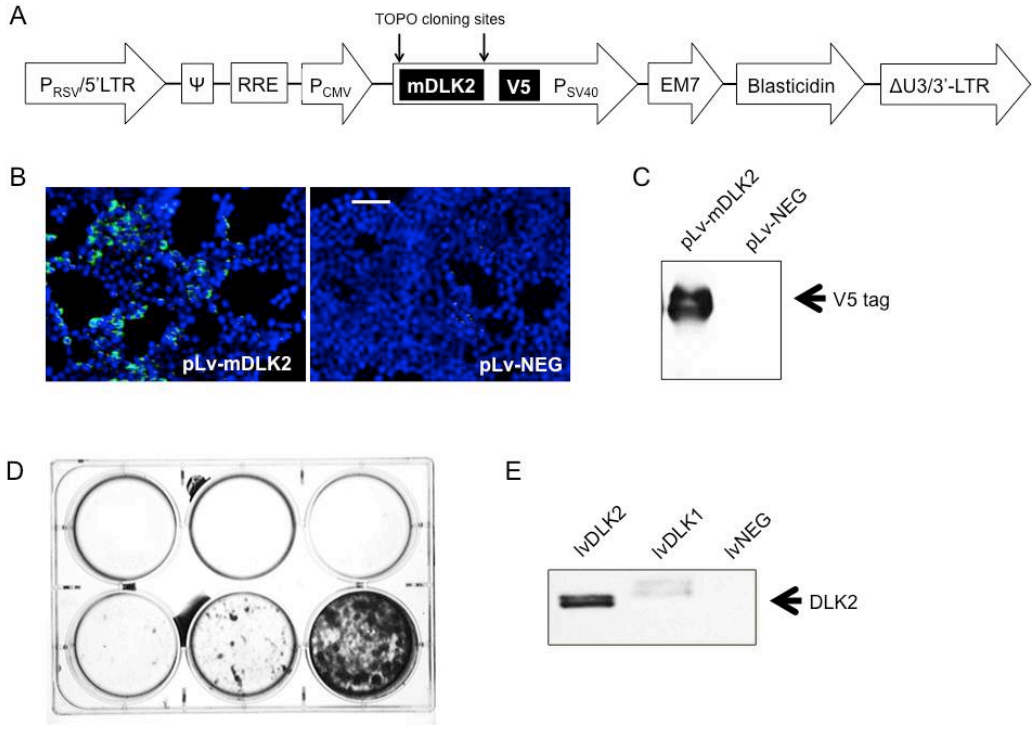

Figure 16. Production of recombinant lvDLK2 lentivirus.

(A) Schematic of the plasmid construct encoding full-length murine DLK2. The plasmid contains the following elements: pRSV/5' LTR, RSV LTR and HIV LTR chimeric promoter, HIV psi (Ψ) packaging sequence, HIV Rev response element (RRE), CMV promoter, full length murine DLK2 gene with V5 reporter tag, SV40p early promoter and origin, EM7 promoter, blasticidin gene,ΔU3/HIV 3′LTR self-inactivating system. This plasmid was subsequently transfected into 293T cells and the resulting cells analyzed for V5 protein expression by **(B)** immunofluorescence microscopy and **(C)** western blotting. Lentiviral vectors recombinant for murine DLK2 were then generated and used to infect HT-1080 cells. Live functional virus was confirmed by the **(D)** formation of blasticidin-resistant colonies imaged after crystal violet staining and by **(E)** western blotting for DLK2 after specific lentiviral infection with lvDLK2 vs. control virus (lvDLK1 or lvNEG). All data are representative of those obtained in 3 independent experiments in (**B-D**). Scale bar = 1 mm

3.4.2 Coordinate vaccination with lvDLK1 + lvDLK2 provides superior therapeutic benefit against established RENCA tumors

To test the hypothesis that therapeutic vaccination against both DLK1 and DLK2 would yield greater protection against tumor progression vs. single antigen-based vaccines, recombinant lentiviral vectors encoding full-length murine DLK1 (lvDLK1) or DLK2 (lvDLK2) were generated (**Figure 16**). Based on a previous report that single intradermal (i.d.) injection of a lentiviral vector-based vaccine results in sustained anti-tumor $CD8^+$ T cell responses *in vivo* [277], we performed a single i.d. injection of lentiviral vectors (lvDLK1 +/- lvDLK2 or the lvNEG negative control virus) 7 days after the s.c implantation of RENCA tumor cells. Vaccines were provided on the contralateral flank to that in which the tumor was placed. Untreated animals were included as a negative control cohort. We then monitored tumor growth progression and specific T cell responses across all treatment groups. Consistent with our previous report [302], we confirmed that lvDLK1-based vaccination inhibited tumor growth (**Figure 17a**). However, tumor growth was inhibited to a greater degree in animals treated with the combined lvDLK1 + lvDLK 2 vaccine. Notably, therapeutic vaccination against DLK2 alone failed to impact tumor growth. As the target DLK2 protein was not highly-expressed in RENCA tumors unless DLK1 expression was first silenced in tumor pericytes (**Figures 15d, 15e, 17e**), this result might merely reflect the lack of a salient target within the TME for recognition by DLK2 vaccine-induced $CD8^+$ T cells in mice vaccinated using only lvDLK2. Overall, we observed that the extent of tumor growth inhibition was associated with the degree of $CD8^+$ TIL infiltration, with the most robust $CD8^+Tbet^+$ T cell infiltrates observed in the lvDLK1 + lvDLK2 treatment cohort (**Figures 17b and 17c**).

We observed that increased $CD8^+$ T cell infiltration of tumors in lvDLK1- and lvDLK1 + lvDLK2-vaccinated animals was associated with a significant decline in $NG2^+$ pericytes within the TME (**Figure 17b**). These results are consistent with a model in which our lentivirus-based vaccines promote the activation of specific $CD8^+$ T cells that target $DLK1^+/DLK2^+$ ($NG2^+$) tumor-associated pericytes *in vivo*. To further monitor antigen-specific $CD8^+$ T cell responses after lentivirus-based vaccination, DCs transduced with recombinant adenovirus encoding full-length mDLK1 or mDLK2 were used to (re)stimulate splenocytes harvested from control or lv-treated animals *in vitro* for 5 days. $CD8^+$ T cells were then isolated from these cultures and DLK1- and DLK2-specific responses were subsequently analyzed in IFN-γ ELISPOT assays. We found that when applied individually, the lvDLK1 and lvDLK2 vaccines promoted DLK1- or DLK2-specific responses, respectively. Predictably, the combination lvDLK1 + lvDLK2 vaccine induced both DLK1- and DLK2-specific $CD8^+$ T cell responses in treated animals (**Figure 17d**). We were also able to confirm the induction of DLK1-specific $CD8^+$ T cell responses in the lvDLK1 and lvDLK1 + lvDLK2 treatment cohorts using DC pulsed with defined synthetic DLK1 peptide epitopes [302] as a stimulus in IFN-γ ELISPOT assays **(Figure 18)**.

Following the observation that the lvDLK1 + lvDLK2 vaccination induced the activation of DLK1- and DLK2-specific T cells, we next investigated how the various vaccine formulations affected DLK1 and DLK2 protein expression by cells within the tumor stroma. We determined that DLK1 expression by $NG2^+$ pericytes was diminished after vaccination with lvDLK1 (either alone or in combination with lvDLK2; **Figure 17e**). Vaccination against lvDLK2 alone did not affect DLK1 expression in the TME, however, DLK2 became expressed by $NG2^+$ pericytes after lvDLK1 vaccination (**Figure 17f**). Remarkably, co-vaccination using lvDLK1 and lvDLK2

resulted in NG2^{+} pericytes that failed to express either DLK1 or DLK2 in the therapeutic TME (**Figure 17e, 17f**).

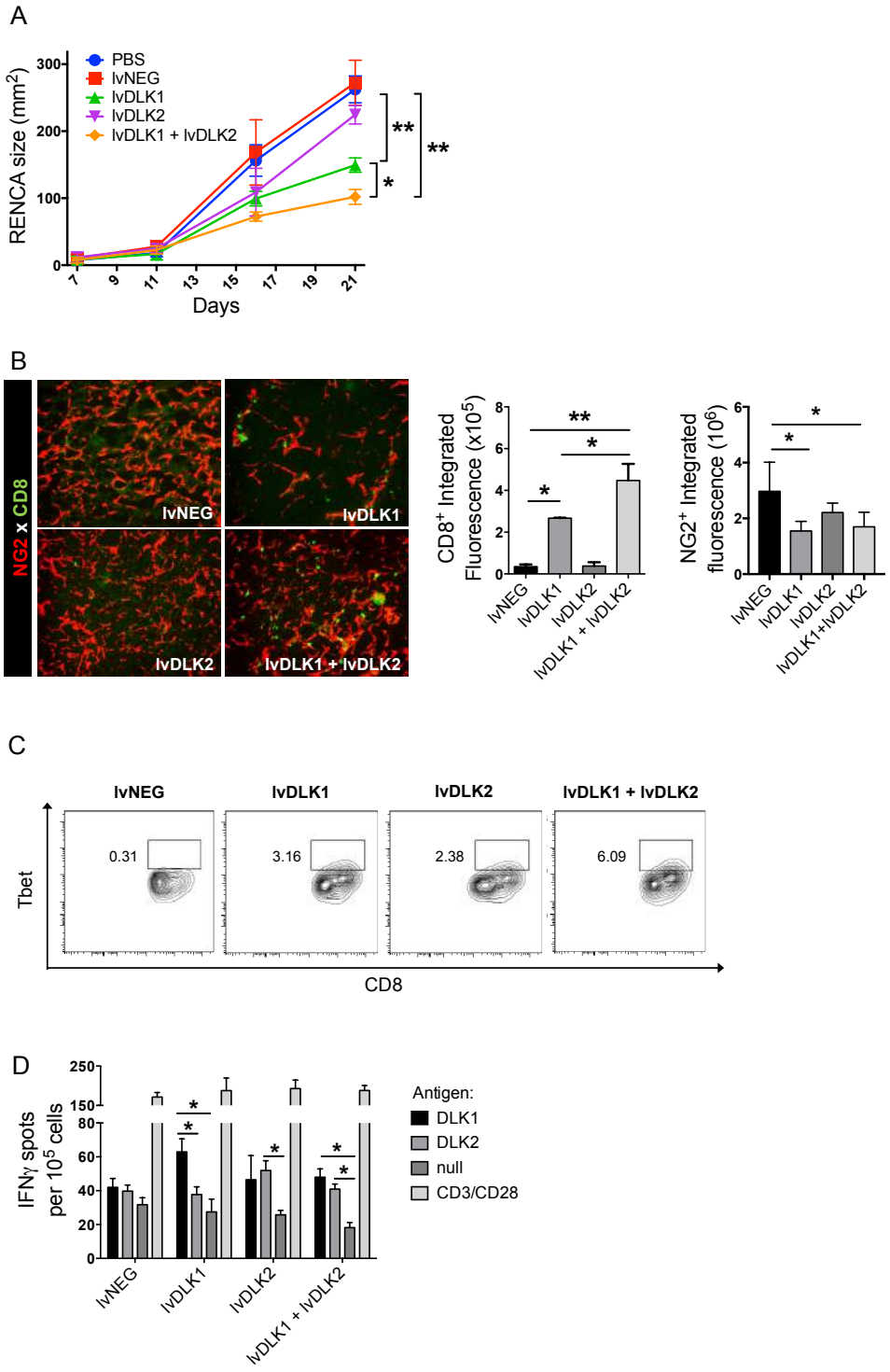

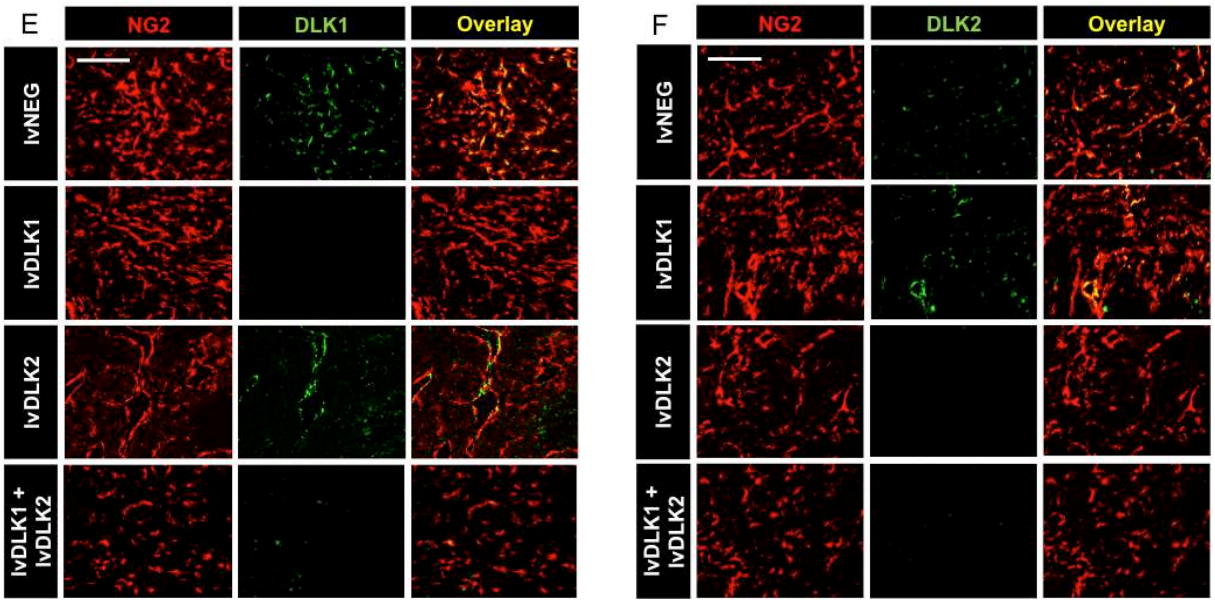

Figure 17. Coordinate vaccination with lvDLK1 and lvDLK2 is immunogenic and therapeutic in the RENCA model.

Female Balb/c mice bearing established day 7 s.c. RENCA tumors were treated with i.d. injection of PBS, 10^4 lvNEG, 10^4 lvDLK1, 10^4 lvDLK2 or 10^4 lvDLK1 + 10^4 lvDLK2. **(A)** Tumor growth was monitored every 3-4 days through day 20, at which time the animals were euthanized. Tumor sizes are reported as the mean ± SEM for 5 animals per group. $*P < 0.05$, two-way ANOVA. Tumors were then harvested to generate tumor sections or they were mechanically/enzymatically-digested to generate single-cell suspensions. **(B)** Tumor sections were analyzed by immunofluorescence microscopy for $NG2^+$ pericytes (red) and infiltrating $CD8^+$ T cells (green). Using Metamorph software (Materials and Methods), $CD8^+$ T cell infiltrates and $NG2^+$ pericytes in the images were quantified and reported as mean integrated fluorescence ± SEM. $*P < 0.05$ and $**P < 0.01$, one-way ANOVA **(C)** Flow cytometry was also performed on the resulting cell suspensions to quantify $Tbet^+$ $CD8^+$ TIL**.** Tumor sections were analyzed for $CD8^+$ TIL (green) infiltration and $NG2^+$ (red) expression. In **(D)**, splenocytes harvested from day 21 tumor-beating mice were stimulated *in vitro* with syngeneic DC infected with rAd.DLK1 (DC.DLK1), rAd.DLK2 (DC.DLK2) or a mixture of both DC populations (i.e. DC.DLK1 + DC.DLK2) for 5 days. Responder T cells were the isolated and restimulated with control or rAd-infected DC as indicated for 18h, and the resultant culture supernatants analyzed for IFN-γ content using a cytokine-specific ELISPOT assay. $*P < 0.05$, one-way ANOVA. In **(E)** and **(F)**, tumor sections were analyzed for $NG2^+$ pericyte co-expression of DLK1 and DLK2, respectively, via immunofluorescence

microscopy. Scale bar = 1mm. Data in A, B, C, E, and F are representative of those obtained in 3 independent experiments. Data in D is representative of 2 independent experiments.

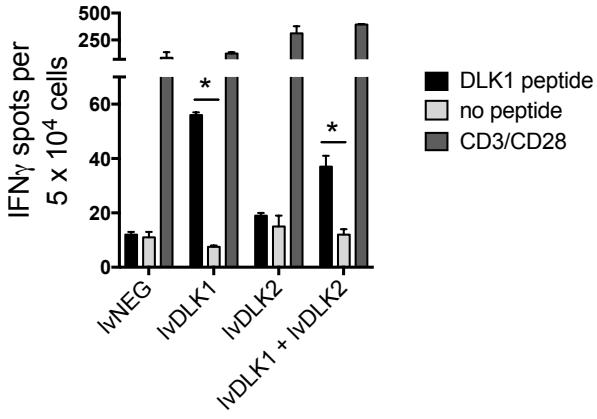

Figure 18. CD8$^+$ T cells in RENCA-bearing mice treated with lvDLK1 or lvDLK1 + lvDLK2 recognize peptide epitopes derived from DLK1.

Female Balb/c mice bearing established day 7 s.c. RENCA tumors were treated with i.d. injection of PBS, 10^4 lvNEG, 10^4 lvDLK1, 10^4 lvDLK2 or 10^4 lvDLK1 + 10^4 lvDLK2. On Day 21, splenocytes harvested from the treated and control mice were stimulated *in vitro* with DCs pulsed with a pool of the $DLK1_{158–166}$, $DLK1_{161–169}$, and $DLK1_{259–270}$ peptide epitopes (10 μM each) for 5 days. Responder CD8$^+$ T cells were the isolated and re-stimulated with DC (no peptide; negative control), DLK1 pooled peptide-pulsed DC or anti-CD3/CD28 (positive control) for 18h in IFN-γ ELISPOT assays. Results are reported as the mean +/- SD of triplicate determinations. *$P < 0.05$. Data are representative of those obtained from 2 independent experiments performed.

Since TBVA are overexpressed in the TME of solid cancers independent of tumor histology [197], TBVA-based vaccines should offer therapeutic benefit against a wide range of vascularized tumors, leading us to next evaluate the anti-tumor efficacy of DLK1- and DLK2-based vaccines against (RENCA-unrelated) B16 melanomas established s.c. in C57BL/6 mice (**Figure 19a**). Syngenic DCs were infected with recombinant adenovirus encoding full-length DLK1 and/or DLK2 for 48h *in vitro*, then injected s.c. in the contralateral flank to that

containing a progressively growing B16 melanoma. An identical booster vaccine was administered one week later. We observed that the combined DLK1 + DLK2-based vaccine yielded optimal anti-tumor efficacy in association with the induction of the most robust antigen-specific $CD8^+$ T cell responses (**Figure 19b**). Furthermore, we noted that successful vaccination against DLK1/DLK2 in these animals was also associated with the development of $CD8^+$ T cell responses against the (vaccine-unrelated) melanoma antigen gp100 (**Figure 19c**), presumably via an "epitope spreading" mechanism.

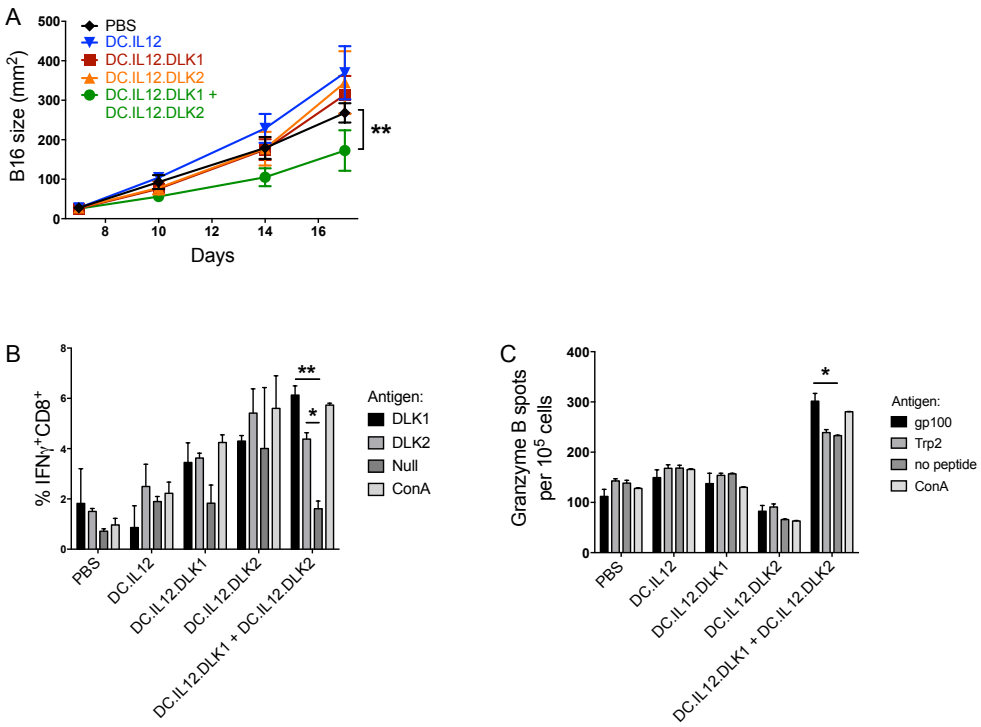

Figure 19. Combined vaccination against DLK1 and DLK2 provides superior therapy benefit against established s.c. B16 melanomas.

On days 7 and 14 post-s.c. inoculation of B16 melanoma cells, mice were injected s.c. on the contralateral flank with 10^6 DC transduced with a recombinant adenovirus encoding murine (DC.IL12) +/- recombinant adenoviruses encoding murine DLK1 (DC.IL12.DLK1) or murine DLK2 (DC.IL12.DLK2) or both DLK1 and

DLK2 (DC.IL12.DLK1 + DC.IL12.DLK2). (A) B16 tumor growth was monitored and measured every 3-4 days, with tumor size reported as mean ± SEM (n = 5 mice/group). Splenocytes were harvested from the animals on day 17 post-tumor inoculation and analyzed for (B) DLK1- and DLK2-specific $CD8^+$ T cells via intracellular staining for IFN-γ, or for (C) gp100- and Trp2- specific $CD8^+$ T cells using a granzyme B ELISPOT assay as described in Materials and Methods. *P < 0.05 and **P < 0.01. All data are representative of those obtained in 3 independent experiments.

3.4.3 DLK1/DLK2-based vaccines promote VN within the TME

Our ability to drive Type-1 $CD8^+$ T cell responses against tumor-associated vascular pericytes using DLK1/DLK2-based vaccines, allows for the possibility of therapeutically proctoring a state of VN [303]. To investigate this further, tumor sections from treated vs. control mice were stained for the VEC marker CD31 and the pericyte marker NG2 (**Figure 20a**). Adopting the method of Weidner *et al.* [304], we quantified microvessel densities (MVD) and we observed that tumors in mice treated with lvDLK1- or lvDLK1 + lvDLK2-based vaccine exhibited significant vascular pruning when compared to tumors in control or lvDLK2-only vaccinated mice (**Figure 20b**). In addition, when pericyte-VEC co-localization was evaluated in tumor-associated blood vessels, we observed that CD31- and NG2-associated fluorescent signals were also more closely associated with each other in the tumors of mice vaccinated with lvDLK1 or with combined lvDLK1 + lvDLK2 versus tumors in all other treatment cohorts (**Figure 20c**). Collectively, the decreased vascular arborization and increased $NG2^+$ pericyte coverage of $CD31^+$ vessels observed in the tumors of lvDLK1- or lvDLK1 + lvDLK2-treated mice is consistent with therapeutic VN as previously described by Jain [139]. Since tumor VN is also characterized by a loss of hypoxia (and a return to normoxia) within the TME [139, 305], we analyzed treated vs. control tumors for expression of the hypoxia-associated biomarker HIF-2α

[305-307]. We determined that tumors in mice vaccinated with lvDLK1 or (more so) lvDLK1 + lvDLK2 displayed significant reductions in HIF-2α transcript levels versus control-untreated tumors (**Figure 20d**), consistent with therapeutic VN in these treatment cohorts.

We also observed that pro-angiogenic biomarkers were repressed as a consequence of lvDLK1/2-based vaccination. In particular, expression of *VEGFR1* and *VEGFR2* mRNA were significantly reduced in the TME of lvDLK1-treated animals, while transcript levels of *VEGFR1, VEGFR2 and* fibroblast growth factor receptor 1 (*FGFR1*) were coordinately decreased in the TME of mice treated with the combined lvDLK1 + lvDLK2 vaccine (**Figure 20e**).

Lastly, combined vaccination against DLK1 and DLK2 led to an increase in expression of vascular cell adhesion molecule-1 (VCAM1) by tumor-associated VECs (**Figure 20f**), consistent with improved tumor infiltration by Type-1 ($Tbet^+$) $CD8^+$ T cells (**Figure 17b, 17c**).

3.4.4 lvDLK1 + lvDLK2-based vaccination decreases frequencies of immunosuppressive cell populations in the TME.

Tumor-associated hypoxia plays a critical role in the maintenance and regulatory activity of myeloid-derived suppressive cells (MDSC), as well as, regulatory T (Treg) cells in the TME [308]. As VN mitigates hypoxia in the TME (**Figure 20d**; ref. [139, 302]), one might predict that vaccines promoting VN would recondition the immunologic landscape within tumors to become less suppressive. We examined this hypothesis in the TME of mice receiving vaccine-based therapy and found that levels of both MDSC (**Figure 21a**) and Tregs (**Figure 21b**) were reduced to a greater extent in the tumors of mice treated with combined lvDLK1 + lvDLK2 vaccination versus all other treatment cohorts.

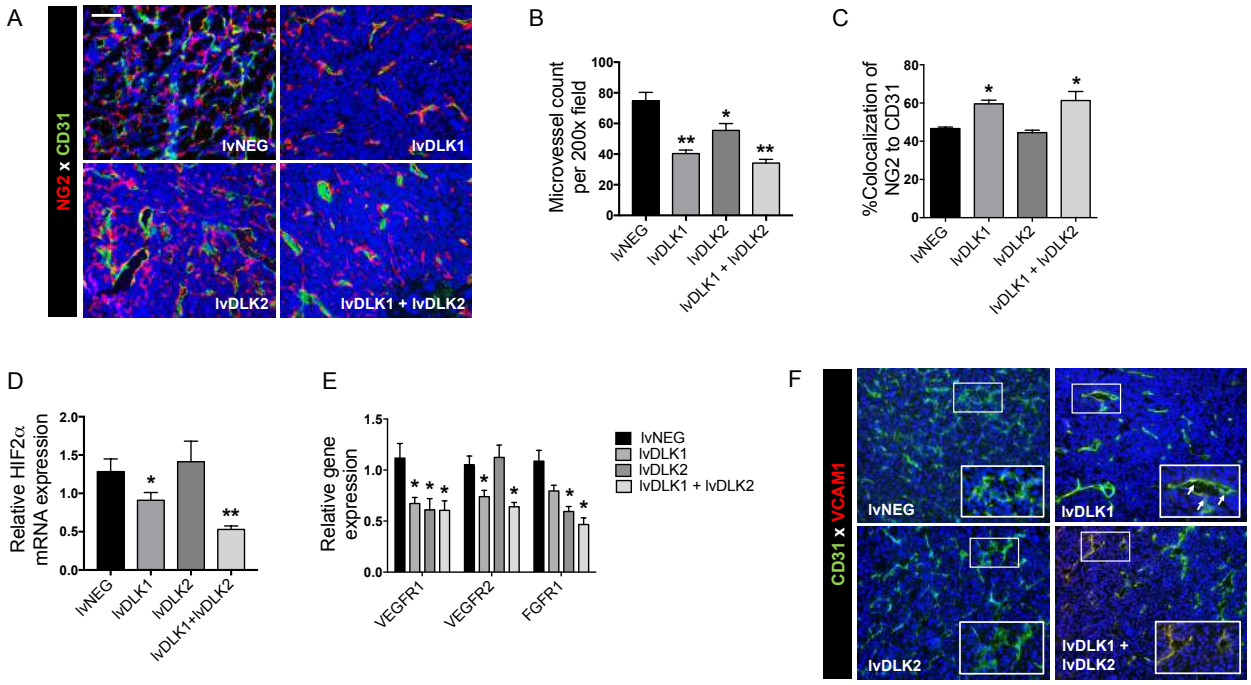

Figure 20. Coordinate vaccination with lvDLK1 and lvDLK2 results in tumor VN.

(A) RENCA tumor sections from **Fig. 15** were stained for $NG2^+$ pericytes (red) and $CD31^+$ VECs (green) to characterize blood vessel morphology. **(B)** Mean vessel density was determined by quantitating distinct (green) VECs or VEC clusters. **(C)** Colocalization of $NG2^+$ (red) pericytes and $CD31^+$ (green) VECs was determined using Metamorph software. **(D-E)** RNA extracted from Day 21 RENCA tumors was analyzed for *HIF2α, VEGFR1*, *VEGFR2*, and *FGFR1* transcript levels by quantitative real-time PCR. In **(E)**, tumor $CD31^+$ VEC (green) were analyzed for co-expression of VCAM1 (red) by immunofluorescence microscopy. Scale bar = 1mm. $*P < 0.05$ and $**P < 0.01$, one-way ANOVA compared to the negative control (lvNEG). All data are representative of those obtained in 3 independent experiments.

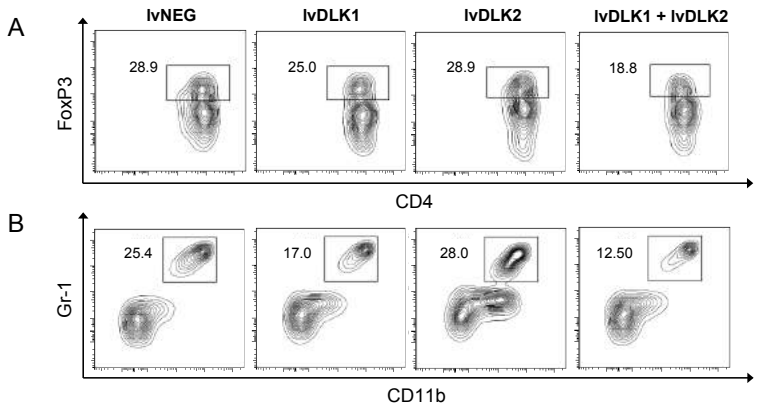

Figure 21. Coordinate vaccination with lvDLK1 and lvDLK2 results in a superior level of reduction in Treg and MDSC content in the therapeutic TME.

Day 21 tumors from untreated or treated mice per **Fig. 1** were dissociated into single-cell suspensions and analyzed by flow cytometry for **(A)** $CD11b^{+}Gr1^{+}$ MDSC and **(B)** $FoxP3^{+}CD4^{+}$ Treg populations. Data are representative of those obtained in 3 independent experiments.

3.4.5 lvDLK1 + lvDLK2-based vaccination combined with PD-L1 blockade further enhances therapeutic efficacy.

Cancer vaccines have previously been shown to be both safe and immunogenic, but rarely curative, based on a variety of immune escape mechanisms employed by residual tumor cells, including elevated expression levels of immune checkpoint/co-inhibitory molecules [309, 310]. Transcript analysis of RENCA tumors vs. normal kidney tissue (from tumor-matched animals) revealed that RENCA tissues overexpress a number of co-inhibitory receptors including B7H3, Gal9, PD-L1 and PD-L2 (**Figure 22a**) that would be expected to negatively impact anti-tumor $CD8^{+}$ T cell activity *in vivo* [309, 310]. Consistent with the known capacity of IFNγ to upregulate PD-L1 expression in some tumors [311], we observed that culturing RENCA cells in media supplemented with rmIFNγ resulted in increased PD-L1 expression (**Figure 22b**).

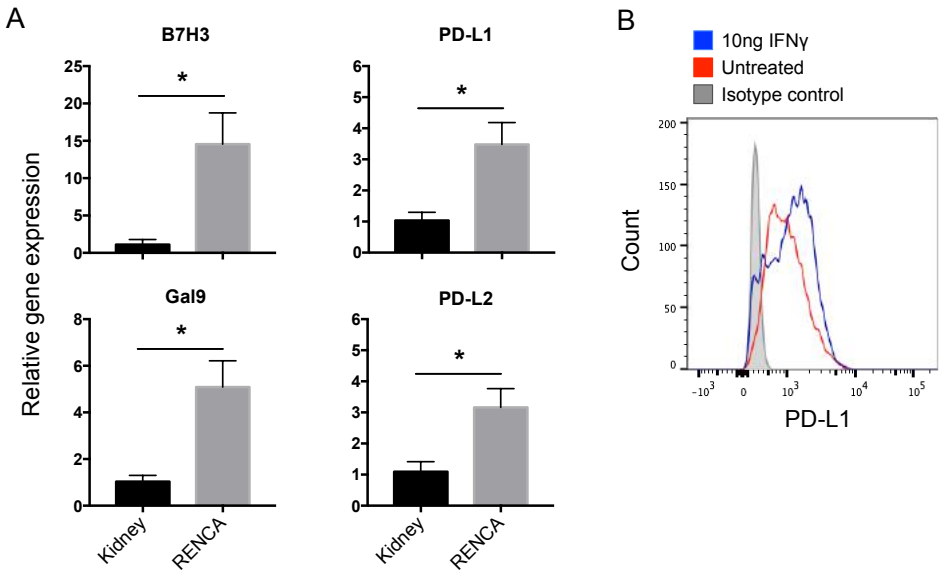

Figure 22. Expression of co-inhibitory molecules in RENCA tumors in vivo.

(**A**) Female Balb/c mice (n=3) were inoculated s.c. with $1x10^6$ RENCA cells and were left untreated. On Day 21, RNA was extracted from harvested tumors and analyzed for expression of B7H3, Gal9, PD-L1, and PD-L2 transcripts via real-time PCR. $*P < 0.05$. (**B**) RENCA cells were incubated in complete RPMI media supplemented with 10 ng/ml rmIFN-γ. After 24 hours, tumor cells were harvested and analyzed for PD-L1 expression via flow cytometry. The presented data are representative of those obtained in 2 independent experiments.

Since we noted a dramatic influx of inflammatory $CD8^+$ TIL in RENCA tumors sponsored by combined lvDLK1 + lvDLK2 vaccination (**Figures 17b, 17c**), we next evaluated PD1 and PD-L1 protein expression levels on TIL and tumors, respectively, in treated vs. control tumor-bearing mice. We found that PD1 protein expression on $CD8^+$ TIL was comparable across all cohorts (**Figure 23a**). On the other hand, PD-L1 protein expression on tumor cells was upregulated in lvDLK1- and lvDLK1 + lvDLK2-vaccinated mice when compared with mice in the other treatment cohorts (**Figure 23b**). Based on these findings, we next investigated the therapeutic benefit of combining lvDLK1 + lvDLK2-based vaccination with systemic delivery of an antagonist anti-PD-L1 antibody. We observed that the degree of RENCA growth inhibition

was greatest in animals that received the combined lvDLK1/lvDLK2 + anti-PD-L1 antibody treatment regimen versus cohorts of tumor-bearing mice receiving either the lvDLK1/lvDLK2 vaccine alone or anti-PD-L1 monotherapy (**Figure 23c**). This superior level of anti-tumor efficacy was association with the greatest magnitude of increased recruitment/maintenance of Tbet^{+} CD8^{+} T cells within the TME (**Figure 23d**) and the greatest degree of reduction in CD4^{+}FoxP3^{+} TIL (**Figure 23e**).

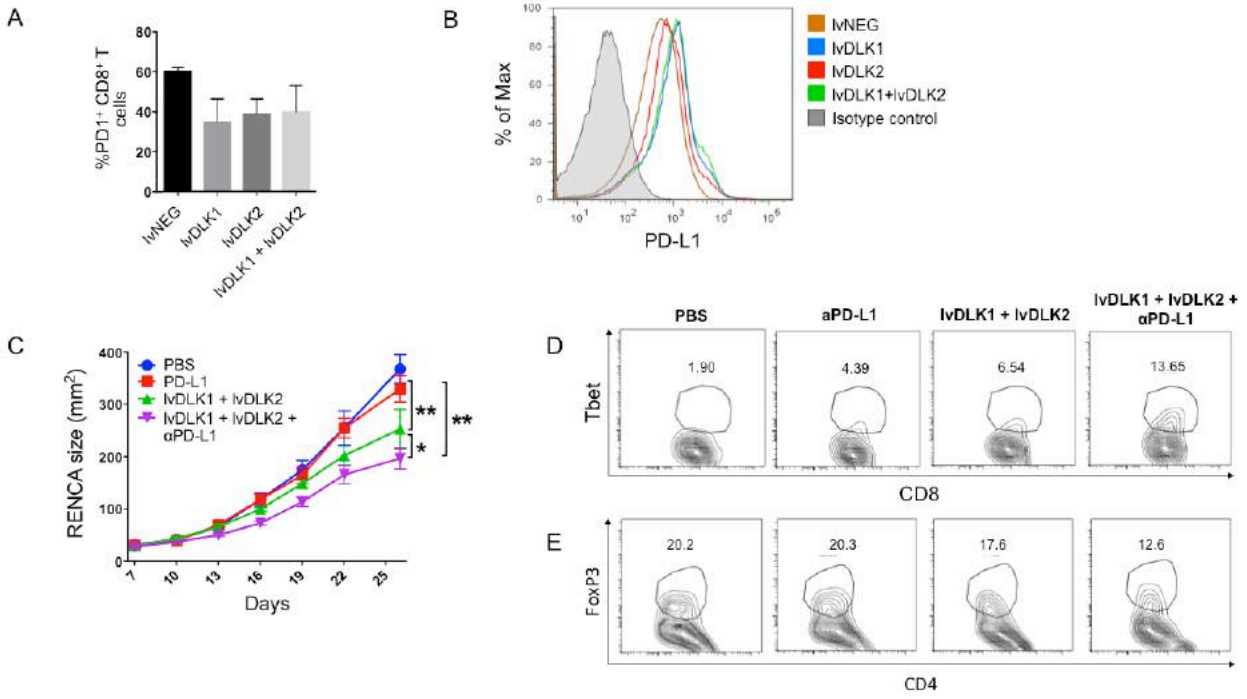

Figure 23. PD-L1 blockade fails as a monotherapy against RENCA tumors, but improves the anti-tumor efficacy of combined lvDLK1 + lvDLK2 vaccination.

(A) CD8^{+} TILs and **(B)** bulk RENCA single-cell suspensions (per **Fig. 1**) were analyzed for expression of PD-1 and PD-L1, respectively, by flow cytometry. In (**C**), mice bearing established day 7 RENCA tumors (right flank) were vaccinated i.d. with lvDLK1 + lvDLK2 (left flank) as a therapeutic vaccine. Anti-mPD-L1 blocking antibody was injected i.p. on days 7, 10, 13, and 17 post-tumor inoculation as described in Materials and Methods. Tumor growth was monitored longitudinally and is reported as the mean ± SEM for 5 animals per group. In (**D**), RENCA tumors

were harvested on day 26 and dissociated single-cell suspensions analyzed for **(D)** $Tbet^{+}CD8^{+}$ TILs and **(E)** $FoxP3^{+}CD4^{+}$ Tregs by flow cytometry. $*P < 0.05$ and $**P < 0.01$.

3.5 DISCUSSION

An ideal cancer vaccine antigen is one that is overexpressed by cells within the TME versus normal tissues, allowing for selective T cell targeting of disease sites. We have previously reported that the non-canonical Notch ligand, DLK1, is overexpressed by vascular pericytes in murine colon and renal carcinomas, and melanomas, when compared to tumor-uninvolved kidneys in these same animals, and that vaccination against DLK1 is capable of yielding therapeutic anti-tumor benefits (Chapter 2; [302]). In the current report, we demonstrate that the expression of DLK2, a homolog of DLK1, is upregulated in tumor-associated vascular pericytes following successful DLK1-targeted vaccination, consistent with the reciprocal expression profiles of these two related Notch antagonists. Given this phenotypic adaptation by tumor pericytes, we hypothesized that a combination vaccine targeting both DLK1 and DLK2 would have greater potential to promote an extended state of VN in the TME in association with improved treatment benefits. Combined vaccination against DLK1 and DLK2 resulted in superior activation of peripheral Type-1 antigen-specific $CD8^+$ T cell responses and more robust recruitment of T effector cells into the TME. Therapeutic TIL modified the tumor landscape by promoting the loss of $DLK1^+$ and $DLK2^+$ pericytes, effectively pruning immature tumor blood vessels. The normalization/maturation of the vascular network, which allows a switch from the hypoxic to a normoxic TME [312], also resulted in tumors that were coordinately deficient in $CD11b^+Gr1^+$ MDSCs and $FoxP3^+$ Tregs that are typically associated with immunosuppression.

Studies from other groups have previously shown that DLK1 and DLK2 reciprocally modulate each other's expression [251, 252]. For instance, during murine neonatal liver development, when DLK1 expression is elevated during the first few days of life, DLK2 is absent, but once DLK1 expression starts to decline, DLK2 expression is turned on. Furthermore,

forced ectopic expression of DLK1 or DLK2 in cells results in the loss of expression of the alternate homolog. The mechanism responsible for the coordinated control of DLK1 and DLK2 gene expression remains poorly-defined. When considered within the context of our DLK1-based vaccine strategy, we hypothesize that the change in the oxygenation level in the therapeutically normalized TME may play a role in flipping a transcriptional switch favoring *DLK2* expression. The *DLK1* promoter contains hypoxia regulatory elements (HRE), placing gene expression under the control of the HIF-1α transcription factor [245]. On the other hand, *DLK2* transcription does not seem to be directly driven by hypoxia but is rather controlled by the Sp1 and KLF4 transcription factors [313, 314], whose activities may be augmented under normoxic conditions [315, 316].

The role of DLK1 and DLK2 in blood vessel formation and maintenance in normal and disease settings remains underinvestigated. Our previous and current studies, however, suggest that DLK1 and DLK2, when expressed by tumor pericytes, contribute to pathological characteristics of the tumor blood vessel network by inhibiting Notch1 signaling in the perivascular region. Notch1 signaling in normal endothelial cells is critical in embryonic vascular development, endothelial cell fate determination, and vascular homeostasis [317]. Notch signaling also plays a role in tumor neovascularization, as suppression of the DLL4-Notch1 interaction leads to the formation of excessive immature blood vessel branches as a result of uncontrolled endothelial proliferation [20, 229, 230]. Both DLK1 and DLK2 block downstream Notch1 receptor signaling by interacting with the EGF-like repeat 12 of the receptor [252], known to be the binding site for canonical ligands [318, 319]. Thus, DLK1 and DLK2 impede Notch signaling by blocking receptor activation and by competing with ligands for binding sites. Vaccine-induced removal of $DLK1^+$ and $DLK2^+$ pericytes from the TME leads to VN that is

correlated with NICD activation and Hes1 expression in endothelial cells **(Appendix Figure 2)**. Consistent with a model in which activation of the Wnt/β-catenin/NOTCH signaling pathway in tumor endothelia leads to VN [289], we observed that reduced mean vascular density and improved pericyte-VEC interaction in the TME are biologic correlates associated with therapeutic vaccination against DLK1/DLK2 in tumor-bearing mice.

In order for cancer vaccines to work effectively, effector T cells must extravasate through the tumor blood vessel wall and into the interstitial space in order to interact with antigen-presenting stromal cell or tumor cell targets. However, conditions within the TME may suppress VEC expression of adhesion molecules such as intercellular adhesion molecule-1 (ICAM-1) and VCAM1, that may limit tumor infiltration by circulating (anti-tumor) T cells [320]. This situation may be remedied by combined administration of anti-angiogenic agents (such as the TKIs axitinib, dasatinib or sunitinib) along with a tumor-specific vaccine [206, 207, 321]. Our DLK1/DLK2-targeted vaccine has an advantage over conventional TAA-targeted vaccine due to the proximal accessibility of circulating T effector cells to tumor-associated vascular pericyte targets in contrast to tumor cells that require T cells to enter, transmigrate and functionally persist within the TME to mediate meaningful therapeutic action. Furthermore, our vaccine promotes sustainable immune-mediated VN that would be envisioned to improve the deliverability of co-delivered chemotherapies or adoptively-transferred (TCR- or CAR-engineered) T cells, theoretically without invoking the development of drug resistance or the adverse side-effects associated with anti-VEGF monoclonal antibodies and TKIs. However, it is possible that low-doses of anti-angiogenic drugs, such as sunitinib, might further reduce immunoregulatory cell populations in support of an even more robust pro-inflammatory TME when combined with DLK1/DLK2-targeted vaccines [322].

When taken in the context to existing paradigms for temporal cascades of T cell infiltration into the TME [323, 324], we would propose that the vaccine-induced DLK1- and DLK2-specific T cells might represent an initial wave of effector TILs that trim and promote the maturation of tumor-associated blood vessels, leading to VN. The normalized TME is conducive to DC maturation and the subsequent cross-priming of "second set" $CD8^+$ T cell responses reactive against tumor-associated antigens acquired by DC within the TME [302, 325]. This effectively drives a broadening in the anti-tumor T cell repertoire based on an "epitope spreading" paradigm [325, 326], such as we observed in the case of DLK1/DLK2-based therapeutic vaccines leading to the development of anti-gp100 $CD8^+$ T cell responses in the B16 melanoma model (**Figure 19**).

One of the anticipated problems with immunotherapy is the development of immune evasion mechanisms in the tumor that would lead to treatment resistance. Vaccines induce anti-tumor protection by expanding the size and specificity of the tumor-specific T response, with superior vaccines also promoting TIL recruitment. However, chronic inflammation in the TME (mediated by T cells or NK cells) may lead to upregulated expression of immune checkpoint molecules such PD-L1 [311, 327, 328] in the tumor which can subvert or delete protective PD-1^+ T effector cells. Consistent with this paradigm, we observed that effective vaccination against DLK1/DLK2 led to increased numbers of inflammatory (IFN-γ^+) TIL and to upregulated PD-L1 expression in the TME. While we did not discern any significant benefit to tumor-bearing mice upon treatment with anti-PD-L1 monotherapy, we observed that the addition of PD-L1 blockade to our DLK1/DLK2-based vaccine regimen resulted in improved Type-1 $CD8^+$ T cell-mediated control of tumor growth vs. either monotherapy. Our data support a model in which PD1/PD-L1 blockade and anti-vascular vaccines complement each other in their ability to promote, recruit

and sustain therapeutic anti-tumor immunity within the TME. However even this "optimized" treatment strategy did not achieve tumor regression, suggesting room for further translational improvement by combination with additional immune checkpoint antagonists (such as anti-B7H3, anti-Gal9 or -Tim3, and anti-PD-L2 or -PD1) in extended treatment protocols, prior to the translation of such approaches into the clinic.

4.0 GENERAL DISCUSSION

Due to its significant role in the proliferation and maintenance of tumor cells and its distinct physiological and molecular signature that distinguishes it from normal blood vessels, the tumor vasculature represents a promising target the generalized for immunotherapy of cancer. However, currently available treatments, such as anti-VEGF and TKIs that attack the tumor blood vessel and/or tumor angiogenesis are only transiently effective [158, 159, 259, 260]. Resistance to anti-angiogenic agents occurs when tumors activate alternative, compensatory pathways that can continue to support neovascularization and/or when tumor cells are reprogrammed so that they can invade deeper into normal tissue and co-opt the normal vasculature [299]. One possible approach to circumvent this problem is to induce immune-targeting that preferentially eliminates "aberrant" tumor-associated vascular cells while sparing the vasculature in normal organs. Immunotherapy has the potential to provide long term control or even complete eradication of tumors due to its capacity to induce durable anti-tumor responses and memory cells [202, 203].

In this thesis, I present two novel antigens, DLK1 and DLK2, as targets for cancer therapeutic vaccines. DLK1 and DLK2 are preferentially expressed by tumor-associated pericytes in RENCA renal cell carcinomas growing s.c. in Balb/c mice but not in the animal-matched tumor-uninvolved kidney vasculature (which serves to limit concerns for off-target pathologic effects). In Chapter 2, I show that immune-targeting of DLK1 via specific peptide- or

gene-based therapeutic vaccination *in vivo* resulted in immune-mediated reduction in RENCA tumor growth. However, tumors in DLK1-vaccinated animals ultimately progressed. I show in Chapter 3 that vaccine-induced removal of $DLK1^+$ pericytes in the TME leads to a compensatory increase in DLK2 expression by tumor-associated vascular pericytes. DLK1 and DLK2 are homologous members of the EGF-like protein family that regulate each other's expression such that the forced downregulation of one gene product results in the upregulation of the other gene product and vice versa [251, 252]. I show that gene-based vaccination against both DLK1 and DLK2 provides superior anti-tumor therapeutic benefit when compared to vaccination against either single antigen alone as demonstrated by the tighter control of treated RENCA and B16 tumor growth *in vivo*. Altogether, I've shown in this thesis that TBVA-targeted immunotherapy results in the activation of antigen-specific T cells, the actions of which lead to the inhibition of progressive tumor growth and to the reconditioning of the TME (i.e. vascular normalization, reduced hypoxia, reduced immunosuppressive cell populations and reduced CSC-like populations).

There are several means to target TBVAs immunotherapeutically and in the studies described here, I employed peptide- and gene-based vaccination strategies to assess anti-TBVA immune-targeting in the RENCA tumor model. Our group has previously demonstrated that vaccine formulations composed of DCs that are engineered to express IL12 (DC.IL12) and then pulsed with MHC class I-presented peptides promote robust antigen-specific $CD8^+$ T cells independent of $CD4^+$ T cell help [197, 275]. As shown in Chapter 2, this formulation was successfully implemented using syngeneic DC.IL12 pulsed with DLK1-derived peptides (DC.IL12.pDLK1) to activate DLK1-specific $CD8^+$ T cells. I implemented a similar vaccine strategy to target tumor pericyte-associated antigen DLK2. Based on Immune Epitope Database

(http://www.iedb.org/) predictions, I picked MHC class I H-2^d-restricted DLK2 peptide sequences that might be immunogenic, generated a DC.IL12 vaccine based on these peptides (DC.IL12.pDLK2), and injected naïve tumor-free Balb/c mice with the vaccine. Assessment of $CD8^+$ splenocytes from the animals showed that some epitopes are putatively immunogenic (**Appendix Figure 3a**). However, application of the DC.IL12.pDLK2 vaccine in addition to DC.IL12.pDLK1 did not provide additional therapeutic benefits in RENCA-bearing Balb/c mice (**Appendix Figure 3b**). I suspect that the DLK2 peptide epitopes chosen may have been only weakly immunogenic and unable to induce a discernable immune response or that while immunogenic as synthetic sequences, these peptides were only inefficiently processed and presented in tumor MHC I complexes naturally. Therefore, in order to develop a more universal platform that would include all possible natural epitopes, I generated cDNA-based vaccines that would virally deliver the full-length gene product into host antigen presenting cells (APC), utilize the host APC's gene expression and antigen presentation machineries, and lead to the cross-priming of more comprehensive DLK1- and DLK2-specific T cell repertoires. For this platform, I utilized a lentivirus system, as it has been shown that cutaneous injection with lentivirus results in the transduction and activation of skin-derived $DEC205^+CD8^{-/lo}$ (cross-priming) DCs [277]. For instance, cutaneous immunization of lentivirus recombinant for ovalbumin in mice led to the transport of transduced, OVA antigen-presenting skin-derived DCs to the vaccine site-draining lymph nodes where it was gound to stimulate Ag-specific $CD8^+$ T cells capable of inhibiting the growth of OVA-expressing melanoma cells (i.e. B16.OVA) *in vivo*.

Both DC.IL12.pDLK1 and lvDLK1 vaccines induced antigen-specific $CD8^+$ effector T cells that targeted and eradicated $DLK1^+$ pericytes, resulting in the remodeling of the tumor

vasculature in the RENCA tumor model. The remodeled tumor vasculature has a more mature phenotype: the immature microvessels are pruned, the VECs and pericytes in remaining vessels are more closely associated with the VECs, and the vessels are less leaky. All these vascular changes are associated with a decrease in hypoxia within the TME. I hypothesize that the shift from a hypoxic TME to a more normoxic condition may be one of the major factors for the preferential expression of DLK2 over DLK1 in the pericytes after treatment. DLK1 expression is controlled by hypoxia-related transcription factor HIF-1α [245] while DLK2 expression is controlled by the transcription factors Sp1 and KLF4 [313, 314], which are more active under normoxic environments [315, 316].

Immunization of RENCA-bearing Balb/c mice and B16-bearing C57BL/6 mice with DLK1- and DLK2-targeted vaccines led to the coordinate activation of both DLK1- and DLK2-specific $CD8^+$ T cells. I postulate that the activation of a broader anti-TBVA T cell repertoire and the removal of both $DLK1^+$ and $DLK2^+$ pericytes (via T cell-mediated cytolysis or promotion of pericyte maturation and loss of DLK1/2 expression) would result in sustainable VN. In this context, I have presented data n support of the conclusion that lvDLK1 and lvDLK2 vaccination alleviates hypoxia, which is one of the important cues for pro-tumor angiogenesis in the TME [23]. Corollary to this is the downregulation of pro-angiogenic receptors, which also represent hypoxia-responsive gene products. These findings suggest that the TBVA-targeted vaccines not only induce VN but also inhibits a rebound in further formation of aberrant neovessels in treated animals. Furthermore, preliminary investigation of the TIL phenotype in B16 tumors suggests that there is an increase in central memory (T_{CM})-like $CD8^+$ T cell population in animals treated with combined DLK1/DLK2 vaccine (**Appendix Figure 4**). In this regard, Restifo *et. al.* have previously shown that tumor infiltrating gp100-specific T_{CM} cells, which have greater

proliferative capacity and ability to persist in the TME, promote a significant delay in B16 tumor growth *in vivo* when compared to adoptively-transferred effector memory T cells [329]. The (T_{CM})-like $CD8^+$ T cells I observed prospectively provide a durable anti-DLK1/DLK2 activity that presumably underlies sustained VN in my tumor models.

I would propose the following comprehensive mechanism by which the DLK1/DLK2-targeted vaccines may effectively regulate tumor progression *in vivo*: first, the vaccine elicits anti-DLK1 and anti-DLK2 $CD8^+$ T cells that preferentially react with $DLK1^+$/$DLK2^+$ pericytes in the TME, resulting in the significant ablation and remodeling (i.e. trimming) of the tumor-associated vasculature and VN. Second, the increased pericyte coverage on VECs post-vaccination limits leakage of plasma nutrients deep into the tumor and without these nutrients, tumor cells that are not adjacent (within 50-60 microns) to the vasculature undergo apoptosis. Such apoptotic tumor cells become a source of antigenic determinants that may subsequently be taken up by APCs recruited into the therapeutically "normalized" TME via stromal cell/VEC-produced chemokines. Lastly, the activated APCs may then cross-prime a "second wave" of protective T cells that are broadly reactive against both TBVAs and TAAs [325], effectively expanding the protective anti-tumor T cell repertoire based on an "epitope spreading" paradigm [325, 326]. Indeed, I report that such is the case in DLK1/DLK2-based therapeutic vaccines, where I also observed therapy-associated induction of anti-gp100 $CD8^+$ T cell responses in the B16 melanoma model. Treatment-linked upregulation of CXCL10 and VCAM1 expression in the remodeled tumor stroma promote the recruitment of this "second wave" of T cells into the tumor bed.

The priming of naïve T cells classically occurs in secondary lymphoid organs (SLO), however, some recent evidence suggests that it can also occur within the tumor in extra-nodal

structures termed as tertiary lymphoid organs (TLO; [330, 331]). The formation of TLOs in the tumor lesion may be promoted by Type-1 proinflammatory DCs ($Tbet^+$ DC) that recruit natural killer cells, B cells, and naïve T cells into the TME [330]. These recruited naïve T cells encounter their cognate antigen for the first time and develop into antigen-specific T effector cells within the TME. One of the features of TLO formation is the presence of high endothelial venules (HEV), which are generated only after the initial recruitment of the immune cells producing lymphotoxins or TNFα that serve as so-called TLO "initiator cells" [331]. Although I have not comprehensively investigated TLO within the therapeutic TME, my preliminary immunofluorescence data show that TBVA-targeted vaccination promotes the development of HEV-like structures *in vivo* i.e. DLK1-vaccinated RENCAs exhibit increased number of $PNAd^+$ VEC in the TME when compared to tumors in the control treatment cohort (**Appendix Figure 5**). Hence, I would infer that the initial wave of anti-DLK1 and anti-DLK2 TILs may be cross-primed in the draining lymph node of the site of vaccine injection while the "second wave" of TILs that respond to a broader range of antigens may be cross-primed in either secondary lymphoid organs or in TLOs within the TME. This hypothesis will need to be investigated by others using informative models lacking SLO or in which SLO or TLO may be differentially perturbed.

Another therapeutic effect of the DLK1/DLK2 vaccine is the reduction of tumor-promoting cell populations, such as CSC-like cells ($CD44^+$, $CD133^+$, and $Jarid1B^+$ cells [283-285]) and regulatory immune cells (MDSC and Tregs) in the TME. This could reflect the ability of the vaccine-induced TILs to recondition the TME such that the recruitment, accumulation and/or expansion of these CSCs and regulatory immune cells are inhibited. For instance, in some types of tumors, the perivascular region provides a niche for CSCs wherein VECs provide

soluble factors that support CSC self-renewal [132-137, 281]. Therapeutic VN could potentially abrogate these CSC niches and disrupt cues for CSC maintenance. The observed decrease in hypoxia in the TME post-therapy may also suppress signals required for the survival/maintenance of tumor-initiating cells. Reduction in the expression of HIFs in the TME could lead to the transcriptional silencing of hypoxia-responsive stem cell-associated gene produces [283-285], in the disruption of the function of MDSCs [308], and in the inhibition of the generation and accumulation of Tregs [111]. Our data support a model wherein TBVA immunotherapy has multi-faceted effects in the TME – it induces effector cells to abolish abnormal vascular cells (and tumor cells via epitope spreading), reconditions the tumor stroma, and mitigates immune suppression.

Notch signaling is critical in the resolution of physiological angiogenesis and maturation of the newly-formed blood vessels [20]. In tumors, blockade of Notch signaling via obstruction of DLL4-Notch1 interactions has been demonstrated to instigate the formation of excessive immature blood vessel branches as a result of uncontrolled endothelial proliferation [229, 230]. The role of DLK1 and DLK2 in angiogenesis and in the vasculature is largely unknown but the data presented in this thesis suggest that these members of the EGF-like family of proteins contribute significantly to the pathologic characteristics of the tumor vasculature by inhibiting Notch1 signaling. Vaccine-induced removal of $DLK1^+$ and $DLK2^+$ pericytes in the TME is correlated with the upregulation of Notch signaling elements, notably the activation of NICD and the expression of Hes1 in tumor perivascular regions. Furthermore, Wnt signaling also appears to be activated in the vaccinated TME as indicated by the increased expression Frzd2, Frzd4 and Frzd7 transcripts [290]. As such, DLK1 and DLK2 inhibition in the tumor vasculature may reinforce Notch/Wnt signaling to negatively regulate tumor-associated angiogenesis, consistent

with the proposed model in which activation of the Wnt/β-catenin/Notch signaling pathways in tumor endothelia leads to VN [289]. The collaboration between DLK1/DLK2 vaccine and Wnt/β-catenin/Notch signaling axis in the anti-tumor response needs to be further elucidated in future studies. My data suggest that Notch signaling plays a role in the therapeutic activity of DLK1/DLK2 vaccine based on the partial ablation of tumor growth control when a pharmacological Notch antagonist (i.e. DAPT) was combined with the vaccine protocol.

Although coordinate targeting of both DLK1 and DLK2 led to a decrease in immunosuppressive cell populations, immune evasion by the tumor is still possible through other means. For instance the generation of IFNγ by TILs contributes of high levels of PD-L1 in tumors, providing the tumors a mechanism to develop adaptive resistance to the evolving anti-tumor immune response [311, 328]. This means that vaccine-induced effector cells may successfully infiltrate the tumor via the vaccine-normalized vasculature only to be deleted or subverted by the PD-L1 signals contributed by tumor cells or stromal cells within the TME. Thus, the application of immune checkpoint inhibitors may augment the activity of the vaccine-induced T cells. Indeed, application of PD-L1 blocking antibodies in addition to DLK1/DLK2-targeted vaccine resulted in improved Type-1 $CD8^+$ T cell-mediated control of tumor growth when compared to either monotherapy. This demonstrates that the complementary action of PD1/PD-L1 blockade and anti-vascular vaccines may sustain the anti-tumor activity of immunotherapy-induced TIL in our tumor models.

In conclusion, the immune targeting of pericyte-associated antigens DLK1 and DLK2 is therapeutic in RENCA and B16 tumor models. The combination of DLK1- and DLK2-targeted vaccine generates potent effector T cells that remodel the tumor stroma, contributing to further anti-tumor effects. I also show that this TBVA-targeted therapeutic regimen is amenable to

complementation using immune checkpoint blockade, thus defining an innovative treatment strategy applicable to a broad range of solid cancers.

5.0 FUTURE DIRECTIONS

5.1 ELUCIDATION OF THE ROLE OF NOTCH IN THE THERAPEUTIC IMMUNE RESPONSE INDUCED BY DLK1/DLK2 IMMUNE TARGETING

Although I have shown that vaccine-induced VN is associated with the activation of Notch signaling, the exact role of Notch in the therapeutic efficacy of the vaccine remains unknown. Dependency of the vaccine on Notch signaling to generate anti-tumor responses was partially demonstrated when inhibitor DAPT was shown to diminish the anti-tumor efficacy of the DLK1-based vaccines. However, γ-secretase inhibitors applied systematically suppress Notch signaling not only in the tumor vasculature but in other tissue compartments as well. Hence, to precisely define the consequence Notch activation on DLK1/DLK2 vaccine, conditional mouse knockout models could be generated in which Notch signaling is only deficient in VECs or pericytes (or only under conditions of hypoxia in the TME).

In addition to the VECs, I also observed that Hes1 expression was also enhanced in other cells in the perivascular region after therapeutic vaccination against DLK1/DLK2. The identification/characterization of these $Hes1^{+}$ cells would contribute to a better understanding to the therapeutic mechanism of action associated with these vaccines and the suitability of combining DLK1/DLK2 vaccination with other anti-cancer agents, especially those that are involved in Notch modulation. These $Hes1^{+}$ stromal cells may include immune cells, such as

DCs and T cells that are known to be regulated by Notch signaling. Indeed, Notch activation has been implicated in the maturation and activation of DCs, as well as, in the differential secretion of cytokines and chemokines by DC subsets [293, 332]. In T cells, Notch inhibition has been shown to decrease $CD4^+$ and $CD8^+$ cell proliferation, NF-κB activity, and IFN-γ production in peripheral T cells [333].

5.2 COMBINATION OF DLK1/DLK2 VACCINE WITH OTHER ANTI-TUMOR THERAPIES

The abnormal tumor-associated blood vasculature results in spatial and temporal heterogeneity in blood perfusion, limiting the access of drugs and effector immune cells to poorly perfused regions of the tumor [88, 90, 140, 334]. Immune targeting of $DLK1^+$ and $DLK2^+$ pericytes could improve the delivery and efficacy of chemotherapies and other immunotherapies by promoting VN. The vaccine-induced VN could restore fluid pressure gradients that would allow uniform flow-driven penetration of chemotherapeutic agents into the tumor [334]. Furthermore, increased oxygenation in the TME could contribute to the efficacy of chemotherapy. The DLK1/DLK2 vaccine could improve other immune-based therapies (such as ACT and TAA-based vaccines) by enhancing effector cell extravasation and by alleviating immunosuppression in the TME. Conventional anti-angiogenic drugs only normalize the vasculature transiently, signifying that there is only a limited window of time during which they may assist the delivery of chemo/immune-therapeutic agents into the TME. TBVA-targeted vaccines may provide more durable VN in the TME, however, particularly in the context of combination regimens, collateral toxicities (such as autoimmune pathology resulting from specific vaccine targeting or as a

consequence of "epitope spreading" in the therapeutic T cell repertoire) will need to be carefully investigated/monitored.

The activity of the DLK1/DLK2 vaccine could be improved through combination with TKIs and immune checkpoint inhibitors. TKIs such as sunitinib have been shown to have immunogenic modulating capabilities that could synergize with the DLK1/DLK2 anti-tumor activity [208, 335]. TKIs could reduce immunosuppressive cell populations, promote a pro-inflammatory TME, and induce phenotypic changes in the tumor cells that would make them more susceptible to T cell killing (i.e. T cells activated after vaccination via epitope spreading mechanisms). Development of adaptive immune evasion is one of the hurdles of immunotherapy [309, 310]. As presented in Chapter 3, PD-L1 blockade augmented the therapeutic efficacy of DLK1/DLK2-targeted vaccination but only to a degree, indicating that other molecules and pathways may participate to underlie tumor evasion of vaccine-induced effector T cells. Inclusion of other checkpoint inhibitors such as anti-CTLA-4, anti-Tim3, and anti-Lag3 should be considered for inclusion in combination vaccines in order to promote and sustain more robust anti-tumor T cell activity *in vivo*.

5.3 ADDITION OF OTHER TBVA IN THE DLK1/DLK2 VACCINE FORMULATION

Although I infer that the DLK1/DLK2 vaccine could provide a durable anti-tumor response, resistance to the vaccine is always a possibility. In particular, the therapeutic TME (after vaccination against DLK1/DLK2) should be investigated for expression of alternate gene products postulated to serve as NOTCH antagonists. If such targets are preferentially expressed

in the TME and not in normal somatic tissues, they should be considered for inclusion in prospective interventional approaches. As with anti-angiogenic drugs, the tumor could also utilize alternative pathways to compensate for the loss of DLK1 and DLK2 in the tumor vasculature. An anti-vascular vaccine that includes a broader range of VEC-associated and pericyte-associated antigens (i.e. EphA2, HBB, NRP-1, PDGFRβ, TEM1, VEGFR1, and VEGFR2 [197] in addition to DLK1 and DLK2) could avert vaccine resistance. Novel TBVAs should also be identified and investigated for the suitability as cancer vaccine targets.

6.0 APPENDIX

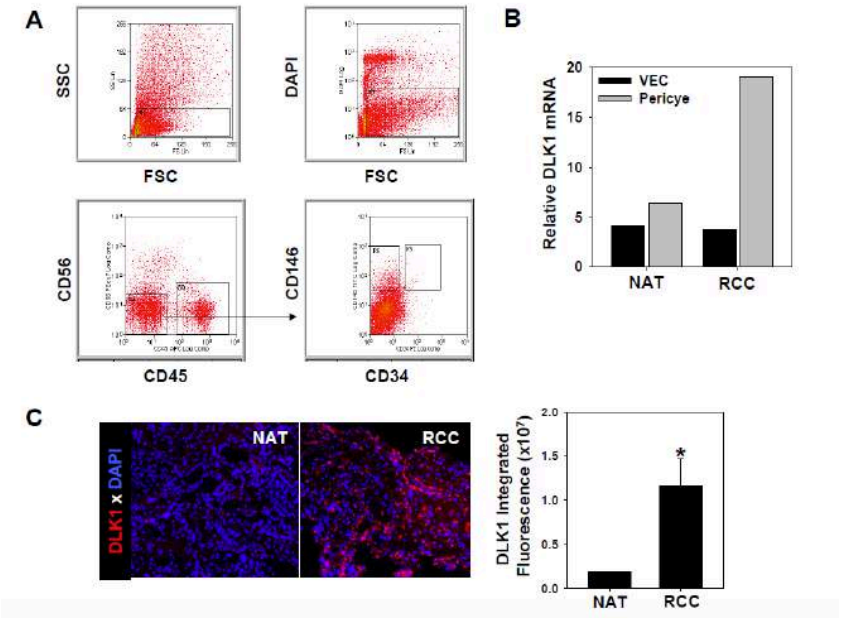

Appendix Figure 1. DLK1 is differentially expressed by human RCC-associated pericytes.

(**a**) Freshly-harvested RCC tumor and patient-matched normal adjacent kidney tissues (NAT) were mechanically and enzymatically digested into single-cell suspension and sorted by flow cytometry based on forward scatter and side scatter, DAPI exclusion (to exclude dead cells), a $CD56^{neg}CD45^{neg}$ phenotype, and then selectively into $CD146^{+}CD34^{neg}$ pericytes and $CD146^{+}CD34^{+}$ VEC populations. (**b**) mRNA was isolated from sorted pericytes and VEC from NAT and RCC tumor and analyzed for DLK1 expression by real-time PCR. Relative mRNA expression was normalized to housekeeping HPRT1 transcript expression. (**c**) RCC tumor and NAT sections were analyzed for expression of DLK1 (red) by immunofluorescence microscopy. Mean fluorescence intensity +/- SD was quantitated from 3 independent fields per slide as described in Materials and Methods. Data are representative those obtained in 3 independent experiments performed. *$p < 0.05$ (t-Test).

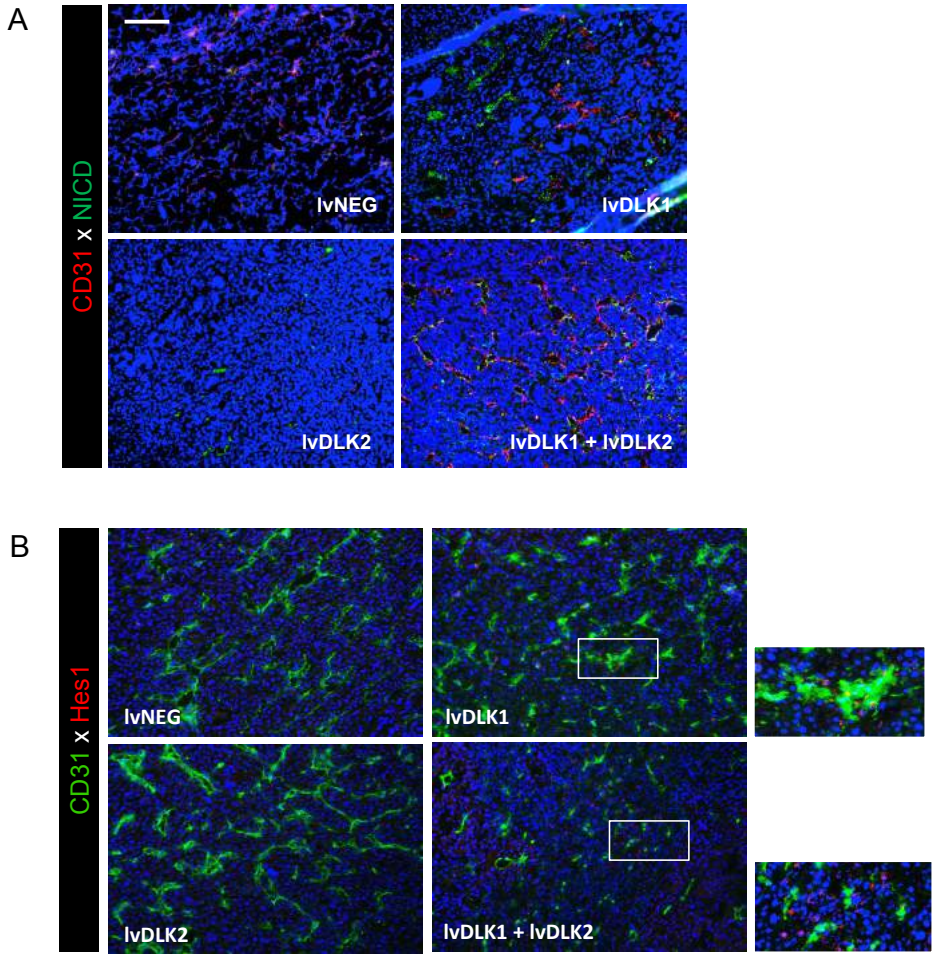

Appendix Figure 2. Activation of Notch signaling in RENCA treated with lvDLK1 + lvDLK2 vaccine.

Tumors harvested from day 21 RENCA-bearing mice receiving the indicated vaccines were sectioned and assessed for VECs (red) and for expression of the cleaved intracellular domain of Notch1 (NICD, green) in (**A**), or for VECs (green) and for expression of the NOTCH down-stream target Hes1 (red) in (**B**) by fluorescence microscopy as described in Materials and Methods. Scale bar = 1mm. All data are representative of those obtained in 3 independent experiments.

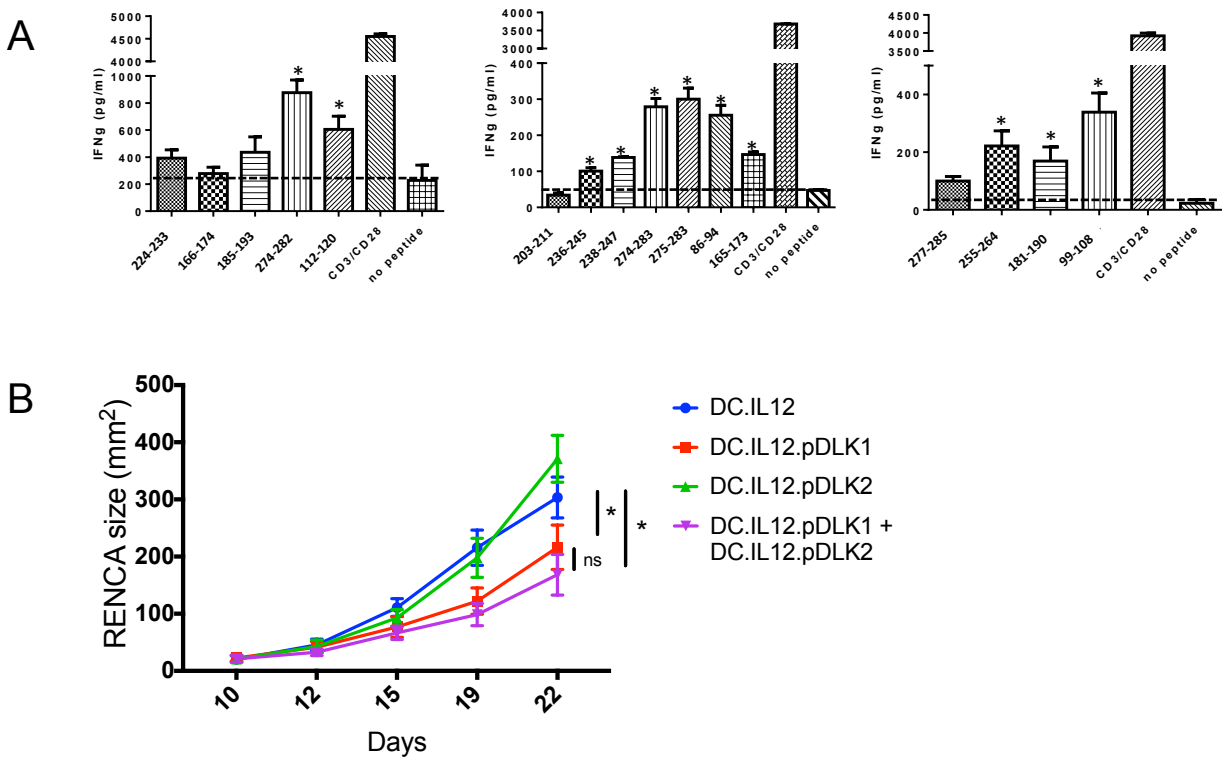

Appendix Figure 3. Immunization with peptide-based DLK2 vaccine is not therapeutic even in combination with DLK1 peptide-based vaccine.

(**a**) SYFPEITHI and IEDB were utilized to predict DLK2 epitopes and high scoring peptides were synthesized as described in [197]. Balb/c DCs ectopically expressing IL12 (as described in Chapter 3) were pulsed with equimolar (10mM) mixture of DLK2 peptides. These pools of peptide-based vaccines were used to immunize naïve Balb/c mice (as described in Chapters 2 and 3) twice, with each injection being 1 week apart. Spleens were harvested from the mice 7 days after the second immunization. Splenocytes were stimulated with individual peptides (as described in Chapter 3) and IFN-γ production was measured by ELISA. (**b**) RENCA-bearing Balb/c mice were vaccinated with DC.IL12 that had been pre-loaded with DLK1 peptides, DLK2 peptides or combination of both on Days 10 and 17 post-tumor inoculation. Tumor growth was monitored longitudinally and is reported as the mean ± SEM for 5 animals per group. * $P < 0.05$, representative of 2 experiments.

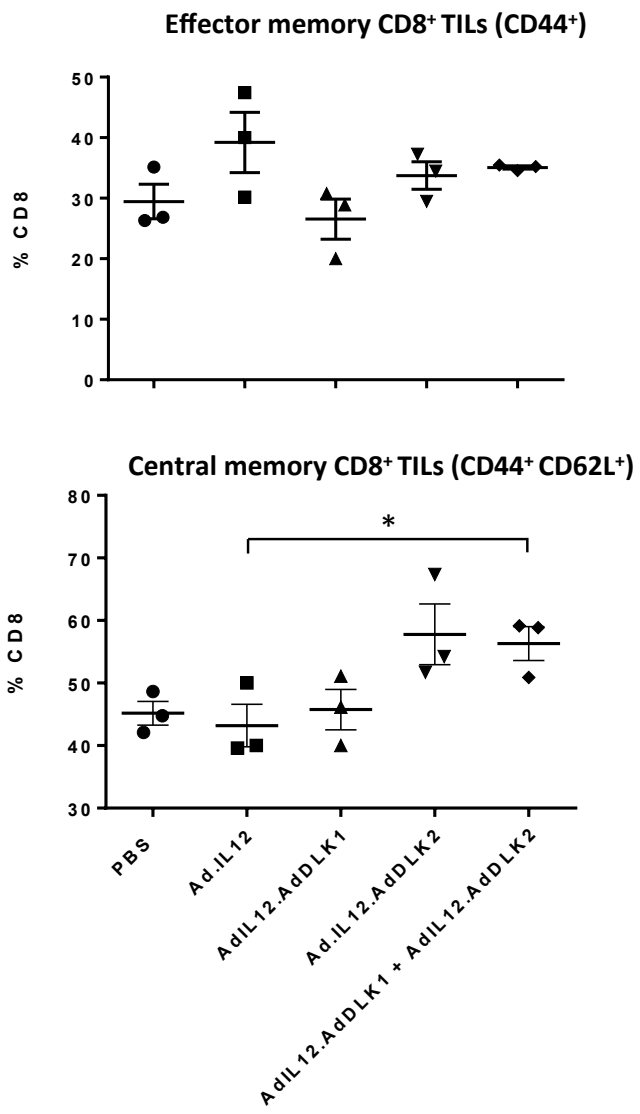

Appendix Figure 4. Characterization of memory TILs in DLK/DLK2-treated B16 tumors.

Day 20 tumors from animal cohorts in Figure 17 were harvested and digested into single cell suspensions as described in the **Chapter 3.3.5**. The $CD44^+$ T_{EM} and $CD44^+$ $CD62L^+$ T_{CM} $CD3^+CD8^+$ TIL populations were identified via flow cytometry.

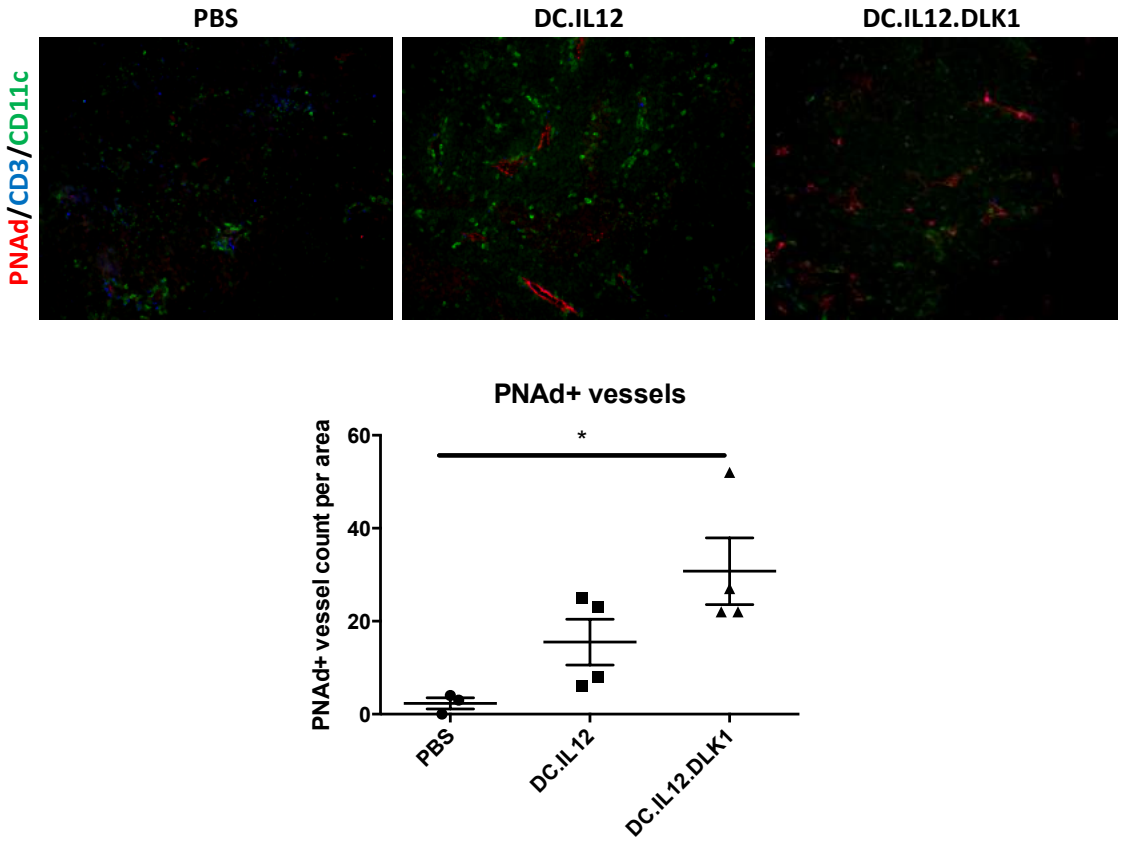

Appendix Figure 5. Formation of HEV-like structures in the DLK1-immune targeted RENCA TME.

Tumor sections from untreated and DC.IL12- and DC.IL12.pDLK1- vaccinated RENCA (**Figure 15)** were immunostained for CD11c (eBioscience), CD3 (BD Pharmingen), and PNAd (BD Pharmingen). $PNAd^{+}$ structures were counted per 200x view field. $*P < 0.05$

BIBLIOGRAPHY

1. Galon, J., et al., *Type, density, and location of immune cells within human colorectal tumors predict clinical outcome.* Science, 2006. **313**(5795): p. 1960-4.
2. Gao, Q., et al., *Intratumoral balance of regulatory and cytotoxic T cells is associated with prognosis of hepatocellular carcinoma after resection.* J Clin Oncol, 2007. **25**(18): p. 2586-93.
3. Gooden, M.J., et al., *The prognostic influence of tumour-infiltrating lymphocytes in cancer: a systematic review with meta-analysis.* Br J Cancer, 2011. **105**(1): p. 93-103.
4. Pages, F., et al., *Immune infiltration in human tumors: a prognostic factor that should not be ignored.* Oncogene, 2010. **29**(8): p. 1093-102.
5. Zhang, L., et al., *Intratumoral T cells, recurrence, and survival in epithelial ovarian cancer.* N Engl J Med, 2003. **348**(3): p. 203-13.
6. Weigelin, B., M. Krause, and P. Friedl, *Cytotoxic T lymphocyte migration and effector function in the tumor microenvironment.* Immunol Lett, 2011. **138**(1): p. 19-21.
7. Ostrand-Rosenberg, S., *CD4+ T lymphocytes: a critical component of antitumor immunity.* Cancer Invest, 2005. **23**(5): p. 413-9.
8. Protti, M.P., L.D. Monte, and G.D. Lullo, *Tumor antigen-specific CD4+ T cells in cancer immunity: from antigen identification to tumor prognosis and development of therapeutic strategies.* Tissue Antigens, 2014. **83**(4): p. 237-46.
9. Leone, P., et al., *MHC class I antigen processing and presenting machinery: organization, function, and defects in tumor cells.* J Natl Cancer Inst, 2013. **105**(16): p. 1172-87.
10. Chen, L., *Co-inhibitory molecules of the B7-CD28 family in the control of T-cell immunity.* Nat Rev Immunol, 2004. **4**(5): p. 336-47.
11. Dong, H., et al., *Tumor-associated B7-H1 promotes T-cell apoptosis: a potential mechanism of immune evasion.* Nat Med, 2002. **8**(8): p. 793-800.
12. Rabinovich, G.A., D. Gabrilovich, and E.M. Sotomayor, *Immunosuppressive strategies that are mediated by tumor cells.* Annu Rev Immunol, 2007. **25**: p. 267-96.
13. Chanmee, T., et al., *Tumor-associated macrophages as major players in the tumor microenvironment.* Cancers (Basel), 2014. **6**(3): p. 1670-90.
14. Lindau, D., et al., *The immunosuppressive tumour network: myeloid-derived suppressor cells, regulatory T cells and natural killer T cells.* Immunology, 2013. **138**(2): p. 105-15.
15. Kerkar, S.P. and N.P. Restifo, *Cellular constituents of immune escape within the tumor microenvironment.* Cancer Res, 2012. **72**(13): p. 3125-30.
16. Hanahan, D. and R.A. Weinberg, *Hallmarks of cancer: the next generation.* Cell, 2011. **144**(5): p. 646-74.

17. Bates, D., et al., *Regulation of microvascular permeability by vascular endothelial growth factors.* J Anat, 2002. **200**(6): p. 581-97.
18. Holash, J., et al., *Vessel cooption, regression, and growth in tumors mediated by angiopoietins and VEGF.* Science, 1999. **284**(5422): p. 1994-8.
19. Gerhardt, H., et al., *VEGF guides angiogenic sprouting utilizing endothelial tip cell filopodia.* J Cell Biol, 2003. **161**(6): p. 1163-77.
20. Hellstrom, M., et al., *Dll4 signalling through Notch1 regulates formation of tip cells during angiogenesis.* Nature, 2007. **445**(7129): p. 776-80.
21. Carmeliet, P. and R.K. Jain, *Molecular mechanisms and clinical applications of angiogenesis.* Nature, 2011. **473**(7347): p. 298-307.
22. Bergers, G. and S. Song, *The role of pericytes in blood-vessel formation and maintenance.* Neuro Oncol, 2005. **7**(4): p. 452-64.
23. Dor, Y., R. Porat, and E. Keshet, *Vascular endothelial growth factor and vascular adjustments to perturbations in oxygen homeostasis.* Am J Physiol Cell Physiol, 2001. **280**(6): p. C1367-74.
24. Bottos, A. and A. Bardelli, *Oncogenes and angiogenesis: a way to personalize anti-angiogenic therapy?* Cell Mol Life Sci, 2013. **70**(21): p. 4131-40.
25. Morikawa, S., et al., *Abnormalities in pericytes on blood vessels and endothelial sprouts in tumors.* Am J Pathol, 2002. **160**(3): p. 985-1000.
26. Baluk, P., et al., *Abnormalities of basement membrane on blood vessels and endothelial sprouts in tumors.* Am J Pathol, 2003. **163**(5): p. 1801-15.
27. Plate, K.H., A. Scholz, and D.J. Dumont, *Tumor angiogenesis and anti-angiogenic therapy in malignant gliomas revisited.* Acta Neuropathol, 2012. **124**(6): p. 763-75.
28. McDonald, D.M. and P.L. Choyke, *Imaging of angiogenesis: from microscope to clinic.* Nat Med, 2003. **9**(6): p. 713-25.
29. Baluk, P., H. Hashizume, and D.M. McDonald, *Cellular abnormalities of blood vessels as targets in cancer.* Curr Opin Genet Dev, 2005. **15**(1): p. 102-11.
30. Alexander, M.R. and G.K. Owens, *Epigenetic control of smooth muscle cell differentiation and phenotypic switching in vascular development and disease.* Annu Rev Physiol, 2012. **74**: p. 13-40.
31. Wragg, J.W., et al., *Shear stress regulated gene expression and angiogenesis in vascular endothelium.* Microcirculation, 2014. **21**(4): p. 290-300.
32. Marshall, C.J., et al., *Detailed characterization of the human aorta-gonad-mesonephros region reveals morphological polarity resembling a hematopoietic stromal layer.* Dev Dyn, 1999. **215**(2): p. 139-47.
33. Sumpio, B.E., J.T. Riley, and A. Dardik, *Cells in focus: endothelial cell.* Int J Biochem Cell Biol, 2002. **34**(12): p. 1508-12.
34. Ruoslahti, E., *Specialization of tumour vasculature.* Nat Rev Cancer, 2002. **2**(2): p. 83-90.
35. Smith, N.R., et al., *Vascular endothelial growth factor receptors VEGFR-2 and VEGFR-3 are localized primarily to the vasculature in human primary solid cancers.* Clin Cancer Res, 2010. **16**(14): p. 3548-61.
36. Schwartz, J.D., et al., *Vascular endothelial growth factor receptor-1 in human cancer: concise review and rationale for development of IMC-18F1 (Human antibody targeting vascular endothelial growth factor receptor-1).* Cancer, 2010. **116**(4 Suppl): p. 1027-32.

37. Otsubo, T., et al., *Identification of novel targets for antiangiogenic therapy by comparing the gene expressions of tumor and normal endothelial cells.* Cancer Sci, 2014. **105**(5): p. 560-7.
38. St Croix, B., et al., *Genes expressed in human tumor endothelium.* Science, 2000. **289**(5482): p. 1197-202.
39. Nanda, A. and B. St Croix, *Tumor endothelial markers: new targets for cancer therapy.* Curr Opin Oncol, 2004. **16**(1): p. 44-9.
40. Michiels, C., *Endothelial cell functions.* J Cell Physiol, 2003. **196**(3): p. 430-43.
41. Cines, D.B., et al., *Endothelial cells in physiology and in the pathophysiology of vascular disorders.* Blood, 1998. **91**(10): p. 3527-61.
42. Dejana, E., E. Tournier-Lasserve, and B.M. Weinstein, *The control of vascular integrity by endothelial cell junctions: molecular basis and pathological implications.* Dev Cell, 2009. **16**(2): p. 209-21.
43. Dejana, E., et al., *Organization and signaling of endothelial cell-to-cell junctions in various regions of the blood and lymphatic vascular trees.* Cell Tissue Res, 2009. **335**(1): p. 17-25.
44. Lampugnani, M.G., *Endothelial cell-to-cell junctions: adhesion and signaling in physiology and pathology.* Cold Spring Harb Perspect Med, 2012. **2**(10).
45. Wallez, Y. and P. Huber, *Endothelial adherens and tight junctions in vascular homeostasis, inflammation and angiogenesis.* Biochim Biophys Acta, 2008. **1778**(3): p. 794-809.
46. Dudley, A.C., *Tumor endothelial cells.* Cold Spring Harb Perspect Med, 2012. **2**(3): p. a006536.
47. Hashizume, H., et al., *Openings between defective endothelial cells explain tumor vessel leakiness.* Am J Pathol, 2000. **156**(4): p. 1363-80.
48. Dvorak, H.F., et al., *Identification and characterization of the blood vessels of solid tumors that are leaky to circulating macromolecules.* Am J Pathol, 1988. **133**(1): p. 95-109.
49. Roberts, W.G., et al., *Host microvasculature influence on tumor vascular morphology and endothelial gene expression.* Am J Pathol, 1998. **153**(4): p. 1239-48.
50. Claesson-Welsh, L., *Blood vessels as targets in tumor therapy.* Ups J Med Sci, 2012. **117**(2): p. 178-86.
51. Jain, R.K., L.L. Munn, and D. Fukumura, *Dissecting tumour pathophysiology using intravital microscopy.* Nat Rev Cancer, 2002. **2**(4): p. 266-76.
52. Barlow, K.D., et al., *Pericytes on the tumor vasculature: jekyll or hyde?* Cancer Microenviron, 2013. **6**(1): p. 1-17.
53. Armulik, A., A. Abramsson, and C. Betsholtz, *Endothelial/pericyte interactions.* Circ Res, 2005. **97**(6): p. 512-23.
54. Birbrair, A., et al., *Pericytes at the intersection between tissue regeneration and pathology.* Clin Sci (Lond), 2015. **128**(2): p. 81-93.
55. Sims, D.E., *The pericyte--a review.* Tissue Cell, 1986. **18**(2): p. 153-74.
56. Armulik, A., G. Genove, and C. Betsholtz, *Pericytes: developmental, physiological, and pathological perspectives, problems, and promises.* Dev Cell, 2011. **21**(2): p. 193-215.
57. von Tell, D., A. Armulik, and C. Betsholtz, *Pericytes and vascular stability.* Exp Cell Res, 2006. **312**(5): p. 623-9.

58. Gerhardt, H. and C. Betsholtz, *Endothelial-pericyte interactions in angiogenesis.* Cell Tissue Res, 2003. **314**(1): p. 15-23.
59. Lindahl, P., et al., *Endothelial-perivascular cell signaling in vascular development: lessons from knockout mice.* Curr Opin Lipidol, 1998. **9**(5): p. 407-11.
60. Hellstrom, M., et al., *Lack of pericytes leads to endothelial hyperplasia and abnormal vascular morphogenesis.* J Cell Biol, 2001. **153**(3): p. 543-53.
61. Diaz-Flores, L., et al., *Pericytes. Morphofunction, interactions and pathology in a quiescent and activated mesenchymal cell niche.* Histol Histopathol, 2009. **24**(7): p. 909-69.
62. Hall, A.P., *Review of the pericyte during angiogenesis and its role in cancer and diabetic retinopathy.* Toxicol Pathol, 2006. **34**(6): p. 763-75.
63. Benjamin, L.E., et al., *Selective ablation of immature blood vessels in established human tumors follows vascular endothelial growth factor withdrawal.* J Clin Invest, 1999. **103**(2): p. 159-65.
64. Bergers, G., et al., *Benefits of targeting both pericytes and endothelial cells in the tumor vasculature with kinase inhibitors.* J Clin Invest, 2003. **111**(9): p. 1287-95.
65. Reinmuth, N., et al., *Induction of VEGF in perivascular cells defines a potential paracrine mechanism for endothelial cell survival.* Faseb j, 2001. **15**(7): p. 1239-41.
66. Shaheen, R.M., et al., *Tyrosine kinase inhibition of multiple angiogenic growth factor receptors improves survival in mice bearing colon cancer liver metastases by inhibition of endothelial cell survival mechanisms.* Cancer Res, 2001. **61**(4): p. 1464-8.
67. Kharaishvili, G., et al., *The role of cancer-associated fibroblasts, solid stress and other microenvironmental factors in tumor progression and therapy resistance.* Cancer Cell Int, 2014. **14**: p. 41.
68. Ohlund, D., E. Elyada, and D. Tuveson, *Fibroblast heterogeneity in the cancer wound.* J Exp Med, 2014. **211**(8): p. 1503-23.
69. Kalluri, R. and M. Zeisberg, *Fibroblasts in cancer.* Nat Rev Cancer, 2006. **6**(5): p. 392-401.
70. Fukumura, D., et al., *Tumor induction of VEGF promoter activity in stromal cells.* Cell, 1998. **94**(6): p. 715-25.
71. Cirri, P. and P. Chiarugi, *Cancer associated fibroblasts: the dark side of the coin.* Am J Cancer Res, 2011. **1**(4): p. 482-97.
72. Kryczek, I., et al., *Stroma-derived factor (SDF-1/CXCL12) and human tumor pathogenesis.* Am J Physiol Cell Physiol, 2007. **292**(3): p. C987-95.
73. Orimo, A., et al., *Stromal fibroblasts present in invasive human breast carcinomas promote tumor growth and angiogenesis through elevated SDF-1/CXCL12 secretion.* Cell, 2005. **121**(3): p. 335-48.
74. Erez, N., et al., *Cancer-Associated Fibroblasts Are Activated in Incipient Neoplasia to Orchestrate Tumor-Promoting Inflammation in an NF-kappaB-Dependent Manner.* Cancer Cell, 2010. **17**(2): p. 135-47.
75. Lederle, W., et al., *MMP13 as a stromal mediator in controlling persistent angiogenesis in skin carcinoma.* Carcinogenesis, 2010. **31**(7): p. 1175-84.
76. Kalluri, R., *Basement membranes: structure, assembly and role in tumour angiogenesis.* Nat Rev Cancer, 2003. **3**(6): p. 422-33.
77. Paulsson, M., *Basement membrane proteins: structure, assembly, and cellular interactions.* Crit Rev Biochem Mol Biol, 1992. **27**(1-2): p. 93-127.

78. Form, D.M., B.M. Pratt, and J.A. Madri, *Endothelial cell proliferation during angiogenesis. In vitro modulation by basement membrane components.* Lab Invest, 1986. **55**(5): p. 521-30.
79. Xu, J., et al., *Proteolytic exposure of a cryptic site within collagen type IV is required for angiogenesis and tumor growth in vivo.* J Cell Biol, 2001. **154**(5): p. 1069-79.
80. Geevarghese, A. and I.M. Herman, *Pericyte-endothelial crosstalk: implications and opportunities for advanced cellular therapies.* Transl Res, 2014. **163**(4): p. 296-306.
81. Stratman, A.N., et al., *Pericyte recruitment during vasculogenic tube assembly stimulates endothelial basement membrane matrix formation.* Blood, 2009. **114**(24): p. 5091-101.
82. Stratman, A.N. and G.E. Davis, *Endothelial cell-pericyte interactions stimulate basement membrane matrix assembly: influence on vascular tube remodeling, maturation, and stabilization.* Microsc Microanal, 2012. **18**(1): p. 68-80.
83. Ausprunk, D.H., D.R. Knighton, and J. Folkman, *Vascularization of normal and neoplastic tissues grafted to the chick chorioallantois. Role of host and preexisting graft blood vessels.* Am J Pathol, 1975. **79**(3): p. 597-618.
84. Gimbrone, M.A., Jr., et al., *Tumor growth and neovascularization: an experimental model using the rabbit cornea.* J Natl Cancer Inst, 1974. **52**(2): p. 413-27.
85. Micke, P. and A. Ostman, *Exploring the tumour environment: cancer-associated fibroblasts as targets in cancer therapy.* Expert Opin Ther Targets, 2005. **9**(6): p. 1217-33.
86. Kaneko, T., et al., *Bcl-2 orchestrates a cross-talk between endothelial and tumor cells that promotes tumor growth.* Cancer Res, 2007. **67**(20): p. 9685-93.
87. Neiva, K.G., et al., *Cross talk initiated by endothelial cells enhances migration and inhibits anoikis of squamous cell carcinoma cells through STAT3/Akt/ERK signaling.* Neoplasia, 2009. **11**(6): p. 583-93.
88. Narang, A.S. and S. Varia, *Role of tumor vascular architecture in drug delivery.* Adv Drug Deliv Rev, 2011. **63**(8): p. 640-58.
89. Boucher, Y., L.T. Baxter, and R.K. Jain, *Interstitial pressure gradients in tissue-isolated and subcutaneous tumors: implications for therapy.* Cancer Res, 1990. **50**(15): p. 4478-84.
90. Azzi, S., J.K. Hebda, and J. Gavard, *Vascular permeability and drug delivery in cancers.* Front Oncol, 2013. **3**: p. 211.
91. Cordon-Cardo, C., et al., *Expression of the multidrug resistance gene product (P-glycoprotein) in human normal and tumor tissues.* J Histochem Cytochem, 1990. **38**(9): p. 1277-87.
92. Chen, G.Y. and G. Nunez, *Sterile inflammation: sensing and reacting to damage.* Nat Rev Immunol, 2010. **10**(12): p. 826-37.
93. Scott, D.W. and R.P. Patel, *Endothelial heterogeneity and adhesion molecules N-glycosylation: implications in leukocyte trafficking in inflammation.* Glycobiology, 2013. **23**(6): p. 622-33.
94. Bevilacqua, M.P., *Endothelial-leukocyte adhesion molecules.* Annu Rev Immunol, 1993. **11**: p. 767-804.
95. von Andrian, U.H. and C.R. Mackay, *T-cell function and migration. Two sides of the same coin.* N Engl J Med, 2000. **343**(14): p. 1020-34.
96. Delfortrie, S., et al., *Egfl7 promotes tumor escape from immunity by repressing endothelial cell activation.* Cancer Res, 2011. **71**(23): p. 7176-86.

97. Wu, N.Z., et al., *Diminished leukocyte-endothelium interaction in tumor microvessels.* Cancer Res, 1992. **52**(15): p. 4265-8.
98. Balabanov, R., et al., *CNS microvascular pericytes express macrophage-like function, cell surface integrin alpha M, and macrophage marker ED-2.* Microvasc Res, 1996. **52**(2): p. 127-42.
99. Edelman, D.A., et al., *Cytokine production in lipopolysaccharide-exposed rat lung pericytes.* J Trauma, 2007. **62**(1): p. 89-93.
100. Stark, K., et al., *Capillary and arteriolar pericytes attract innate leukocytes exiting through venules and 'instruct' them with pattern-recognition and motility programs.* Nat Immunol, 2013. **14**(1): p. 41-51.
101. Verbeek, M.M., et al., *T lymphocyte adhesion to human brain pericytes is mediated via very late antigen-4/vascular cell adhesion molecule-1 interactions.* J Immunol, 1995. **154**(11): p. 5876-84.
102. Balabanov, R., T. Beaumont, and P. Dore-Duffy, *Role of central nervous system microvascular pericytes in activation of antigen-primed splenic T-lymphocytes.* J Neurosci Res, 1999. **55**(5): p. 578-87.
103. Maier, C.L. and J.S. Pober, *Human placental pericytes poorly stimulate and actively regulate allogeneic CD4 T cell responses.* Arterioscler Thromb Vasc Biol, 2011. **31**(1): p. 183-9.
104. Proebstl, D., et al., *Pericytes support neutrophil subendothelial cell crawling and breaching of venular walls in vivo.* J Exp Med, 2012. **209**(6): p. 1219-34.
105. Bose, A., et al., *Tumor-derived vascular pericytes anergize Th cells.* J Immunol, 2013. **191**(2): p. 971-81.
106. Huang, Y., et al., *Vascular normalization as an emerging strategy to enhance cancer immunotherapy.* Cancer Res, 2013. **73**(10): p. 2943-8.
107. Barsoum, I.B., et al., *A mechanism of hypoxia-mediated escape from adaptive immunity in cancer cells.* Cancer Res, 2014. **74**(3): p. 665-74.
108. Chouaib, S., et al., *Hypoxia promotes tumor growth in linking angiogenesis to immune escape.* Front Immunol, 2012. **3**: p. 21.
109. Lukashev, D., et al., *Cutting edge: hypoxia-inducible factor 1alpha and its activation-inducible short isoform I.1 negatively regulate functions of CD4+ and CD8+ T lymphocytes.* J Immunol, 2006. **177**(8): p. 4962-5.
110. Zuckerberg, A.L., L.I. Goldberg, and H.M. Lederman, *Effects of hypoxia on interleukin-2 mRNA expression by T lymphocytes.* Crit Care Med, 1994. **22**(2): p. 197-203.
111. Clambey, E.T., et al., *Hypoxia-inducible factor-1 alpha-dependent induction of FoxP3 drives regulatory T-cell abundance and function during inflammatory hypoxia of the mucosa.* Proc Natl Acad Sci U S A, 2012. **109**(41): p. E2784-93.
112. Stockmann, C., et al., *The Impact of the Immune System on Tumor: Angiogenesis and Vascular Remodeling.* Frontiers in Oncology, 2014. **4**(69).
113. Jin, X., Z. Zhu, and Y. Shi, *Metastasis mechanism and gene/protein expression in gastric cancer with distant organs metastasis.* Bull Cancer, 2014. **101**(1): p. E1-12.
114. Cao, Z., et al., *Tumor cell-mediated neovascularization and lymphangiogenesis contrive tumor progression and cancer metastasis.* Biochim Biophys Acta, 2013. **1836**(2): p. 273-86.
115. Moserle, L. and O. Casanovas, *Anti-angiogenesis and metastasis: a tumour and stromal cell alliance.* J Intern Med, 2013. **273**(2): p. 128-37.

116. Tsai, Y.P. and K.J. Wu, *Hypoxia-regulated target genes implicated in tumor metastasis.* J Biomed Sci, 2012. **19**: p. 102.
117. Thiery, J.P., *Epithelial-mesenchymal transitions in tumour progression.* Nat Rev Cancer, 2002. **2**(6): p. 442-54.
118. Friedl, P. and D. Gilmour, *Collective cell migration in morphogenesis, regeneration and cancer.* Nat Rev Mol Cell Biol, 2009. **10**(7): p. 445-57.
119. Gaggioli, C., et al., *Fibroblast-led collective invasion of carcinoma cells with differing roles for RhoGTPases in leading and following cells.* Nat Cell Biol, 2007. **9**(12): p. 1392-400.
120. Wolf, K., et al., *Multi-step pericellular proteolysis controls the transition from individual to collective cancer cell invasion.* Nat Cell Biol, 2007. **9**(8): p. 893-904.
121. Beerling, E., et al., *Intravital microscopy: new insights into metastasis of tumors.* J Cell Sci, 2011. **124**(Pt 3): p. 299-310.
122. Gerhardt, H. and H. Semb, *Pericytes: gatekeepers in tumour cell metastasis?* J Mol Med (Berl), 2008. **86**(2): p. 135-44.
123. Xian, X., et al., *Pericytes limit tumor cell metastasis.* J Clin Invest, 2006. **116**(3): p. 642-51.
124. Yonenaga, Y., et al., *Absence of smooth muscle actin-positive pericyte coverage of tumor vessels correlates with hematogenous metastasis and prognosis of colorectal cancer patients.* Oncology, 2005. **69**(2): p. 159-66.
125. Welen, K., et al., *Pericyte coverage decreases invasion of tumour cells into blood vessels in prostate cancer xenografts.* Prostate Cancer Prostatic Dis, 2009. **12**(1): p. 41-6.
126. Chabottaux, V., et al., *Membrane-type 4 matrix metalloproteinase (MT4-MMP) induces lung metastasis by alteration of primary breast tumour vascular architecture.* J Cell Mol Med, 2009. **13**(9b): p. 4002-13.
127. Sohail, A., et al., *Characterization of the dimerization interface of membrane type 4 (MT4)-matrix metalloproteinase.* J Biol Chem, 2011. **286**(38): p. 33178-89.
128. Reymond, N., B.B. d'Agua, and A.J. Ridley, *Crossing the endothelial barrier during metastasis.* Nat Rev Cancer, 2013. **13**(12): p. 858-70.
129. Garcia, A. and J.J. Kandel, *Notch: a key regulator of tumor angiogenesis and metastasis.* Histol Histopathol, 2012. **27**(2): p. 151-6.
130. Frohlich, C., et al., *ADAM12 is expressed in the tumour vasculature and mediates ectodomain shedding of several membrane-anchored endothelial proteins.* Biochem J, 2013. **452**(1): p. 97-109.
131. Giannotta, M., M. Trani, and E. Dejana, *VE-cadherin and endothelial adherens junctions: active guardians of vascular integrity.* Dev Cell, 2013. **26**(5): p. 441-54.
132. Morrison, S.J. and A.C. Spradling, *Stem cells and niches: mechanisms that promote stem cell maintenance throughout life.* Cell, 2008. **132**(4): p. 598-611.
133. Charles, N. and E.C. Holland, *The perivascular niche microenvironment in brain tumor progression.* Cell Cycle, 2010. **9**(15): p. 3012-21.
134. Ritchie, K.E. and J.E. Nor, *Perivascular stem cell niche in head and neck cancer.* Cancer Lett, 2013. **338**(1): p. 41-6.
135. Calabrese, C., et al., *A perivascular niche for brain tumor stem cells.* Cancer Cell, 2007. **11**(1): p. 69-82.
136. Krishnamurthy, S., et al., *Endothelial cell-initiated signaling promotes the survival and self-renewal of cancer stem cells.* Cancer Res, 2010. **70**(23): p. 9969-78.

137. Shen, Q., et al., *Endothelial cells stimulate self-renewal and expand neurogenesis of neural stem cells.* Science, 2004. **304**(5675): p. 1338-40.
138. Folkman, J., *Angiogenesis: an organizing principle for drug discovery?* Nat Rev Drug Discov, 2007. **6**(4): p. 273-286.
139. Jain, R.K., *Normalization of tumor vasculature: an emerging concept in antiangiogenic therapy.* Science, 2005. **307**(5706): p. 58-62.
140. Jain, R.K., *Normalizing tumor microenvironment to treat cancer: bench to bedside to biomarkers.* J Clin Oncol, 2013. **31**(17): p. 2205-18.
141. Mazzone, M., et al., *Heterozygous deficiency of PHD2 restores tumor oxygenation and inhibits metastasis via endothelial normalization.* Cell, 2009. **136**(5): p. 839-51.
142. Bellone, M. and A. Calcinotto, *Ways to enhance lymphocyte trafficking into tumors and fitness of tumor infiltrating lymphocytes.* Front Oncol, 2013. **3**: p. 231.
143. Curnis, F., et al., *Enhancement of tumor necrosis factor alpha antitumor immunotherapeutic properties by targeted delivery to aminopeptidase N (CD13).* Nat Biotechnol, 2000. **18**(11): p. 1185-90.
144. Bellone, M., A. Calcinotto, and A. Corti, *Won't you come on in? How to favor lymphocyte infiltration in tumors.* Oncoimmunology, 2012. **1**(6): p. 986-8.
145. Lorusso, D., et al., *Phase II study of NGR-hTNF in combination with doxorubicin in relapsed ovarian cancer patients.* Br J Cancer, 2012. **107**(1): p. 37-42.
146. Kerbel, R.S. and B.A. Kamen, *The anti-angiogenic basis of metronomic chemotherapy.* Nat Rev Cancer, 2004. **4**(6): p. 423-36.
147. Maiti, R., *Metronomic chemotherapy.* J Pharmacol Pharmacother, 2014. **5**(3): p. 186-92.
148. Pasquier, E., M. Kavallaris, and N. Andre, *Metronomic chemotherapy: new rationale for new directions.* Nat Rev Clin Oncol, 2010. **7**(8): p. 455-65.
149. Hermans, I.F., et al., *Synergistic effect of metronomic dosing of cyclophosphamide combined with specific antitumor immunotherapy in a murine melanoma model.* Cancer Res, 2003. **63**(23): p. 8408-13.
150. Chen, G. and L.A. Emens, *Chemoimmunotherapy: reengineering tumor immunity.* Cancer Immunol Immunother, 2013. **62**(2): p. 203-16.
151. De Vita, S., et al., *Secondary Ph+ acute lymphoblastic leukemia after temozolomide.* Ann Hematol, 2005. **84**(11): p. 760-2.
152. Presta, L.G., et al., *Humanization of an anti-vascular endothelial growth factor monoclonal antibody for the therapy of solid tumors and other disorders.* Cancer Res, 1997. **57**(20): p. 4593-9.
153. Ciombor, K.K., J. Berlin, and E. Chan, *Aflibercept.* Clin Cancer Res, 2013. **19**(8): p. 1920-5.
154. Byrne, A.T., et al., *Vascular endothelial growth factor-trap decreases tumor burden, inhibits ascites, and causes dramatic vascular remodeling in an ovarian cancer model.* Clin Cancer Res, 2003. **9**(15): p. 5721-8.
155. Rosen, L.S., *VEGF-targeted therapy: therapeutic potential and recent advances.* Oncologist, 2005. **10**(6): p. 382-91.
156. Shih, T. and C. Lindley, *Bevacizumab: an angiogenesis inhibitor for the treatment of solid malignancies.* Clin Ther, 2006. **28**(11): p. 1779-802.
157. Verheul, H.M., et al., *Vascular endothelial growth factor trap blocks tumor growth, metastasis formation, and vascular leakage in an orthotopic murine renal cell cancer model.* Clin Cancer Res, 2007. **13**(14): p. 4201-8.

158. Ma, J. and D.J. Waxman, *Combination of antiangiogenesis with chemotherapy for more effective cancer treatment.* Mol Cancer Ther, 2008. **7**(12): p. 3670-84.
159. Tejpar, S., H. Prenen, and M. Mazzone, *Overcoming Resistance to Antiangiogenic Therapies.* Oncologist, 2012. **17**(8): p. 1039-50.
160. De Falco, S., *Antiangiogenesis therapy: an update after the first decade.* Korean J Intern Med, 2014. **29**(1): p. 1-11.
161. Lemmon, M.A. and J. Schlessinger, *Cell signaling by receptor tyrosine kinases.* Cell, 2010. **141**(7): p. 1117-34.
162. Hojjat-Farsangi, M., *Small-molecule inhibitors of the receptor tyrosine kinases: promising tools for targeted cancer therapies.* Int J Mol Sci, 2014. **15**(8): p. 13768-801.
163. Dabney, R., et al., *New agents in renal cell carcinoma.* Target Oncol, 2014. **9**(3): p. 183-93.
164. Iyer, R., et al., *Sorafenib: a clinical and pharmacologic review.* Expert Opin Pharmacother, 2010. **11**(11): p. 1943-55.
165. Nguewa, P.A., et al., *Tyrosine kinase inhibitors with antiangiogenic properties for the treatment of non-small cell lung cancer.* Expert Opin Investig Drugs, 2011. **20**(1): p. 61-74.
166. Sonpavde, G., T.E. Hutson, and C.N. Sternberg, *Pazopanib, a potent orally administered small-molecule multitargeted tyrosine kinase inhibitor for renal cell carcinoma.* Expert Opin Investig Drugs, 2008. **17**(2): p. 253-61.
167. Harris, P.A., et al., *Discovery of 5-[[4-[(2,3-dimethyl-2H-indazol-6-yl)methylamino]-2-pyrimidinyl]amino]-2-methyl-b enzenesulfonamide (Pazopanib), a novel and potent vascular endothelial growth factor receptor inhibitor.* J Med Chem, 2008. **51**(15): p. 4632-40.
168. Hu-Lowe, D.D., et al., *Nonclinical antiangiogenesis and antitumor activities of axitinib (AG-013736), an oral, potent, and selective inhibitor of vascular endothelial growth factor receptor tyrosine kinases 1, 2, 3.* Clin Cancer Res, 2008. **14**(22): p. 7272-83.
169. Huang, D., et al., *Sunitinib acts primarily on tumor endothelium rather than tumor cells to inhibit the growth of renal cell carcinoma.* Cancer Res, 2010. **70**(3): p. 1053-62.
170. Mangiameli, D.P., et al., *Combination therapy targeting the tumor microenvironment is effective in a model of human ocular melanoma.* J Transl Med, 2007. **5**: p. 38.
171. Hamberg, P., J. Verweij, and S. Sleijfer, *(Pre-)clinical pharmacology and activity of pazopanib, a novel multikinase angiogenesis inhibitor.* Oncologist, 2010. **15**(6): p. 539-47.
172. Mendel, D.B., et al., *In vivo antitumor activity of SU11248, a novel tyrosine kinase inhibitor targeting vascular endothelial growth factor and platelet-derived growth factor receptors: determination of a pharmacokinetic/pharmacodynamic relationship.* Clin Cancer Res, 2003. **9**(1): p. 327-37.
173. O'Farrell, A.M., et al., *SU11248 is a novel FLT3 tyrosine kinase inhibitor with potent activity in vitro and in vivo.* Blood, 2003. **101**(9): p. 3597-605.
174. Ozao-Choy, J., et al., *The novel role of tyrosine kinase inhibitor in the reversal of immune suppression and modulation of tumor microenvironment for immune-based cancer therapies.* Cancer research, 2009. **69**(6): p. 2514-22.
175. Bose, A., et al., *Sunitinib facilitates the activation and recruitment of therapeutic anti-tumor immunity in concert with specific vaccination.* International Journal of Cancer, 2011. **129**(9): p. 2158-2170.

176. Ko, J.S., et al., *Direct and differential suppression of myeloid-derived suppressor cell subsets by sunitinib is compartmentally constrained.* Cancer Res, 2010. **70**(9): p. 3526-36.
177. Finke, J.H., et al., *Sunitinib reverses type-1 immune suppression and decreases T-regulatory cells in renal cell carcinoma patients.* Clin Cancer Res, 2008. **14**(20): p. 6674-82.
178. Gu, Y., et al., *Sunitinib impairs the proliferation and function of human peripheral T cell and prevents T-cell-mediated immune response in mice.* Clin Immunol, 2010. **135**(1): p. 55-62.
179. Alfaro, C., et al., *Influence of bevacizumab, sunitinib and sorafenib as single agents or in combination on the inhibitory effects of VEGF on human dendritic cell differentiation from monocytes.* Br J Cancer, 2009. **100**(7): p. 1111-9.
180. Kim, S., et al., *Clinical response to sunitinib as a multitargeted tyrosine-kinase inhibitor (TKI) in solid cancers: a review of clinical trials.* Onco Targets Ther, 2014. **7**: p. 719-28.
181. Vinik, A.I. and E. Raymond, *Pancreatic neuroendocrine tumors: approach to treatment with focus on sunitinib.* Therap Adv Gastroenterol, 2013. **6**(5): p. 396-411.
182. Ibrahim, N., et al., *Molecular targeted therapies for cancer: sorafenib mono-therapy and its combination with other therapies (review).* Oncol Rep, 2012. **27**(5): p. 1303-11.
183. Thomas, L., et al., *Sorafenib in metastatic thyroid cancer: a systematic review.* Oncologist, 2014. **19**(3): p. 251-8.
184. Deeks, E.D., *Pazopanib: in advanced soft tissue sarcoma.* Drugs, 2012. **72**(16): p. 2129-40.
185. Drabkin, H.A., *Pazopanib and anti-VEGF therapy.* Open Access J Urol, 2010. **2**: p. 35-40.
186. Cheever, M.A. and C.S. Higano, *PROVENGE (Sipuleucel-T) in prostate cancer: the first FDA-approved therapeutic cancer vaccine.* Clin Cancer Res, 2011. **17**(11): p. 3520-6.
187. Ghilardi, C., et al., *Identification of novel vascular markers through gene expression profiling of tumor-derived endothelium.* BMC Genomics, 2008. **9**: p. 201.
188. Schaer, D.A., A.M. Lesokhin, and J.D. Wolchok, *Hiding the road signs that lead to tumor immunity.* J Exp Med, 2011. **208**(10): p. 1937-40.
189. Dong, Y., et al., *Identification of H-2Db-specific CD8+ T-cell epitopes from mouse VEGFR2 that can inhibit angiogenesis and tumor growth.* J Immunother, 2006. **29**(1): p. 32-40.
190. Ishizaki, H., et al., *Inhibition of tumor growth with antiangiogenic cancer vaccine using epitope peptides derived from human vascular endothelial growth factor receptor 1.* Clin Cancer Res, 2006. **12**(19): p. 5841-9.
191. Wada, S., et al., *Rationale for antiangiogenic cancer therapy with vaccination using epitope peptides derived from human vascular endothelial growth factor receptor 2.* Cancer Res, 2005. **65**(11): p. 4939-46.
192. Yamaue, H., et al., *Randomized phase II/III clinical trial of elpamotide for patients with advanced pancreatic cancer; PEGASUS-PC Study.* Cancer Sci, 2015.
193. Hazama, S., et al., *A phase I study of combination vaccine treatment of five therapeutic epitope-peptides for metastatic colorectal cancer; safety, immunological response, and clinical outcome.* J Transl Med, 2014. **12**: p. 63.

194. Okamoto, I., et al., *Clinical phase I study of elpamotide, a peptide vaccine for vascular endothelial growth factor receptor 2, in patients with advanced solid tumors.* Cancer Sci, 2012. **103**(12): p. 2135-8.
195. Okuyama, R., et al., *Immunological responses to a multi-peptide vaccine targeting cancer-testis antigens and VEGFRs in advanced pancreatic cancer patients.* Oncoimmunology, 2013. **2**(11): p. e27010.
196. Suzuki, H., et al., *Multiple therapeutic peptide vaccines consisting of combined novel cancer testis antigens and anti-angiogenic peptides for patients with non-small cell lung cancer.* J Transl Med, 2013. **11**: p. 97.
197. Zhao, X., et al., *Vaccines targeting tumor blood vessel antigens promote CD8(+) T cell-dependent tumor eradication or dormancy in HLA-A2 transgenic mice.* J Immunol, 2012. **188**(4): p. 1782-8.
198. Sharpe, M. and N. Mount, *Genetically modified T cells in cancer therapy: opportunities and challenges.* Dis Model Mech, 2015. **8**(4): p. 337-50.
199. Maude, S.L., et al., *CD19-targeted chimeric antigen receptor T cell therapy for acute lymphoblastic leukemia.* Blood, 2015.
200. Fu, X., et al., *Genetically modified T cells targeting neovasculature efficiently destroy tumor blood vessels, shrink established solid tumors, and increase nanoparticle delivery.* Int J Cancer, 2013. **133**(10): p. 2483-92.
201. Chinnasamy, D., et al., *Local delivery of interleukin-12 using T cells targeting VEGF receptor-2 eradicates multiple vascularized tumors in mice.* Clin Cancer Res, 2012. **18**(6): p. 1672-83.
202. Vujanovic, L. and L.H. Butterfield, *Melanoma cancer vaccines and anti-tumor T cell responses.* J Cell Biochem, 2007. **102**(2): p. 301-10.
203. Yu, Z. and N.P. Restifo, *Cancer vaccines: progress reveals new complexities.* J Clin Invest, 2002. **110**(3): p. 289-94.
204. Shi, S., L. Chen, and G. Huang, *Antiangiogenic therapy improves the antitumor effect of adoptive cell immunotherapy by normalizing tumor vasculature.* Med Oncol, 2013. **30**(4): p. 698.
205. Griffioen, A.W., et al., *The emerging quest for the optimal angiostatic combination therapy.* Biochem Soc Trans, 2014. **42**(6): p. 1608-15.
206. Bose, A., et al., *Combined vaccine+axitinib therapy yields superior antitumor efficacy in a murine melanoma model.* Melanoma Res, 2012. **22**(3): p. 236-43.
207. Lowe, D.B., et al., *Dasatinib promotes the expansion of a therapeutically superior T-cell repertoire in response to dendritic cell vaccination against melanoma.* Oncoimmunology, 2014. **3**(1): p. e27589.
208. Farsaci, B., J.P. Higgins, and J.W. Hodge, *Consequence of dose scheduling of sunitinib on host immune response elements and vaccine combination therapy.* Int J Cancer, 2012. **130**(8): p. 1948-59.
209. Kwilas, A.R., et al., *Immune consequences of tyrosine kinase inhibitors that synergize with cancer immunotherapy.* Cancer Cell Microenviron, 2015. **2**(1).
210. Amato, R.J., et al., *Vaccination of metastatic renal cancer patients with MVA-5T4: a randomized, double-blind, placebo-controlled phase III study.* Clin Cancer Res, 2010. **16**(22): p. 5539-47.

211. Franco, M., et al., *Targeted anti-vascular endothelial growth factor receptor-2 therapy leads to short-term and long-term impairment of vascular function and increase in tumor hypoxia.* Cancer Res, 2006. **66**(7): p. 3639-48.
212. Moserle, L., G. Jimenez-Valerio, and O. Casanovas, *Antiangiogenic therapies: going beyond their limits.* Cancer Discov, 2014. **4**(1): p. 31-41.
213. Sato, C., G. Zhao, and M.X.G. Ilagan, *An Overview of Notch Signaling in Adult Tissue Renewal and Maintenance.* Curr Alzheimer Res, 2012. **9**(2): p. 227-40.
214. Andersson, E.R. and U. Lendahl, *Therapeutic modulation of Notch signalling--are we there yet?* Nat Rev Drug Discov, 2014. **13**(5): p. 357-78.
215. Ntziachristos, P., et al., *From Fly Wings to Targeted Cancer Therapies: A Centennial for Notch Signaling.* Cancer Cell, 2014. **25**(3): p. 318-34.
216. D'Souza, B., A. Miyamoto, and G. Weinmaster, *The many facets of Notch ligands.* Oncogene, 2008. **27**(38): p. 5148-67.
217. Kovall, R.A., *More complicated than it looks: assembly of Notch pathway transcription complexes.* Oncogene, 2008. **27**(38): p. 5099-109.
218. Louvi, A. and S. Artavanis-Tsakonas, *Notch and disease: a growing field.* Semin Cell Dev Biol, 2012. **23**(4): p. 473-80.
219. Penton, A.L., L.D. Leonard, and N.B. Spinner, *Notch signaling in human development and disease.* Semin Cell Dev Biol, 2012. **23**(4): p. 450-7.
220. Koch, U. and F. Radtke, *Notch in T-ALL: new players in a complex disease.* Trends Immunol, 2011. **32**(9): p. 434-42.
221. Koch, U. and F. Radtke, *Notch and cancer: a double-edged sword.* Cellular and Molecular Life Sciences, 2007. **64**(21): p. 2746-2762.
222. Lobry, C., P. Oh, and I. Aifantis, *Oncogenic and tumor suppressor functions of Notch in cancer: it's NOTCH what you think.* The Journal of experimental medicine, 2011. **208**(10): p. 1931-5.
223. Chen, J., et al., *Hypoxia potentiates Notch signaling in breast cancer leading to decreased E-cadherin expression and increased cell migration and invasion.* Br J Cancer, 2010. **102**(2): p. 351-60.
224. Grudzien, P., et al., *Inhibition of Notch signaling reduces the stem-like population of breast cancer cells and prevents mammosphere formation.* Anticancer Res, 2010. **30**(10): p. 3853-67.
225. Rangarajan, A., et al., *Notch signaling is a direct determinant of keratinocyte growth arrest and entry into differentiation.* Embo j, 2001. **20**(13): p. 3427-36.
226. Nicolas, M., et al., *Notch1 functions as a tumor suppressor in mouse skin.* Nat Genet, 2003. **33**(3): p. 416-21.
227. Dumont, A.G., et al., *Anti-tumor effects of the Notch pathway in gastrointestinal stromal tumors.* Carcinogenesis, 2012. **33**(9): p. 1674-83.
228. Jonusiene, V., et al., *Down-regulated expression of Notch signaling molecules in human endometrial cancer.* Med Oncol, 2013. **30**(1): p. 438.
229. Ridgway, J., et al., *Inhibition of Dll4 signalling inhibits tumour growth by deregulating angiogenesis.* Nature, 2006. **444**(7122): p. 1083-7.
230. Noguera-Troise, I., et al., *Blockade of Dll4 inhibits tumour growth by promoting non-productive angiogenesis.* Nature, 2006. **444**(7122): p. 1032-7.
231. Djokovic, D., et al., *Incomplete Dll4/Notch signaling inhibition promotes functional angiogenesis supporting the growth of skin papillomas.* BMC Cancer, 2015. **15**: p. 608.

232. Yan, M., et al., *Chronic DLL4 blockade induces vascular neoplasms.* Nature, 2010. **463**(7282): p. E6-7.
233. Li, J.L., A.M. Jubb, and A.L. Harris, *Targeting DLL4 in tumors shows preclinical activity but potentially significant toxicity.* Future Oncol, 2010. **6**(7): p. 1099-103.
234. Gil-Garcia, B. and V. Baladron, *The complex role of NOTCH receptors and their ligands in the development of hepatoblastoma, cholangiocarcinoma and hepatocellular carcinoma.* Biol Cell, 2016. **108**(2): p. 29-40.
235. Carvalho, F.L.F., et al., *Notch Signaling in Prostate Cancer: A Moving Target.* Prostate, 2014. **74**(9): p. 933-45.
236. Avila, J.L. and J.L. Kissil, *Notch signaling in pancreatic cancer: Oncogene or tumor suppressor?* Trends Mol Med, 2013. **19**(5): p. 320-7.
237. Smas, C.M. and H.S. Sul, *Pref-1, a protein containing EGF-like repeats, inhibits adipocyte differentiation.* Cell, 1993. **73**(4): p. 725-734.
238. Wang, Y., et al., *Pref-1, a preadipocyte secreted factor that inhibits adipogenesis.* The Journal of nutrition, 2006. **136**(12): p. 2953-6.
239. Laborda, J., *The role of the epidermal growth factor-like protein dlk in cell differentiation.* Histol Histopathol, 2000. **15**(1): p. 119-29.
240. Baladron, V., et al., *dlk acts as a negative regulator of Notch1 activation through interactions with specific EGF-like repeats.* Experimental cell research, 2005. **303**(2): p. 343-59.
241. Traustadóttir, G.Á., et al., *Evidence of non-canonical NOTCH signaling: Delta-like 1 homolog (DLK1) directly interacts with the NOTCH1 receptor in mammals.* Cellular Signalling, 2016. **28**(4): p. 246-254.
242. Falix, F.A., et al., *Possible roles of DLK1 in the Notch pathway during development and disease.* Biochimica et Biophysica Acta (BBA) - Molecular Basis of Disease, 2012. **1822**(6): p. 988-995.
243. Begum, A., et al., *DLK1, delta-like 1 homolog (Drosophila), regulates tumor cell differentiation in vivo.* Cancer letters, 2012. **318**(1): p. 26-33.
244. Espina, A.G., et al., *Induction of Dlk1 by PTTG1 inhibits adipocyte differentiation and correlates with malignant transformation.* Mol Biol Cell, 2009. **20**(14): p. 3353-62.
245. Kim, Y., et al., *Hypoxia-regulated delta-like 1 homologue enhances cancer cell stemness and tumorigenicity.* Cancer research, 2009. **69**(24): p. 9271-80.
246. Xu, X., et al., *DLK1 as a potential target against cancer stem/progenitor cells of hepatocellular carcinoma.* Mol Cancer Ther, 2012. **11**(3): p. 629-38.
247. Fukuzawa, R., et al., *Imprinting, expression, and localisation of DLK1 in Wilms tumours.* J Clin Pathol, 2005. **58**(2): p. 145-50.
248. Yin, D., et al., *DLK1: increased expression in gliomas and associated with oncogenic activities.* Oncogene, 2006. **25**(13): p. 1852-61.
249. Orr, B., et al., *Reduction of pro-tumorigenic activity of human prostate cancer-associated fibroblasts using Dlk1 or SCUBE1.* Disease Models & Mechanisms, 2013. **6**(2): p. 530-536.
250. Moon, Y.S., et al., *Mice Lacking Paternally Expressed Pref-1/Dlk1 Display Growth Retardation and Accelerated Adiposity.* Mol Cell Biol, 2002. **22**(15): p. 5585-92.
251. Nueda, M.L., et al., *The novel gene EGFL9/Dlk2, highly homologous to Dlk1, functions as a modulator of adipogenesis.* Journal of molecular biology, 2007. **367**(5): p. 1270-80.

252. Sanchez-Solana, B., et al., *The EGF-like proteins DLK1 and DLK2 function as inhibitory non-canonical ligands of NOTCH1 receptor that modulate each other's activities.* Biochimica et biophysica acta, 2011. **1813**(6): p. 1153-64.
253. Nueda, M.L., et al., *The proteins DLK1 and DLK2 modulate NOTCH1-dependent proliferation and oncogenic potential of human SK-MEL-2 melanoma cells.* Biochim Biophys Acta, 2014. **1843**(11): p. 2674-84.
254. Gaengel, K., et al., *Endothelial-mural cell signaling in vascular development and angiogenesis.* Arterioscler Thromb Vasc Biol, 2009. **29**(5): p. 630-8.
255. Fukumura, D., et al., *Tumor microvasculature and microenvironment: novel insights through intravital imaging in pre-clinical models.* Microcirculation, 2010. **17**(3): p. 206-25.
256. Finke, J.H., et al., *Tumor-infiltrating lymphocytes in patients with renal-cell carcinoma.* Annals of the New York Academy of Sciences, 1988. **532**: p. 387-94.
257. Muul, L.M., et al., *Identification of specific cytolytic immune responses against autologous tumor in humans bearing malignant melanoma.* J Immunol, 1987. **138**(3): p. 989-95.
258. Lokich, J., *Spontaneous regression of metastatic renal cancer. Case report and literature review.* Am J Clin Oncol, 1997. **20**(4): p. 416-8.
259. Motzer, R.J., et al., *Overall survival and updated results for sunitinib compared with interferon alfa in patients with metastatic renal cell carcinoma.* J Clin Oncol, 2009. **27**(22): p. 3584-90.
260. Escudier, B., et al., *Phase II study of sunitinib administered in a continuous once-daily dosing regimen in patients with cytokine-refractory metastatic renal cell carcinoma.* J Clin Oncol, 2009. **27**(25): p. 4068-75.
261. Helfrich, I., et al., *Resistance to antiangiogenic therapy is directed by vascular phenotype, vessel stabilization, and maturation in malignant melanoma.* The Journal of experimental medicine, 2010. **207**(3): p. 491-503.
262. Najjar, Y.G. and B.I. Rini, *Novel agents in renal carcinoma: a reality check.* Ther Adv Med Oncol, 2012. **4**(4): p. 183-94.
263. Ahmed, F., et al., *Tumor stroma as a target in cancer.* Curr Cancer Drug Targets, 2008. **8**(6): p. 447-53.
264. Hamzah, J., et al., *Vascular normalization in Rgs5-deficient tumours promotes immune destruction.* Nature, 2008. **453**(7193): p. 410-4.
265. Huang, Y., et al., *Vascular normalizing doses of antiangiogenic treatment reprogram the immunosuppressive tumor microenvironment and enhance immunotherapy.* Proc Natl Acad Sci U S A, 2012. **109**(43): p. 17561-6.
266. Komita, H., et al., *CD8+ T-cell responses against hemoglobin-beta prevent solid tumor growth.* Cancer research, 2008. **68**(19): p. 8076-84.
267. Ranganathan, P., K.L. Weaver, and A.J. Capobianco, *Notch signalling in solid tumours: a little bit of everything but not all the time.* Nat Rev Cancer, 2011. **11**(5): p. 338-51.
268. Murphy, G.P. and W.J. Hrushesky, *A murine renal cell carcinoma.* J Natl Cancer Inst, 1973. **50**(4): p. 1013-25.
269. Crisan, M., et al., *A perivascular origin for mesenchymal stem cells in multiple human organs.* Cell Stem Cell, 2008. **3**(3): p. 301-13.

270. Tatsumi, T., et al., *Intratumoral delivery of dendritic cells engineered to secrete both interleukin (IL)-12 and IL-18 effectively treats local and distant disease in association with broadly reactive Tc1-type immunity.* Cancer Res, 2003. **63**(19): p. 6378-86.
271. Klungsoyr, L. and K.F. Stoa, *Spectrophotometric determination of hemoglobin oxygen saturation: the method of Drabkin & Schmidt as modified for its use in clinical routine analysis.* Scand J Clin Lab Invest, 1954. **6**(4): p. 270-6.
272. Stallcup, W.B., *The NG2 proteoglycan: past insights and future prospects.* J Neurocytol, 2002. **31**(6-7): p. 423-35.
273. Trevino-Villarreal, J.H., et al., *Host-derived pericytes and Sca-1+ cells predominate in the MART-1- stroma fraction of experimentally induced melanoma.* J Histochem Cytochem, 2011. **59**(12): p. 1060-75.
274. Crisan, M., et al., *Perivascular cells for regenerative medicine.* J Cell Mol Med, 2012. **16**(12): p. 2851-60.
275. Zhao, X., et al., *Intratumoral IL-12 Gene Therapy Results in the Crosspriming of Tc1 Cells Reactive Against Tumor-associated Stromal Antigens.* Mol Ther, 2011. **19**(4): p. 805-14.
276. Sasaki, K., et al., *Preferential expression of very late antigen-4 on type 1 CTL cells plays a critical role in trafficking into central nervous system tumors.* Cancer Res, 2007. **67**(13): p. 6451-8.
277. He, Y., et al., *Skin-derived dendritic cells induce potent CD8(+) T cell immunity in recombinant lentivector-mediated genetic immunization.* Immunity, 2006. **24**(5): p. 643-56.
278. Huang, Y.H., et al., *Thyroid hormone regulation of miR-21 enhances migration and invasion of hepatoma.* Cancer Res, 2013. **73**(8): p. 2505-17.
279. Matsumoto, S., et al., *Simultaneous imaging of tumor oxygenation and microvascular permeability using Overhauser enhanced MRI.* Proc Natl Acad Sci U S A, 2009. **106**(42): p. 17898-903.
280. Wilson, W.R. and M.P. Hay, *Targeting hypoxia in cancer therapy.* Nat Rev Cancer, 2011. **11**(6): p. 393-410.
281. Cabarcas, S.M., L.A. Mathews, and W.L. Farrar, *The cancer stem cell niche--there goes the neighborhood?* Int J Cancer, 2011. **129**(10): p. 2315-27.
282. Levesque, J.P., et al., *Hematopoietic progenitor cell mobilization results in hypoxia with increased hypoxia-inducible transcription factor-1 alpha and vascular endothelial growth factor A in bone marrow.* Stem Cells, 2007. **25**(8): p. 1954-65.
283. Roesch, A., et al., *A temporarily distinct subpopulation of slow-cycling melanoma cells is required for continuous tumor growth.* Cell, 2010. **141**(4): p. 583-94.
284. Liang, D., et al., *The hypoxic microenvironment upgrades stem-like properties of ovarian cancer cells.* BMC Cancer, 2012. **12**: p. 201.
285. Mathieu, J., et al., *HIF induces human embryonic stem cell markers in cancer cells.* Cancer Res, 2011. **71**(13): p. 4640-52.
286. Saha, B., et al., *Gene modulation and immunoregulatory roles of interferon gamma.* Cytokine, 2010. **50**(1): p. 1-14.
287. Mizuno, T., et al., *Small interfering RNA expression vector targeting hypoxia-inducible factor 1 alpha inhibits tumor growth in hepatobiliary and pancreatic cancers.* Cancer Gene Ther, 2006. **13**(2): p. 131-40.

288. Keith, B., R.S. Johnson, and M.C. Simon, *HIF1alpha and HIF2alpha: sibling rivalry in hypoxic tumour growth and progression.* Nat Rev Cancer, 2011. **12**(1): p. 9-22.
289. Reis, M., et al., *Endothelial Wnt/β-catenin signaling inhibits glioma angiogenesis and normalizes tumor blood vessels by inducing PDGF-B expression.* J Exp Med, 2012. **209**(9): p. 1611-27.
290. Ueno, K., et al., *Frizzled homolog proteins, microRNAs and Wnt signaling in cancer.* Int J Cancer, 2013. **132**(8): p. 1731-40.
291. Wang, Y. and H.S. Sul, *Ectodomain shedding of preadipocyte factor 1 (Pref-1) by tumor necrosis factor alpha converting enzyme (TACE) and inhibition of adipocyte differentiation.* Mol Cell Biol, 2006. **26**(14): p. 5421-35.
292. Zhang, J., et al., *Angiopoietin-1/Tie2 signal augments basal Notch signal controlling vascular quiescence by inducing delta-like 4 expression through AKT-mediated activation of beta-catenin.* J Biol Chem, 2011. **286**(10): p. 8055-66.
293. Perez-Cabezas, B., et al., *Ligation of Notch receptors in human conventional and plasmacytoid dendritic cells differentially regulates cytokine and chemokine secretion and modulates Th cell polarization.* J Immunol, 2011. **186**(12): p. 7006-15.
294. Rini, B.I. and M.B. Atkins, *Resistance to targeted therapy in renal-cell carcinoma.* Lancet Oncol, 2009. **10**(10): p. 992-1000.
295. Faivre, S., et al., *Molecular basis for sunitinib efficacy and future clinical development.* Nat Rev Drug Discov, 2007. **6**(9): p. 734-45.
296. Folkman, J., *Tumor angiogenesis: therapeutic implications.* N Engl J Med, 1971. **285**(21): p. 1182-6.
297. Goel, S., et al., *NORMALIZATION OF THE VASCULATURE FOR TREATMENT OF CANCER AND OTHER DISEASES.* Physiol Rev, 2011. **91**(3): p. 1071-121.
298. Folkman, J., *Angiogenesis: an organizing principle for drug discovery?* Nat Rev Drug Discov, 2007. **6**(4): p. 273-86.
299. Bergers, G. and D. Hanahan, *Modes of resistance to anti-angiogenic therapy.* Nat Rev Cancer, 2008. **8**(8): p. 592-603.
300. Hofmeister, V., D. Schrama, and J.C. Becker, *Anti-cancer therapies targeting the tumor stroma.* Cancer Immunol Immunother, 2008. **57**(1): p. 1-17.
301. Sainson, R.C.A. and A.L. Harris, *Regulation of angiogenesis by homotypic and heterotypic notch signalling in endothelial cells and pericytes: from basic research to potential therapies.* Angiogenesis, 2008. **11**(1): p. 41-51.
302. Chi Sabins, N., et al., *DLK1: a novel target for immunotherapeutic remodeling of the tumor blood vasculature.* Mol Ther, 2013. **21**(10): p. 1958-68.
303. Wentink, M.Q., et al., *Vaccination approach to anti-angiogenic treatment of cancer.* Biochim Biophys Acta, 2015. **1855**(2): p. 155-171.
304. Weidner , N., et al., *Tumor Angiogenesis and Metastasis — Correlation in Invasive Breast Carcinoma.* New England Journal of Medicine, 1991. **324**(1): p. 1-8.
305. Raval, R.R., et al., *Contrasting Properties of Hypoxia-Inducible Factor 1 (HIF-1) and HIF-2 in von Hippel-Lindau-Associated Renal Cell Carcinoma.* Mol Cell Biol, 2005. **25**(13): p. 5675-86.
306. Dengler, V.L., M. Galbraith, and M. Espinosa Jí, *Transcriptional Regulation by Hypoxia Inducible Factors.* Crit Rev Biochem Mol Biol, 2014. **49**(1): p. 1-15.
307. Bertout, J.A., et al., *HIF2α inhibition promotes p53 pathway activity, tumor cell death, and radiation responses.* Proc Natl Acad Sci U S A, 2009. **106**(34): p. 14391-6.

308. Kumar, V. and D.I. Gabrilovich, *Hypoxia-inducible factors in regulation of immune responses in tumour microenvironment.* Immunology, 2014. **143**(4): p. 512-9.
309. van der Burg, S.H., et al., *Vaccines for established cancer: overcoming the challenges posed by immune evasion.* Nat Rev Cancer, 2016. **16**(4): p. 219-233.
310. Melief, C.J.M., et al., *Therapeutic cancer vaccines.* J Clin Invest, 2015. **125**(9): p. 3401-12.
311. Abiko, K., et al., *IFN-γ from lymphocytes induces PD-L1 expression and promotes progression of ovarian cancer.* Br J Cancer, 2015. **112**(9): p. 1501-9.
312. Winkler, F., et al., *Kinetics of vascular normalization by VEGFR2 blockade governs brain tumor response to radiation.* Cancer Cell. **6**(6): p. 553-563.
313. Rivero, S., et al., *DLK2 is a transcriptional target of KLF4 in the early stages of adipogenesis.* Journal of molecular biology, 2012. **417**(1-2): p. 36-50.
314. Rivero, S., et al., *Characterization of a proximal Sp1 response element in the mouse Dlk2 gene promoter.* BMC molecular biology, 2011. **12**: p. 52.
315. Culver, C., et al., *HIF-1alpha depletion results in SP1-mediated cell cycle disruption and alters the cellular response to chemotherapeutic drugs.* Cell Cycle, 2011. **10**(8): p. 1249-60.
316. Jean, J.C., et al., *Transcription factor Klf4, induced in the lung by oxygen at birth, regulates perinatal fibroblast and myofibroblast differentiation.* PLoS One, 2013. **8**(1): p. e54806.
317. Hofmann, J.J. and M.L. Iruela-Arispe, *Notch signaling in blood vessels: who is talking to whom about what?* Circ Res, 2007. **100**(11): p. 1556-68.
318. Rebay, I., et al., *Specific EGF repeats of Notch mediate interactions with Delta and Serrate: implications for Notch as a multifunctional receptor.* Cell, 1991. **67**(4): p. 687-99.
319. Cordle, J., et al., *Localization of the delta-like-1-binding site in human Notch-1 and its modulation by calcium affinity.* J Biol Chem, 2008. **283**(17): p. 11785-93.
320. Griffioen, A.W., *Anti-angiogenesis: making the tumor vulnerable to the immune system.* Cancer Immunol Immunother, 2008. **57**(10): p. 1553-8.
321. Bose, A., et al., *Sunitinib facilitates the activation and recruitment of therapeutic anti-tumor immunity in concert with specific vaccination.* International journal of cancer. Journal international du cancer, 2011. **129**(9): p. 2158-70.
322. Finke, J.H., et al., *Sunitinib reverses type-1 immune suppression and decreases T-regulatory cells in renal cell carcinoma patients.* Clinical cancer research : an official journal of the American Association for Cancer Research, 2008. **14**(20): p. 6674-82.
323. Mrass, P., et al., *Random migration precedes stable target cell interactions of tumor-infiltrating T cells.* The Journal of Experimental Medicine, 2006. **203**(12): p. 2749-2761.
324. Boissonnas, A., et al., *In vivo imaging of cytotoxic T cell infiltration and elimination of a solid tumor.* The Journal of Experimental Medicine, 2007. **204**(2): p. 345-356.
325. Facciponte, J.G., et al., *Tumor endothelial marker 1-specific DNA vaccination targets tumor vasculature.* J Clin Invest, 2014. **124**(4): p. 1497-511.
326. Seavey, M.M., et al., *An anti-vascular endothelial growth factor receptor 2/fetal liver kinase-1 Listeria monocytogenes anti-angiogenesis cancer vaccine for the treatment of primary and metastatic Her-2/neu+ breast tumors in a mouse model.* J Immunol, 2009. **182**(9): p. 5537-46.

327. Blattman, J.N., et al., *Impact of Epitope Escape on PD-1 Expression and CD8 T-Cell Exhaustion during Chronic Infection.* J Virol, 2009. **83**(9): p. 4386-94.
328. Spranger, S., et al., *Up-Regulation of PD-L1, IDO, and T(regs) in the Melanoma Tumor Microenvironment Is Driven by CD8(+) T Cells.* Sci Transl Med, 2013. **5**(200): p. 200ra116.
329. Klebanoff, C.A., et al., *Determinants of successful CD8(+) T cell adoptive immunotherapy for large established tumors in mice.* Clin Cancer Res, 2011. **17**(16): p. 5343-52.
330. Chen, L., et al., *Extranodal induction of therapeutic immunity in the tumor microenvironment after intratumoral delivery of Tbet gene-modified dendritic cells.* Cancer Gene Ther, 2013. **20**(8): p. 469-77.
331. Chen, L., et al., *Therapeutic Use of Dendritic Cells to Promote the Extranodal Priming of Anti-Tumor Immunity.* Front Immunol, 2013. **4**.
332. Weijzen, S., et al., *The Notch ligand Jagged-1 is able to induce maturation of monocyte-derived human dendritic cells.* J Immunol, 2002. **169**(8): p. 4273-8.
333. Adler, S.H., et al., *Notch signaling augments T cell responsiveness by enhancing CD25 expression.* J Immunol, 2003. **171**(6): p. 2896-903.
334. Lunt, S.J., et al., *Interstitial fluid pressure in tumors: therapeutic barrier and biomarker of angiogenesis.* Future Oncol, 2008. **4**(6): p. 793-802.
335. Hodge, J.W., et al., *Attacking malignant cells that survive therapy: Exploiting immunogenic modulation.* Oncoimmunology, 2013. **2**(12).